REPUBLIC OF YEMEN
MINISTRY OF WATER AND ENVIRONMENT
SANA'A BASIN WATER MANAGEMENT PROJECT

(IDA CREDIT 3774-YEM)

Sub-Component 3(d)

Hydro-geological and Water Resources
Monitoring and Investigations

ACTIVITY 4: HYDROLOGICAL MONITORING AND ANALYSES IN SANA'A BASIN

DRAFT FINAL REPORT
(Part IV: Water Quality Report)

by
Dr. Khaled Kheireldin
Regional Consultant

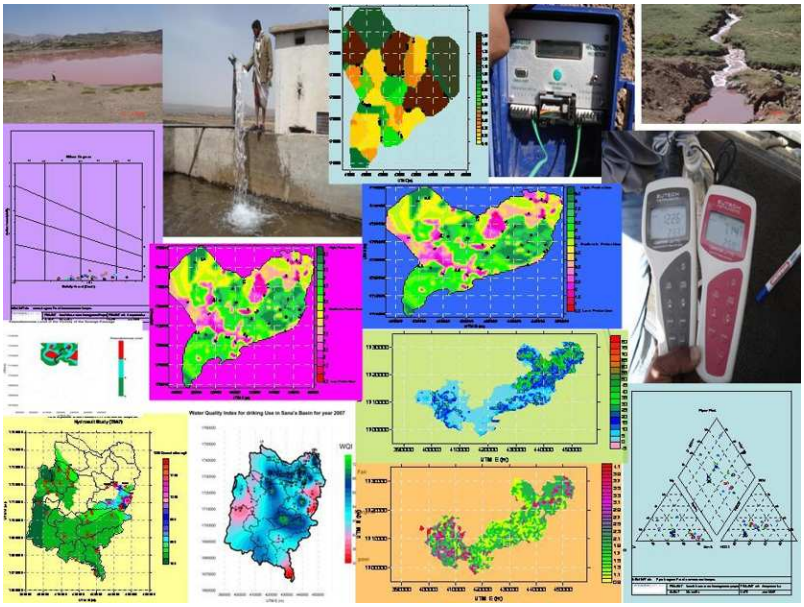

Financed by the World Bank

April, 2008

HYDROSULT Inc.
Consultants, Experts-conseils

TABLE OF CONTENTS

LIST OF FIGURES

LIST OF TABLES

EXECUTIVE SUMMARY

A literature review for the water quality studies within the entire Sana'a Basin was performed in this phase of research. Reliable water quality data from previous studies were collected and analyzed, and available information from other sources was collected. Hydro-chemical maps for the different water quality parameters were developed based on an intensive study that was performed in the Sana'a Basin in 1986. The maps were developed for total dissolved solids; pH, calcium, magnesium, sodium, soleplate, chloride, bicarbonates and carbonates. Thus, these maps are considered as base-maps or bench marks to which any new hydro-chemical maps can be referred and compared.

During the period of March 2007 to April 2007, 150 water samples were collected from throughout the Sana'a Basin from four different aquifers: limestone, sandstone, volcanic and alluvial. The collected water samples were analyzed and new hydro-chemical maps were developed. Comparisons were drawn between hydro-chemical maps that were developed using the 1986 data and the new hydro-chemical maps from 2007 data. The comparison shows significant deterioration of some water quality parameters, while positive changes have been observed in other parameters. Interpretations for all of these comparisons are presented in the current document. In addition, an intensive water quality study was performed for the area around treated wastewater passages, whereby water quality samples were taken from the deep groundwater wells in the vicinity of treated wastewater passages. Routine chemical analyses for anions and cations were performed, as well as microbiological analysis for organisms related to the impact of sewage water. Results show that the groundwater in the vicinity of the treated wastewater passage is not significantly impacted by the proximity. On the other hand, microbiological analysis shows that some wells in the region are significantly polluted with microbiological organisms. Regular monitoring of these wells is essential to a wider understanding of water quality in the area.

Designs for a water-quality monitoring network throughout the Sana'a Basin are presented in the current study, and it has been proposed that, in order to develop this network, it is essential to conduct more intensive study of the water quality and pollution status within the entire basin. Thus, vulnerability maps were constructed for the different aquifers within the Sana'a Basin using the COP method. To finalize the selection of locations for the water quality monitoring network, the 1986 hydro-chemical maps, 2007 hydro-chemical maps and vulnerability maps were integrated. From this integration, critical locations, where it is essential to install water quality monitoring stations, were determined. Thus, a finalized network of monitoring stations throughout the Basin was developed according to three general priorities for the selected locations, based upon the weight of each location.

In addition, the water quality index approach was applied to study the suitability of the water for different intended uses. The CCME water quality index approach has been applied herein. Three maps were developed for the suitability of water quality in Sana'a Basin: for drinking, irrigation and livestock use. These maps are essential to verify the appropriateness of water sources for different intended uses. Also, water type maps were developed for the different aquifers within the Sana'a Basin.

Comment [IN1]: ?What do you mean

Comment [IN2]: Explain

Chapter 1. DEVELOPMENT OF HYDRO-CHEMICAL MAPS FOR THE SANA'A BASIN IN 2007

1.1 Analyzed Parameters

The collected samples were analyzed for total cations and anions, and, in some specific locations, microbiological indicators. This section outlines the parameters that were analyzed.

Analysis of the total cations and anions:

- pH
- Electrical conductivity (EC), µS/cm
- Total dissolved solids (TDS), mg/L
- Calcium, mg/L
- Magnesium, mg/L
- Sodium, mg/L
- Potassium, mg/L
- Carbonate, mg/L
- Bicarbonate, mg/L
- Sulfate, mg/L
- chloride, mg/L
- Microbiological Organisms
- Pseudomonas
- Alcaligenes
- Escherichia coli
- Citrobacter
- Salmonella
- Shigella
- Klebsiella
- Proteus
- Enterobacter

1.2 Procedure for Sample Collection

Special field missions were conducted to collect the water samples for analysis. 500 cm^3 plastic bottles were used to collect the water samples (Figure 1). Samples were then preserved and/or iced and returned to various laboratories for analysis. Conductivity, pH, and temperature were recorded in the field using various types of EUTECH Instruments. The samples were kept at 4 Co until they arrived at the laboratory for analysis. Well water samples were collected from the outlet of an operated pump. The selected wells were usually run for at least 10 minutes prior to the collection procedure. Figure 2 shows how a water sample is collected. After collection in the sample bottle, pH, electrical conductivity, and temperature were directly measured (Figures 3 and 4). The measuring instruments were cleaned with purified water to protect the sensors after each measurement.

Figure 1-1 Bottles for Water Quality Sample Collection

Figure 1-2 Collection of a water quality sample from the pump outlet

Figure 1-3 Measurement of EC and PH in the field directly after collecting water sample

Figure 1-4 Water Quality Sample collection and on-site measurements.

1.3 Interpretation of Water Quality Analyses for the Volcanic Aquifer

In all, 29 samples were collected from 29 wells scattered over the entire volcanic outcrop. Figure 5 shows the locations of the collected water quality sampling stations within the outcrop of the volcanic aquifer. Table 1 presents the list of the selected wells, their locations and UTM coordinates. In the following section a brief description and analysis of different water quality parameters will be introduced.

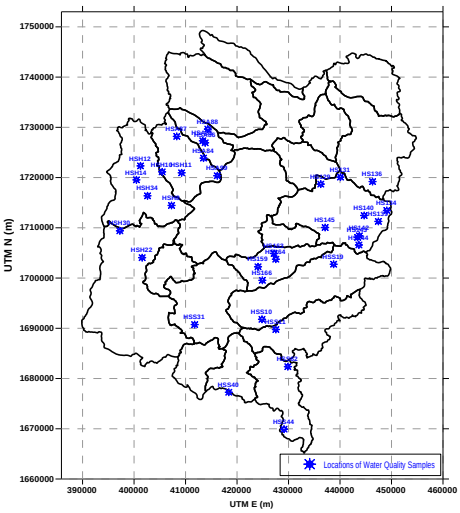

Figure 1-5 Selected locations for water quality samples within the outcrop of the volcanic aquifer

Sample	Well ID	Location	Sample_Date	UTM E (m)	UTM N (m)	Rim Elv (m)
64	HS129	Bite Al abid /nihm	17/03/2007	436267	1718700	2626
65	HS131	Bani Rasam /nihm	17/03/2007	440083	1720084	2570
68	HS134	Sara'a- Khawlan	22/03/2007	449088	1713454	2477
69	HS136	Al mahajirah-Khawlan	22/03/2007	446320	1719200	2406
70	HS139	Alsrar -Khawlan	22/03/2007	447450	1711272	2414
71	HS140	Bani Zamwmah -Bani Husheish	22/03/2007	444695	1712454	2380
73	HS142	Hozayfah -Khawlan	24/03/2007	443756	1708408	2464
74	HS143	Hozayfah -Khawlan	24/03/2007	443420	1708089	2481
75	HS144	Hozayfah -Khawlan	24/03/2007	443669	1706585	2568
77	HS145	aradah -Bani Husheish	24/03/2007	437115	1710061	2343
127	HS164	Al Rowna /Bani Husheish	14/05/2007	427530	1703755	2394
129	HSH12	Garban -Qwla'a / Hamdan	17/05/2007	401253	1722329	2468
130	HSH14	Qwla'a / Hamdan	17/05/2007	400459	1719547	2481
135	HSS10	Al Hadowr/ SANHAN	24/05/2007	424849	1691790	2372
136	HSS11	Al Hijrah/Sanhan	24/05/2007	427537	1689763	2426
137	HSS19	Shahik Khawlan	31/05/2007	438762	1702751	2574
140	HSH30	Hamdan Qa'a Al Munakab	06/06/2007	397248	1709399	2646
141	HSS31	Sna'a /Sanhan	06/06/2007	411771	1690739	2346
142	HSS40	Ruhm / Sanhan	07/06/2007	418400	1677271	2416
143	HSS44	Al Sirin / Sanhan	07/06/2007	429126	1669927	2605
84	HSA84	Al-jahman/baraman / ARHAB	07/04/2007	413496	1723877	2239
85	HSA85	Al-Asmad/Hzam / ARHAB	07/04/2007	413350	1727319	2281
86	HSA86	Al-Asmad/ ARHAB	07/04/2007	413814	1726919	2268
87	HSA87	Hotban/ ARHAB	07/04/2007	408295	1728198	2506
88	HSA88	Bait Dafa'a/ ARHAB	07/04/2007	414334	1729656	2303
90	HSH8	Al Hawry / Hamdan	09/04/2007	407277	1714451	2248
91	HSH10	Bait Al Rafik /Hamdan	09/04/2007	405457	1721136	2248
104	HSH11	Al Hokah /Hamdan	12/04/2007	409246	1720948	2253
105	HSA99	Bit Al Thib Al A'alah /Bani Al harith	12/04/2007	416163	1720363	2182

Table 1-1 List of water quality sample wells and their locations

1.3.1 pH in the volcanic aquifer

The pH value determines whether water is hard or soft and the pH of pure water is 7. The measurement of alkalinity and pH is needed to determine the corrosiveness of the water. In general, water with a low pH (< 6.5) could be acidic, soft, and corrosive. Therefore, the water could contain metal ions such as iron, manganese, copper, lead, and zinc... or, in other words, elevated levels of toxic metals. This can cause premature damage to metal piping and have associated aesthetic problems such as a metallic or sour taste, staining of laundry, and the characteristic "blue-green" staining of sinks and drains. More importantly, there are health risks associated with these toxins. The primary way to treat the problem of low pH water is with the use of a neutralizer.

Water with a pH > 8.5 could indicate that the water is hard. Hard water does not pose a health risk, but can cause aesthetic problems. These problems include an alkaline taste to the water, formation of a deposit on dishes, utensils and laundry basins, difficulty in getting soaps and detergents to lather, and formation of insoluble precipitates on clothing.

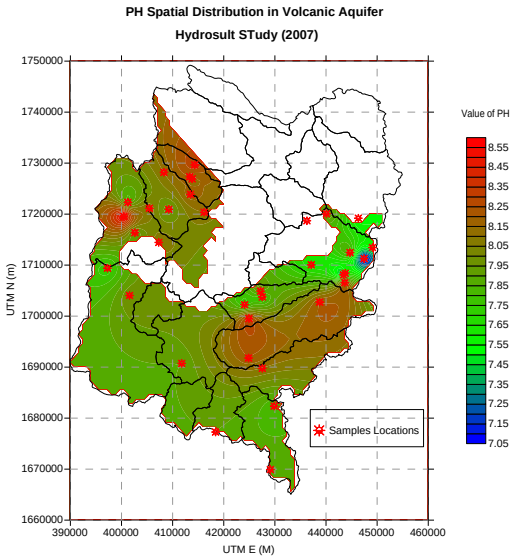

Figure 1-6 pH Distribution within the outcrop of the volcanic aquifer

Accordingly, looking at the map in Figure 6, it can be observed that the green color covers about 65% of the volcanic aquifer. This indicates that most of the aquifer has a pH value between 7 and 8 which is considered ideal. There are some locations where pH is relatively high but does not exceed the critical value of 8.55. The highest pH value within the aquifer is located at Wadi Iqbal on the western side of the basin. Also, pH values within the boundaries of Wadi Shahik and Wadi Al-Qasaba are relatively high.

1.3.2 Chloride in the volcanic aquifer

Almost all natural waters contain chloride ions in varying concentrations that depend on the mineral content of the earth in any given area. Nevertheless, excessive concentrations of chloride ions can make water unpleasant to drink.

The EPA Secondary Drinking Water Regulations recommend a maximum concentration of 250 mg/L for chloride ions (expressed as Cl- and not as CaC03). Chlorides give water a salty flavor, but the concentrations at which this taste becomes noticeable depends upon the individual. In large concentrations, chlorides cause a brackish, briny flavor that definitely is undesirable. Although chlorides are extremely soluble, they possess marked stability. This enables them to resist change and to remain fairly constant in any given water unless the supply is altered by dilution or by industrial or human wastes. Chlorides contribute to the total mineral content of water. As indicated above, the total concentration of minerals may have a variety of effects in the home. High concentrations of chloride ions add to the electrical conductivity of water. Chlorides can be substantially removed from water by reverse osmosis. Deionization (demineralization) or distillation will also remove chlorides and sulfates from water, but these methods are less suitable than reverse osmosis for household use.

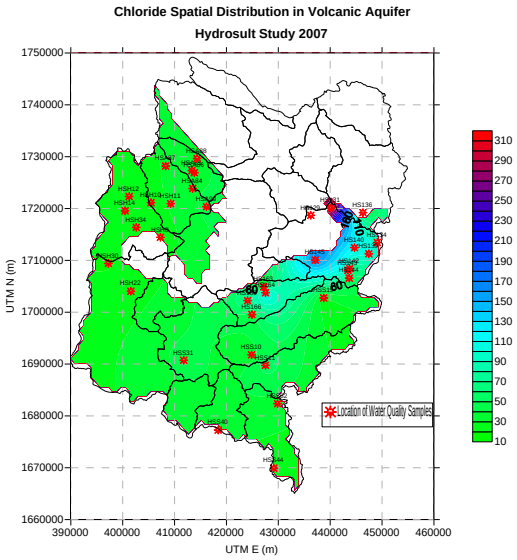

Figure 1-7 Chloride concentration within the outcrop of the volcanic aquifer

The chloride concentration in the volcanic aquifer is presented in Figure 7. It can be noticed that 90% of the aquifer water is suspected to contain a low chloride concentration. The highest chloride concentration occurs in Wadi Al-Sirr, where the value exceeds 300 mg/L. This high concentration occurs in the area of intersection with the sandstone outcrop. The coordinates of the location where the highest value is found are UTM E 440000, N 1720000.

1.3.3 Calcium in the volcanic aquifer

Hard water is high in dissolved minerals, especially calcium and magnesium. As water moves through soil and rock, it dissolves small amounts of these naturally-occurring minerals and carries them into the groundwater supply. The hardness of water is expressed in terms of the amount of calcium carbonate – the principal constituent of limestone – or equivalent minerals that would be formed if the water were evaporated. Water is considered soft if it contains 0 to 60 mg/L of hardness, moderately hard from 61 to 120 mg/L, hard between 121 and 180 mg/L, and very hard if more than 180 mg/L. Hard water interferes with most domestic cleaning tasks, from doing the laundry to washing dishes to taking a shower. Clothes can look dingy and feel rough and scratchy when washed in hard water. Dishes and glasses get spotted and a film may build up on shower doors, bathtubs, sinks and faucets. Washing your hair in hard water may leave it feeling sticky and dull. Finally, hard water can cause a residue to build up in pipes that can lower water pressure throughout the house.

Hardness does not however pose a health risk and is not regulated by any government agency. In fact, calcium and magnesium in drinking water can help ensure that individuals get the average daily requirements for these minerals in their diet. But hard water can be a nuisance due to the mineral buildup on plumbing fixtures and poor soap and detergent performance. It often causes aesthetic problems, such as an alkaline flavor that makes coffee taste bitter; build up of scales on pipes and fixtures than can lead to lower water pressure; build up of deposits on dishes, utensils and laundry basins, difficulty in getting soap and detergent to foam; and lowered efficiency of electric water heaters. The human body needs calcium to develop strong teeth and bones, and a good calcium intake can combat osteoporosis and other bone disorders. It also helps in regulating nerve transmission, blood

coagulation, and muscle contraction. Calcium intake through water sources is shown to protect against death from acute myocardial infarction (heart disease), especially in women. It also protects against rectal and gastric cancers. In general, based on the water quality standards, the lowest desirable limit in Yemen for calcium concentration in water is 75 mg/L while the permissible value is 200 mg/L.

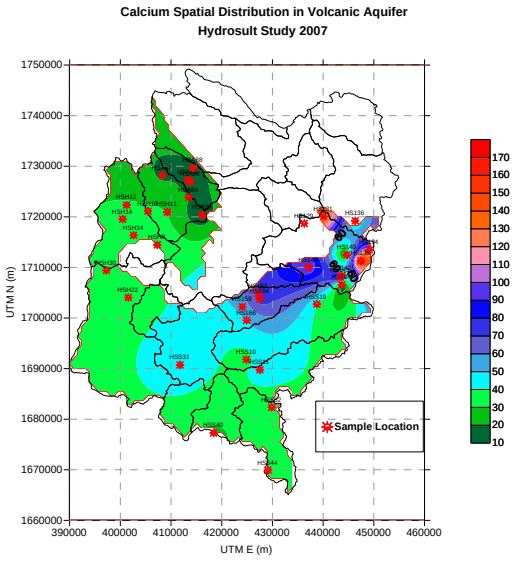

Figure 1-8 Calcium concentration within the outcrop of the volcanic aquifer

Figure 8 presents the distribution of calcium within the boundaries of the volcanic aquifer. It can be concluded that the concentration is less than the maximum permissible limit over the entire aquifer. However, the west part of the aquifer displays a relatively low value of 10 to 30 mg/L. The highest calcium levels are located the Wadi Al-Sirr where a maximum value of 170 mg/L was observed. Then, this value decreases gradually towards the western areas. High concentrations are also found at the basin boundary in the Wadi Al-Sirr area. The coordinates of the two locations where the highest concentrations occurred are UTM E 450000, N 1710000 and UTM E 440000, N 1720000.

1.3.4 Sodium in the volcanic aquifer

Sodium salts are present in variable concentrations in all natural waters from concentrations of a few parts per million in some surface supplies to several hundred grains per gallon in certain well supplies. Sodium is extremely soluble and increases its solubility as the temperature of water rises. Because of this characteristic, sodium salts do not form scales when water is heated. Likewise, sodium salts do not produce curd when combined with soap. In fact, ordinary soap is an organic sodium compound. As such, it does not react with the sodium in water. High concentrations of sodium, on the other hand, mean high total minerals and tend to increase the corrosive action of water. In concentrations over 30 to 40 grains per gallon, sodium salts may give water an unpleasant taste. Further, sodium ions in large amounts hamper the operation of ion exchange softeners used for the removal of water hardness. Where water contains appreciable amounts of both hardness minerals and sodium, several grains of hardness may continue to appear even in softened water. This occurs because of the regenerative action of the sodium ions on the ion exchange material.

Comment [IN3]: May be we do not need this detail

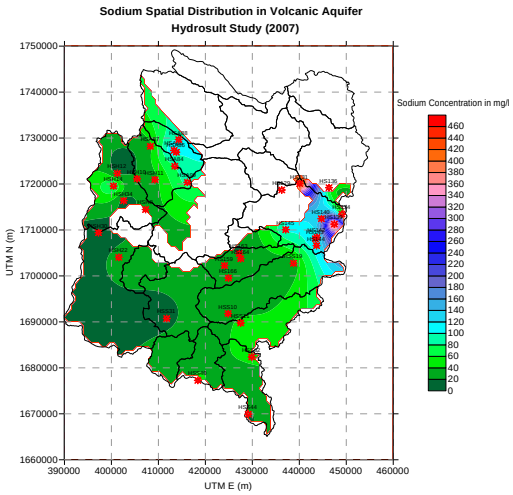

Figure 1-9 Sodium concentration within the outcrop of the volcanic aquifer

Figure 9 presents the spatial distribution of sodium within the outcrop of the volcanic aquifer. The lowest desirable limit for sodium concentrations is 200 mg/L while the maximum permissible limit is 400 mg/L. Thus, it can be concluded that the value of sodium concentration is below the desirable standards value for almost 85% of the aquifer. At the eastern side and close to the Sana'a Basin boundary, the highest values of sodium concentration are found. In the transition zone between the low concentration and high concentration, there is a location where sodium concentration is gradually increased from 30 or below to 330 mg/L. The coordinates of the two locations where the highest concentration has been found are UTM E 450000, N 1710000 and UTM E 440000, N 1720000.

1.3.5 Potassium in the volcanic aquifer

In fresh water, potassium levels are normally low, while higher levels can be observed in brackish waters. The guide level prescribed for drinking water supplies under the EC Regulations is 10 mg/L (ref?). Potassium is not a major component in public or industrial water supplies. Potassium is, however, essential in a well-balanced diet.

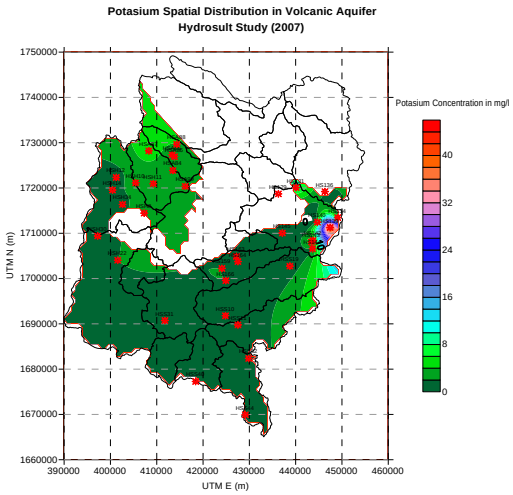

Figure 1-10 Potassium concentration within the outcrop of volcanic aquifer

Figure 10 presents the distribution map for the potassium concentration within the volcanic aquifer. It can be seen that 95% of the aquifer area has very low potassium concentration (within the range of 2 mg/L). The highest concentrations are found at the far eastern side close to the boundary, as shown by the red color. The highest value is in the range of 45 mg/L, which is considered a very high potassium concentration. The coordinates of this location are UTM E 450000, N 1710000.

1.3.6 Sulfate in the volcanic aquifer

Sulfate (SO4) occurs in almost all natural waters. Most sulfate compounds originate from the oxidation of sulfite ores, the presence of shale, and the existence of industrial wastes. Sulfate is one of the major dissolved constituents in rain. High concentrations of sulfate in drinking water have a laxative effect when combined with calcium and magnesium, the two most common components of hardness. Bacteria, which attack and reduce sulfates, causes hydrogen sulfide gas (H2S) to form. Sulfate has a suggested level of 250 mg/L in the Secondary Drinking Water Standards published by the US EPA (ref?).

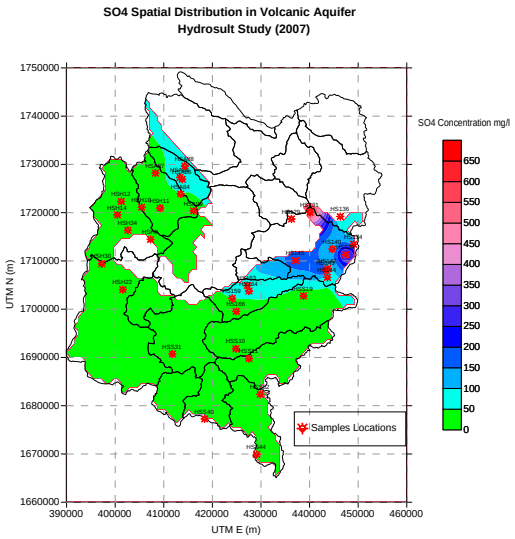

Figure 1-11 Sulfate Concentration in the volcanic aquifer

Figure 11 presents the sulfate distribution over the volcanic aquifer. It can be noticed that 90% of the aquifer has a relatively low concentration of sulfate, within the range of 50 mg/L or less. However, this value is slightly higher at Wadi Al-Qasaba, with values between 50 mg/L and 100 mg/L. The highest value occurred at location UTM E 440000, N 1720000.

1.3.7 Magnesium in the volcanic aquifer

Magnesium (Mg+2) hardness usually makes up approximately 33% of the total hardness of a particular water supply. Magnesium is found in many minerals, including dolomite, magnetite, and many types of clay. Figure 12 presents the distribution of magnesium within the volcanic aquifer. The maximum permissible limit is 30 mg/L. Approximately 98% of the aquifer area has a value below 15 mg/L. The concentration is more elevated at one location towards the eastern boundary of the basin, with a value of 100 mg/L. The coordinates of this location are UTM E 450000, N 1710000.

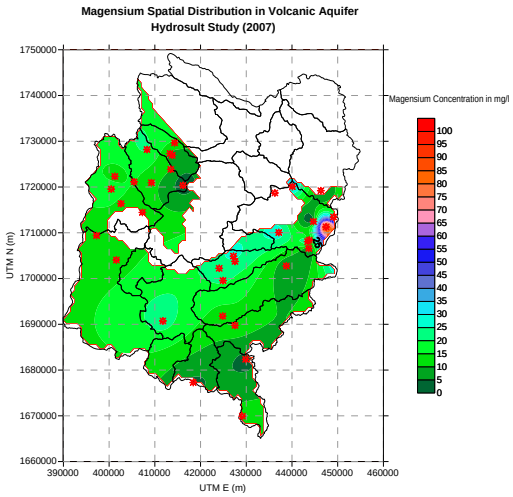

Figure 1-12 Magnesium distribution within the volcanic aquifer

1.3.8 Bicarbonate in the volcanic aquifer

The bicarbonate (HCO3) ion is the principal alkaline constituent in almost all water supplies. Alkalinity in drinking water supplies seldom exceeds 300 mg/L. Bicarbonate alkalinity is introduced into the water by CO2 dissolving carbonate-containing minerals. Alkalinity control is especially important in boiler feed water, cooling tower water, and in the beverage industry. Alkalinity neutralizes the acidity in fruit flavors, and, in the textile industry, it interferes with acid dying. Figure 13 presents the distribution of HCO3 within the volcanic aquifer. The desirable level for HCO3 concentrations is 150 mg/L while the maximum permissible limit is 500 mg/L. It has been found that the value of HCO3 within the volcanic aquifer is relatively low, in the range of 50 to 150 mg/L for 98% of the aquifer. However, the concentration is higher at a certain location on the eastern boundary of the basin, with a value above 1250 mg/L. The coordinates of this location are UTM E 450000, N 1710000.

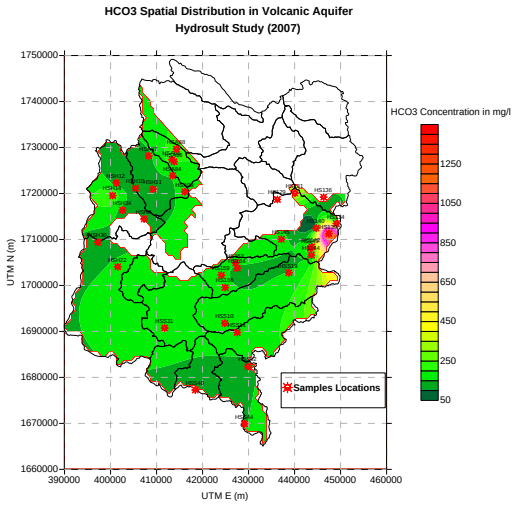

Figure 1-13 The distribution of bicarbonate in the volcanic aquifer

1.3.9 Total Dissolved Solids in the volcanic aquifer

Total Dissolved Solids (TDS) consist mainly of carbonates, bicarbonates, chlorides, sulfates, phosphates, nitrates, calcium, magnesium, sodium, potassium, iron, manganese, and a few others. They do not include gases, colloids, or sediment. TDS can be estimated by measuring the specific conductance of the water. Dissolved solids in natural concentrations can range from less than 10 mg/L for rain to more than 100,000 mg/L for brines. Since TDS is the sum of all materials dissolved in the water, it has many different mineral sources. High levels of total dissolved solids can adversely affect industrial applications requiring the use of water such as cooling tower operations, boiler feed water, food and beverage industries, and electronics manufacturers. High levels of chloride and sulfate will accelerate the corrosion of metals. The desirable level of Total Dissolved solids in Yemen is 650 mg/L while the maximum permissible value is 1500 mg/L.

Figure 14 presents the distribution of TDS in waters throughout the volcanic aquifer. It can be seen that 95% of the aquifer area has a value of TDS below 400 mg/L, and in the western part of the basin the TDS value is much lower still, reaching 100-200 mg/L. On the other hand, in the eastern area bounded by the coordinates of UTM E 450000, N 1710000 and UTM E 440000, N 1720000, the value of TDS reached a value above 2000 mg/L.

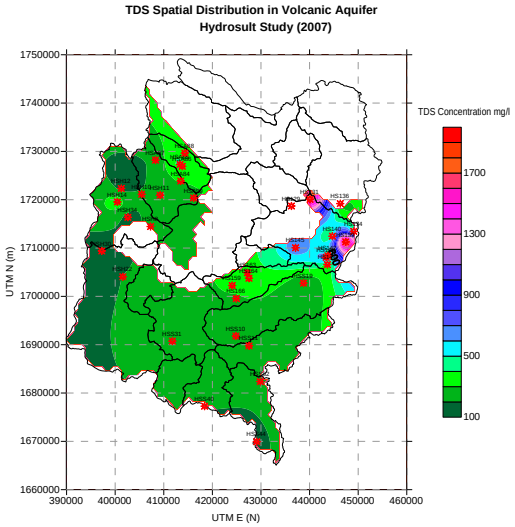

Figure 1-14 Distribution of TDS in the volcanic aquifer

1.4 Interpretation of Water Quality Analyses for the Limestone Aquifer

61 samples were collected from 29 wells located throughout the outcrop of the limestone aquifer. Figure 15 shows the locations of the water quality sampling points within the limestone outcrop. Table 2 presents a list of the selected wells, their locations and UTM coordinates. The following sections will provide a brief description and analysis of the different water quality parameters that were analyzed.

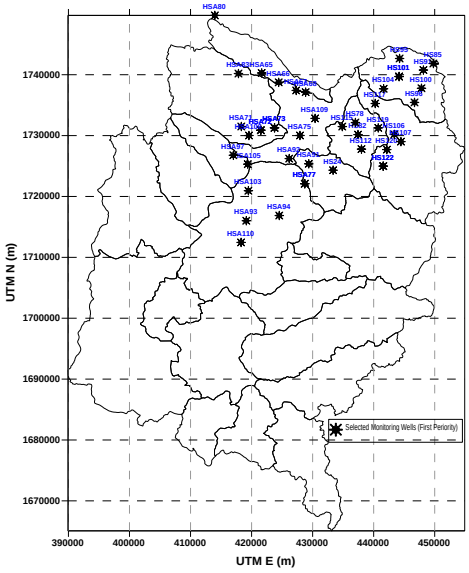

Figure 1-15 The selected locations for water quality samples within the outcrop of the limestone aquifer

Sample	Well ID	Location	Sample Date	UTM E (m)	UTM N (m)	Rim Elv (m)
1	HSA63	Al-Hyfa / ARHAB	3/1/2007	418913	1739978	2407
2	HSA65	Kulak / ARHAB	3/1/2007	421656	1740289	2379
3	HSA66	Aigaz / ARHAB	3/1/2007	424439	1738751	2375
4	HSA67	Bani Al-Hakam / ARHAB	3/1/2007	427306	1737420	2290
5	HSA68	Bani Sabare / ARHAB	3/1/2007	428859	1737137	2281
6	HSA69	AL-Mrahyb / ARHAB	3/1/2007	425724	1731589	2073
7	HSA70	Darb Oubaid / ARHAB	3/6/2007	419702	1731375	2160
8	HSA71	Al ganadiba / ARHAB	3/6/2007	418317	1731495	2186
9	HSA72	Bousaan / ARHAB	3/6/2007	421515	1730889	2124
10	HSA73	gahfal / ARHAB	3/6/2007	423760	1731279	2094
11	HSA74	Simnah / ARHAB	3/6/2007	426751	1729981	2031
12	HSA75	Al safiah / ARHAB	3/6/2007	427928	1730022	2028
13	HSA76	Al abwa'a / Al Swllban / ARHAB	3/6/2007	425304	1728396	2089
14	HS77	Al hayeathim /Nihm	3/7/2007	437787	1732133	1991
15	HS78	Al hayeathim /Nihm	3/7/2007	437008	1732149	2009
16	HS79	Al hayeathim /Nihm	3/7/2007	437909	1732005	1994
17	HS80	Al hayeathim /Nihm	3/7/2007	438198	1730745	2009
18	HS81	Al ghyl/Al hayeathim /Nihm	3/7/2007	437733	1730792	2010
19	HS82	Al raghwa/Al hayeathim / Nihm	3/7/2007	437433	1730165	2014
20	HSA77	Al kibsha'a / bani Al harith	3/7/2007	428717	1722095	2156
21	HSA80	El-zylah / ARHAB	3/10/2007	413979	1749744	2606
22	HSA83	Al-Hyfa / ARHAB	3/10/2007	417850	1740194	2423
23	HS83	Maswarah /Nihm	3/11/2007	446815	1740388	2139
24	HS84	Maswarah /Nihm	3/11/2007	450100	1740787	2173
25	HS85	Maswarah /Nihm	3/11/2007	449783	1741843	2171

Sample	Well ID	Location	Sample Date	UTM E (m)	UTM N (m)	Rim Elv (m)
26	HS88	Al -Kutby /Nihm	3/11/2007	448408	1744413	2198
27	HS89	Al -Kutby /Nihm	3/11/2007	447482	1744952	2195
28	HS90	Al -Kutby /Nihm	3/11/2007	446983	1744691	2201
29	HS91	Eyal Housin /Nihm	3/11/2007	448148	1740768	2116
30	HS93	Bani ghalib /Nihm	3/11/2007	445988	1742985	2215
31	HS95	Al -qadr /Nihm	3/11/2007	444245	1742667	2188
32	HS96	Wadi Mahaly /Nihm	3/12/2007	446690	1735446	2170
33	HS99	Al razoah /Nihm	3/12/2007	447790	1735787	2153
34	HS34	sanany /Nihm	3/12/2007	448854	1736073	2156
35	HS100	Ghaylamah /Nihm	3/12/2007	447830	1737774	2136
36	HS101	Al Ghaydah/Nihm	3/12/2007	444166	1739703	2094
37	HS102	Wadi Al- ma'ady /Nihm	3/12/2007	442135	1737739	2022
38	HS104	Wadi Al- ma'ady /Nihm	3/12/2007	441635	1737691	2019
39	HS106	Wadi Thajer /NIHM	3/13/2007	443383	1730190	2083
40	HS107	Wadi Thajer/Bani Asaem /NIHM	3/13/2007	444468	1729011	2089
41	HS108	Wadi Thajer /NIHM	3/13/2007	445208	1727894	2107
42	HS24	Al mahajer /NIHM	3/14/2007	433352	1724317	2127
43	HS112	KOULAQAH /NIHM	3/14/2007	438002	1727781	2054
44	HS115	Bani Qtra'an /Nihm	3/14/2007	434859	1731484	2093
45	HS117	Ghoubarah/Nihm	3/14/2007	440254	1735268	2012
46	HS119	Bani Zater/Nihm	3/14/2007	440747	1731266	2060
47	HS120	Bait Houmran/Nihm	3/14/2007	442159	1727703	2100
48	HS121	Qourymah/Nihm	3/14/2007	442170	1726064	2128
49	HS122	Qariah Aljarf /nihm	3/15/2007	441564	1724984	2151
50	HS27	Bit Al anz /NIHM	4/10/2007	432478	1724413	2127
51	HS28	Bit Al anz /NIHM	4/10/2007	430758	1724836	2127

Sample	Well ID	Location	Sample Date	UTM E (m)	UTM N (m)	Rim Elv (m)
52	HSA91	Shira'a /ARHAB	4/10/2007	429370	1725365	2066
53	HSA92	Bani Jarmoz /ARHAB	4/10/2007	426167	1726223	2086
54	HSA97	Aomarah /ARHAB	4/11/2007	417010	1726772	2207
55	HSA102	Bit Al Euthari /Bani Al harith	4/12/2007	419534	1723364	2167
56	HSA103	Bit Duqaish /Bani Al harith	4/12/2007	419477	1720943	2166
57	HSA105	Bab Al Rawdah /ARHAB	4/14/2007	419380	1725310	2156
58	HSA106	Al baglan /ARHAB	4/14/2007	419567	1730016	2156
59	HSA107	Bit Swdi /ARHAB	4/14/2007	430467	1729702	2074
60	HSA108	Markan /ARHAB	4/14/2007	430695	1730438	2105
61	HSA109	Bani Al Hakam /ARHAB	4/14/2007	430402	1732830	2001

Table 1-2 List of water quality sample wells and their locations

1.4.1 pH in the limestone aquifer

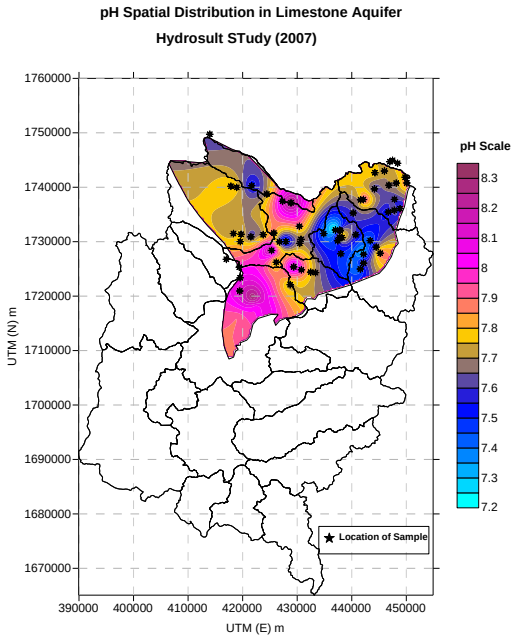

Figure 1-16 pH Concentration within the outcrop of the limestone aquifer

Figure 16 presents the spatial distribution for the pH values over the limestone outcrop. The lowest value occurred within the boundaries of Wadi Khulaga while the highest values occurred mainly in

Wadi Al-Kharid. In general, the pH values of the aquifer are found to be below the permissible limit of 8.5.

1.4.2 Chloride in the Limestone Aquifer

Figure 17 presents the chloride concentrations of the limestone aquifer. The results show that concentrations vary within the desirable and permissible limits for Yemen. The north-western part of the aquifer has a relatively low chloride concentration with an average value of approximately 40 mg/L. The north-eastern part of the limestone outcrop has a higher value at 150 mg/L. However, the highest value occurred at a specific location, which is represented by the red color on the map. This location is found at coordinates of UTM E 442000 and UTM N 1730000.

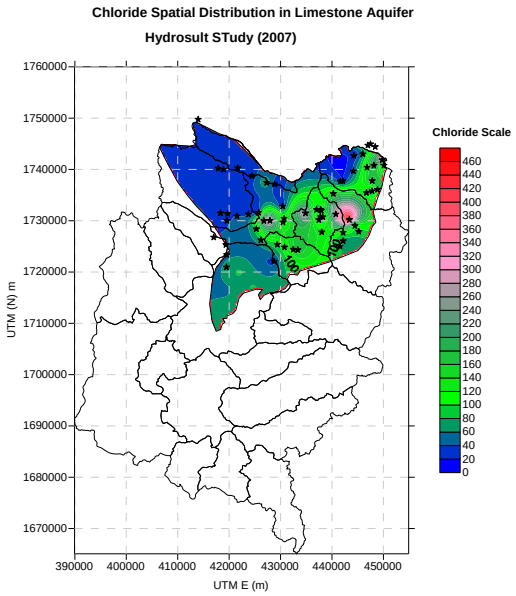

Figure 1-17 Chloride concentration within the outcrop of the limestone aquifer

1.4.3 Calcium in the Limestone Aquifer

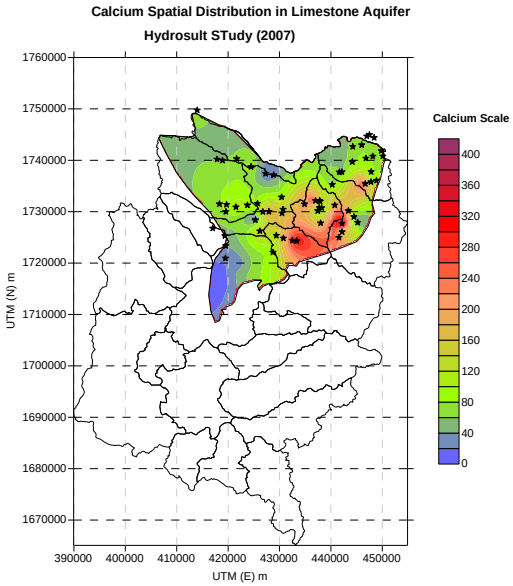

Figure 1-18 Calcium Concentration within the outcrop of the limestone Aquifer

Figure 18 presents the distribution of calcium within the boundaries of the limestone aquifer. The spatial distribution of calcium concentrations within the outcrop of the limestone aquifer indicates that there is an area with a relatively high calcium concentration, spread on a considerably large area. As indicated by the red color in Figure 18, this area represents about 30% of the total outcrop area of limestone. The high concentration level covers Wadis: Khulaga, Thuma, Lafaf and Asir, and some areas in Qatab. The remaining area has a calcium concentration that varies between 40 mg/L and 120 mg/L.

1.4.4 Sodium in the Limestone Aquifer

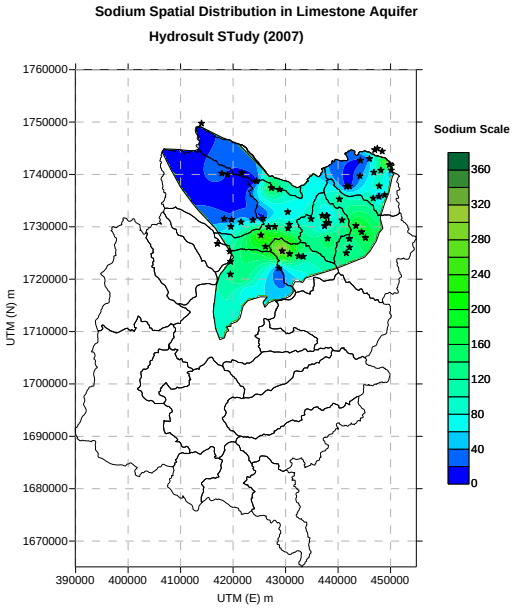

Figure 1-19 Sodium concentration within the outcrop of the limestone aquifer

Figure 19 presents the spatial distribution of sodium within the outcrop of the limestone aquifer. The lowest desirable limit for sodium concentrations is 200 mg/L while the maximum permissible limit is 400 mg/L. Thus, it can be concluded that sodium concentrations are below the desirable standard value for the entire aquifer. The lowest value occurs in the north-western areas within the boundaries of Wadis Madini and Madar. In addition, the northern parts of Wadi Qatab have low values of sodium concentration. The light blue areas, where the concentration of sodium varies between 40 and 120 mg/L, are distributed among several Wadis including Bani Hawat, Khulaga, Al-Kharid, and Thuma. The highest concentration is indicated with the green color and the concentration of sodium in these areas ranges from 140 to 280 mg/L. This area covers some parts of Wadi Thuma, Al-Kharid, Asef and Lafaf and Kholaga.

1.4.5 Potassium in the Limestone Aquifer

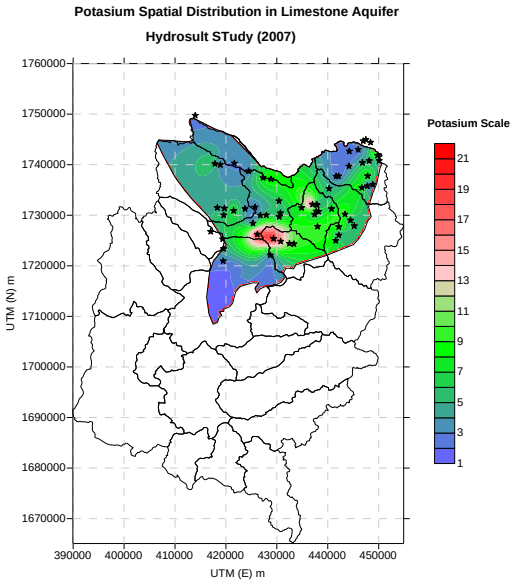

Figure 1-20 Potassium concentration within the outcrop of the limestone aquifer

Figure 20 presents the distribution map for the potassium concentration within the limestone aquifer. It indicates that 95% of the aquifer area has very low concentration (within the range of 2 mg/L). From Figure 20, it can be concluded that many locations over the Sana'a Basin have a considerably low level of potassium that varies between 2 mg/L and 9 mg/L. The highest concentration is found in Wadi Khulaga with a value of 21 mg/L. The coordinates of this location are UTM E 430000, N 1725000.

1.4.6 Sulfate in the Limestone Aquifer

Figure 21 presents the sulfate distribution over the limestone aquifer. The north-western area of the Sana'a Basin has the lowest sulfate value. Wadi Madar and Wadi Medani, as well as the northern part of Wadi Hawat, have considerably low sulfate values, with a maximum value of 100 mg/L. The spatial distribution of sulfate shows that the concentration increases dramatically towards the south-east, from 100 mg/L to 1350 mg/L, more than double the maximum permissible limit for Yemen. The area with high sulfate concentrations is found to be in the range of 120 km2.

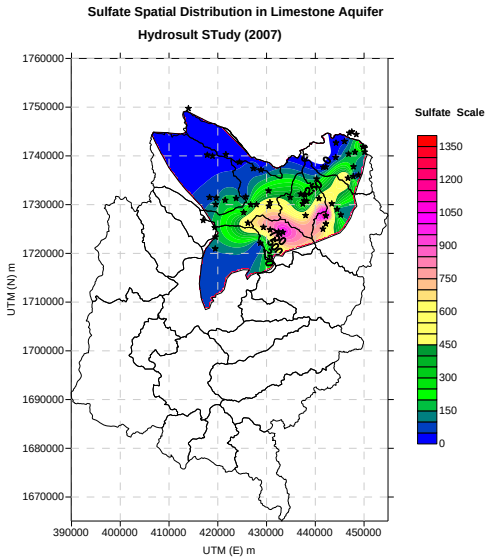

Figure 1-21 Sulfate concentration in the limestone aquifer

1.4.7 Magnesium in the Limestone Aquifer

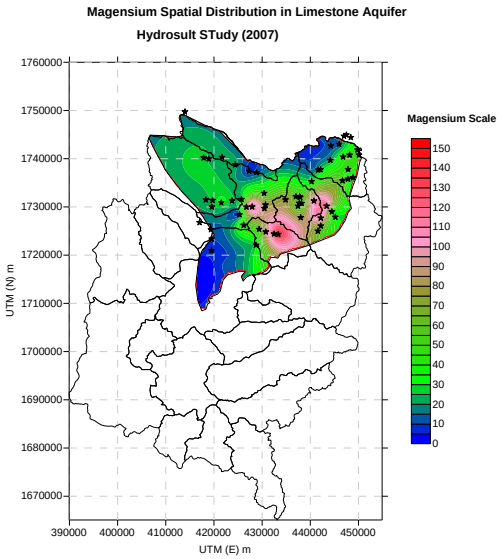

Figure 1-22 Magnesium distribution within the limestone aquifer

Figure 22 presents the distribution of magnesium within the limestone aquifer. The maximum permissible limit is 30 mg/L. The north-western part of the aquifer has a relatively low level of

Magnesium, in the range of 10 mg/L to 30 mg/L. On the other hand, in the north-eastern part of the limestone aquifer, magnesium concentrations are found to increase dramatically, with maximum values reaching 150 mg/L. This is five times the permissible value of magnesium concentration. The boundary of the high concentration area is almost the same as that of the area with a high sulfate concentration.

~~1.4.9~~1.4.8 Bicarbonate in the Limestone Aquifer

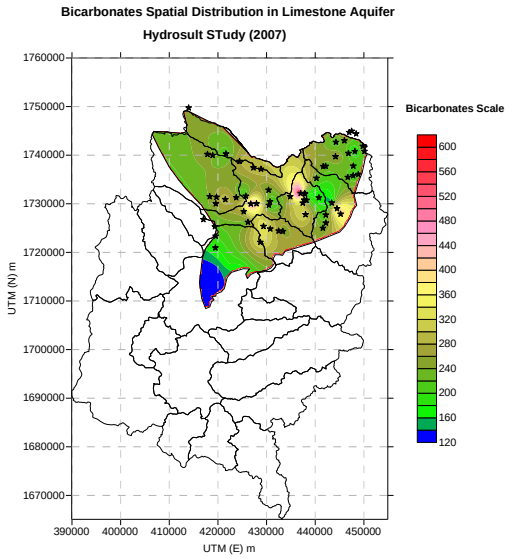

Figure 1-23 The distribution of bicarbonate in the limestone aquifer

Figure 23 presents the distribution of HCO3 within the limestone aquifer. The desirable lowest level for HCO3 concentrations is 150 mg/L while the maximum permissible limit is 500 mg/L. It has been found that the value of HCO3 for nearly 95% of the limestone aquifer ranges between 50 mg/L and 400 mg/L, which is lower than the maximum permissible limit in Yemen.

~~1.4.10~~1.4.9 Total Dissolved Solids in the Limestone Aquifer

Figure 24 presents the distribution of TDS throughout the limestone aquifer. We see that about 75% of the aquifer has a value below the limit of 400 mg/L. The value of TDS is dramatically higher in the south-western part of the aquifer and reaches values of up to 1800 mg/L. In addition, there are some locations where the value is higher still and reaches values of 2200 mg/L.

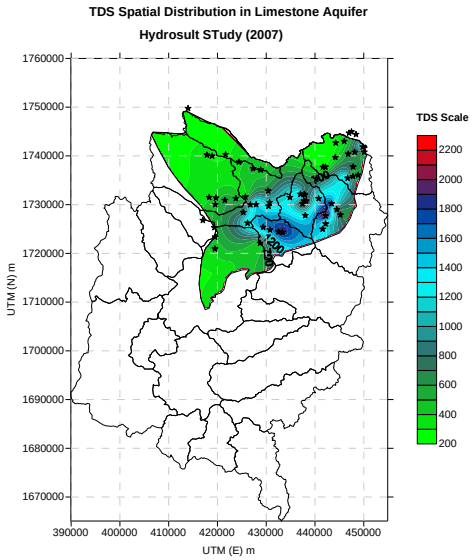

Figure 1-24 Distribution of TDS in the limestone aquifer

1.5 Interpretation of Water Quality Analyses for the Sandstone Aquifer

25 samples were collected from 25 wells over the outcrop of the sandstone aquifer. Figure 25 shows the locations of the water quality sampling points within the sandstone outcrop. Table 3 presents a list of the selected wells, their locations and UTM coordinates. The following sections provide a brief description and analysis of the different water quality parameters that were analyzed.

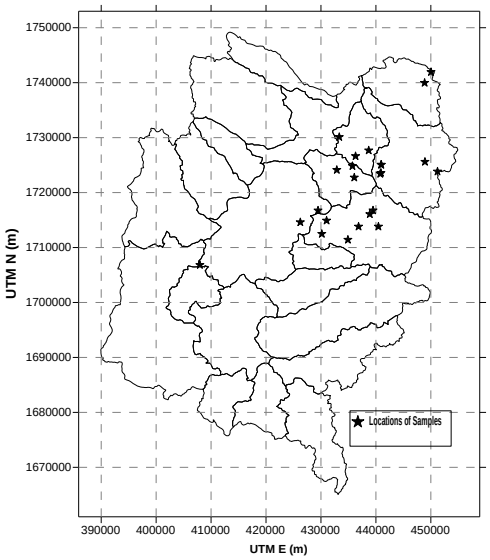

Figure 1-25 The selected locations for water quality samples within the outcrop of the sandstone aquifer

No.	Well ID	Location	Date	UTM E	UTM N
1	HS90	Qariah Aljarf /nihm	3/15/2007	440981	1725057
2	HS91	Hija'ah al makanah/nihm	3/17/2007	435733	1724826
3	HS96	Maswarah /Nihm	3/11/2007	450033	1741936
4	HS99	Al-mahajer /Nihm	3/13/2007	432883	1724121
5	HS34	KOULAQAH /NIHM	3/13/2007	436297	1726629
6	HS100	Ghoulah Aseam/ NIHM	3/13/2007	448929	1725596
7	HS101	Almoa'ainah / NIHM	3/13/2007	451212	1723827
8	HS102	KOULAQAH /NIHM	3/14/2007	438693	1727668
9	HS104	Qariah Aljarf /nihm	3/15/2007	440946	1725071
10	HS25	Al ghidah /nihm	3/15/2007	440794	1723402
11	HS105	Al ghidah /nihm	3/15/2007	440909	1723588
12	HS107	Bani hoshish	3/17/2007	438891	1716072

No.	Well ID	Location	Date	UTM E	UTM N
13	HS108	Alharf -Bani Husheish	3/22/2007	440459	1713806
14	HS110	Aradah -Bani Husheish	3/24/2007	434905	1711413
15	HS24	Rama'a /Bani Husheish	3/25/2007	431026	1714902
16	HS113	Alsatrah /NIHM	3/27/2007	433332	1730112
17	HS119	Hamdan Wadi Zahr	6/5/2007	407966	1706823
18	HS120	Al Ghorzah -Hamdan	6/21/2007	400176	1709097
19	HS95	Maswarah /Nihm	3/11/2007	448870	1739967
20	HS106	Bit Abdalah /nihm	3/17/2007	439478	1716748
21	HS31	Qadran -Bani Husheish	3/24/2007	430155	1712477
22	HS112	Bit Al saieed /Bani Husheish	3/25/2007	436845	1713808
23	HS18	Shibam //Bani Husheish	4/10/2007	426243	1714598
24	HS115	Zijan / Bani Husheish	4/10/2007	429466	1716736
25	HS121	Thomah /nihm	3/17/2007	436064	1722730

Table 1-3 List of water quality sample wells and their locations

1.5.1 pH in the sandstone aquifer

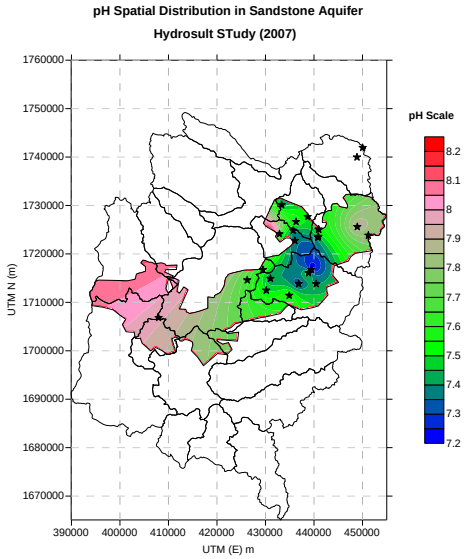

Figure 1-26 pH spatial distribution in the sandstone aquifer

The spatial distribution of pH shown in Figure 26 shows that pH values are within the range of 7.2 to 8.2 (within the permissible Yemeni limits) throughout the sandstone aquifer. The eastern part of the aquifer has values that range between 7.9 and 8.2. The western part of the aquifer has values that range between 7.2 and 7.9.

1.5.2 Chloride in the sandstone aquifer

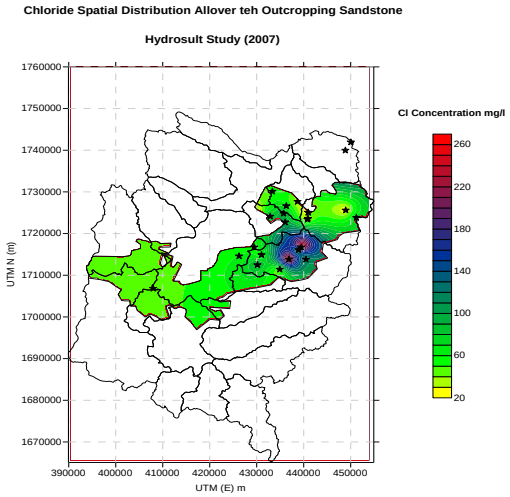

Figure 1-27 Chloride concentration within the outcrop of the sandstone aquifer

Chloride concentrations in the sandstone aquifer are presented in Figure 27. It can be noted that 90% of the aquifer water is suspected to have a low chloride concentration. The most common concentration is found to be in the range of 20 mg/L to 90 mg/L. The highest chloride concentration occurs in Wadi Al-Sirr, where the value exceeds 280 mg/L. This high value occurs in the area of intersection with the limestone outcrop. The coordinates of the location where the highest value is found are UTM E 440000, N 1715000.

1.5.3 Calcium in the sandstone aquifer

Figure 28 presents the distribution of calcium within the boundaries of the sandstone aquifer. It can be concluded that the concentration is less than the maximum permissible limit over the entire aquifer except at the intersection point with the limestone aquifer. However, the western part of the aquifer has a relatively low value of 10 to 30 mg/L. The high value of calcium is located near the Wadi Thomaa where the record value of 290 mg/L was detected. This value then decreases gradually towards the western areas. The coordinates of the location where the highest concentration occurred are UTM E 432000, N 1725000.

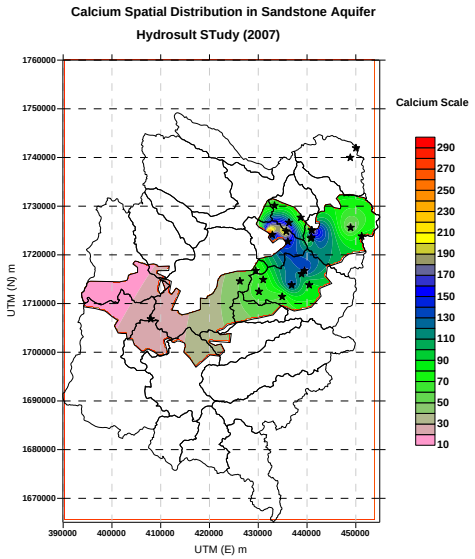

Figure 1-28 Calcium Concentration within the outcrop of sandstone aquifer

1.5.4 Sodium in the sandstone aquifer

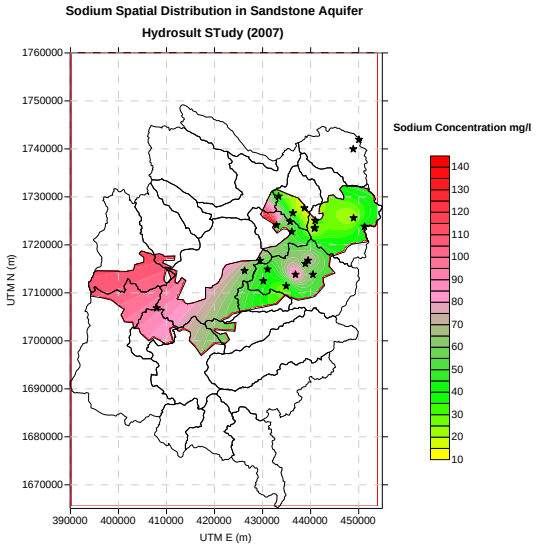

Figure 1-29 Sodium concentration within the outcrop of the sandstone aquifer

Figure 29 presents the spatial distribution of sodium within the outcrop of the sandstone aquifer. The lowest desirable limit for sodium concentration is 200 mg/L while the maximum permissible limit is

400 mg/L. Thus, it can be concluded that the value of sodium concentration is below the desirable standard value for the entire aquifer.

1.5.5 Potassium in the sandstone aquifer

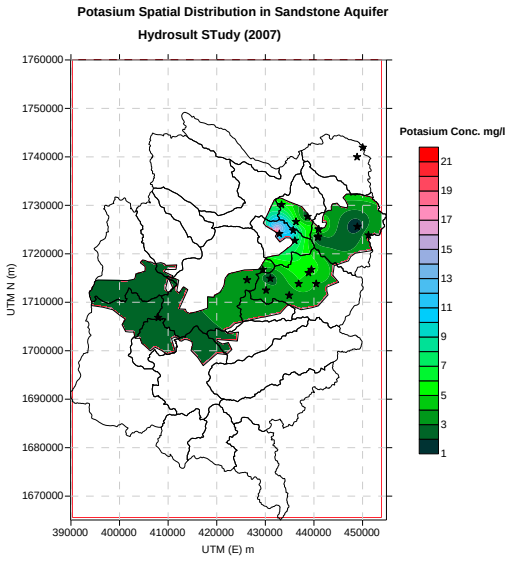

Figure 1-30 Potassium concentration within the outcrop of sandstone aquifer

Figure 30 presents the distribution map for potassium concentrations within the sandstone aquifer. It can be shown that almost all of the aquifer has a concentration varying between 2 and 7 mg/L. The highest concentration is found at the point where the sandstone aquifer intersects the limestone aquifer. The coordinates of the location where the highest concentration occurred are UTM E 432000, N 1725000.

1.5.6 Sulfate in the sandstone aquifer

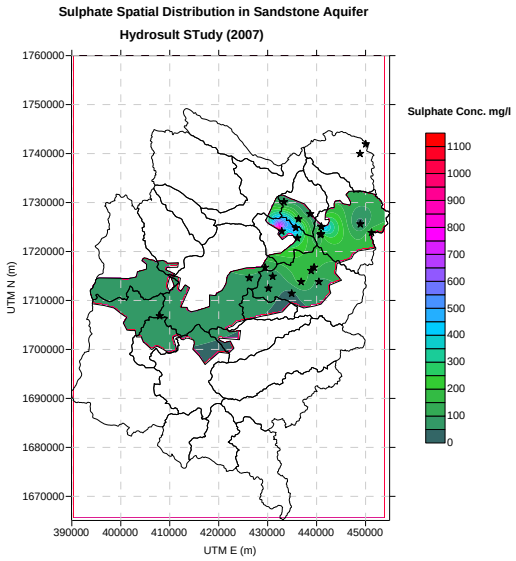

Figure 1-31 Sulfate concentration in sandstone aquifer

Figure 31 presents the sulfate distribution over the sandstone aquifer. It can be noted that almost all of the aquifer has a relatively low concentration of sulfate within the range of 50 mg/L to 300 mg/L. The highest concentration is found at the point where the sandstone aquifer intersects the limestone aquifer. The coordinates of the location where the highest concentration occurred are UTM E 432000, N 1725000.

1.5.7 Magnesium in the sandstone aquifer

Figure 32 presents the distribution of magnesium within the sandstone aquifer. The maximum permissible limit is 30 mg/L. Most of the aquifer area is well below this limit with a value below 7 mg/L. The highest concentration is found at the point where the sandstone aquifer intersects with the limestone aquifer. The coordinates of the location where the highest concentration occurred are UTM E 432000, N 1725000.

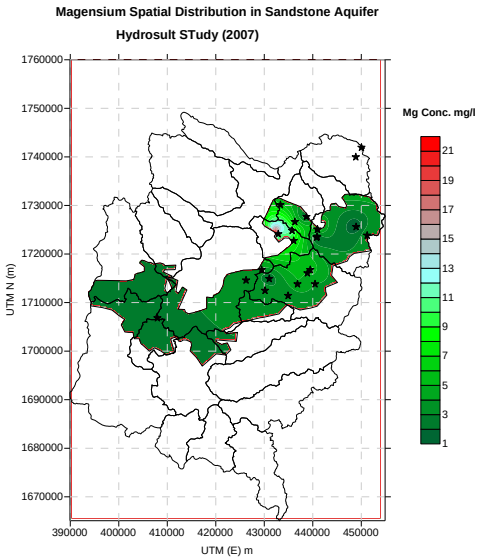

Figure 1-32 Magnesium distribution within the sandstone aquifer

1.5.8 Bicarbonate in the sandstone aquifer

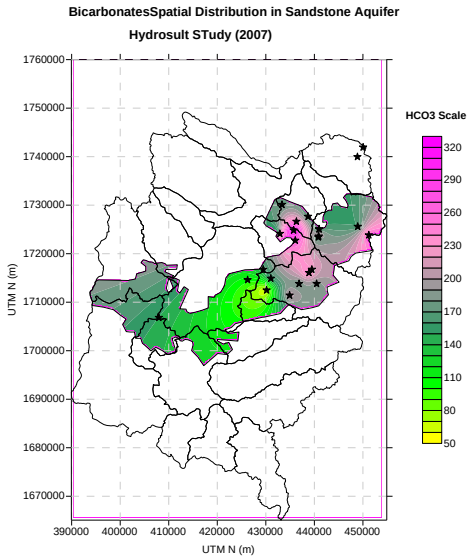

Figure 1-33 The distribution of bicarbonate in the sandstone aquifer

Figure 33 presents the distribution of HCO3 within the sandstone aquifer. The desirable lowest level for HCO3 concentrations is 150 mg/L while the maximum permissible limit is 500 mg/L. Within the

sandstone aquifer, it has been found that the value of HCO3 is relatively low, in the range of 50 to 330 mg/L.

1.5.9 Total Dissolved Solids in the sandstone aquifer

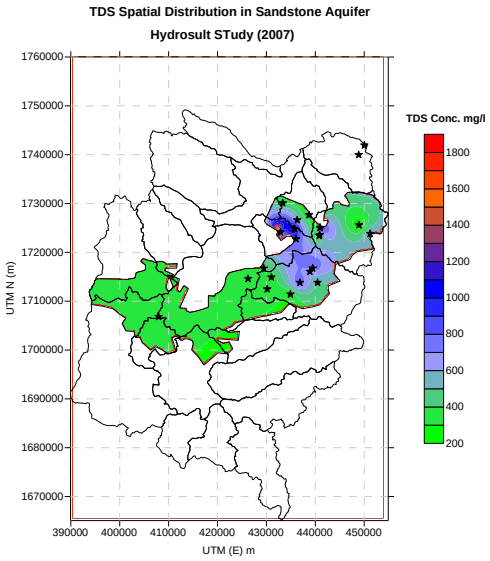

Figure 1-34 Distribution of TDS in the sandstone aquifer

Figure 34 presents the distribution of TDS in the sandstone aquifer. It shows that 70% of the aquifer area has TDS values ranging between 200 and 400 mg/L. On the other hand, TDS in wadis Thomaa, AL-Sirr, Khulaga and Lafaf was found to be higher, in the range of 500 mg/L and 1200 mg/L. The highest concentration was found at the point where the sandstone aquifer intersects the limestone aquifer, where a value of 2000 mg/L was detected. The coordinates of the location where the highest concentration occurred are UTM E 432000, N 1725000.

Chapter 2. WATER QUALITY VARIATION WITHIN THE SANA'A BASIN FROM 1986 TO 2007

2.1 Introduction

In this section, a comparison will be introduced between the Russian Study of 1986 and the Hydrosult study of 2007 (ref). The aim of this comparison is to examine the variation of water quality throughout the Sana'a Basin over an extended period. In 1986, the Russian study collected about 350 water quality samples from different points within the basin. These samples were analyzed and all the data presented in the subsequent report. At that time, the limestone aquifer was not as developed as it is now, so very few samples were collected from this aquifer. By contrast, several water quality samples were collected from the alluvial aquifer, which now has been depleted in many regions. In the 2007 study, only a few samples were collected from this aquifer. In general, only two aquifers can be compared directly between the 1986 and 2007 studies: the volcanic aquifer and the sandstone aquifer. Thus, in the following sections, only these two aquifers are used for the purpose of drawing comparisons.

2.2 Comparison of Water Quality Analyses in the Sana'a Basin between 1986 and 2007

The next sections will compare the water quality analysis performed as part of a Russian water resources study in 1986 and the water quality analysis performed by Hydrosult in 2007. In the Russian study, about 350 samples were collected from the different aquifers throughout the Sana'a basin. The majority of these samples were collected from the alluvial aquifer, which has since been depleted in many locations. In the 2007 study, only a small number of samples was collected from the alluvial aquifer. A comparison of water quality in the alluvial aquifer in 1986 and 2007 would not be significant since the new samples were spatially distributed over a relatively small area as compared to the 1986 mission. In addition, the 1986 Russian study included a very small number of water quality samples from the limestone aquifer. Thus, it was determined that comparing the limestone aquifer water quality data from 1986 and 2007 would not be useful. Accordingly, the current study aims to draw comparisons between water quality data from 1986 and 2007 for the volcanic and sandstone aquifers only**.**

2.3 Comparison of Water Quality between 1986 and 2007 for the Volcanic Aquifer

2.3.1 Comparison of TDS Concentration between 1986 and 2007 for the volcanic aquifer

Figure 35 and Figure 36 present the spatial distribution of total dissolved solids in mg/L for the 2007 study and 1986 study, respectively. In the 1986 study, the highest value of TDS was found to be in the range of 500 mg/L at Wadi Qasabah in the north-eastern part of the Sana'a Basin. TDS concentrations in the rest of the aquifer were less than 500 mg/L. The lowest value occurred at the south-western side of the basin at Wadi Zahr, with a value in the range of 100 mg/L. Thus, TDS concentrations were considered relatively low and acceptably lower than the permissible limit of 600 mg/L.

In the 2007 study, as shown in Figure 35, the TDS concentration was relatively low for 90% of the basin area. Starting from Wadi Qasabah and running counterclockwise up to Wadi Sawan, the entire aquifer that is located within this area has a relatively low value that varies between 100 and 400 mg/L. On the other hand, the far eastern part of the volcanic aquifer that is located in Wadi Al-Sirr displays a relatively high TDS value. TDS concentrations reach 1600 mg/L at two locations: the Al-Gahala in Khwalan area and Bani Rassam. In 1986, TDS in the same location was relatively low, in the range of 100 to 200 mg/L. The reasons behind this dramatic change in the volcanic aquifer are not yet known since there were no measurements made in the 21 years between studies. The most probable reason has to do with significant withdrawal from the groundwater aquifer in this area between 1986 and 2007. Thus, it is recommended that continuous monitoring be set up in this area in order to understand the reasons for the water quality deterioration.

2.3.2 Comparison of sulfate spatial distribution between 1986 and 2007 for the volcanic aquifer

Figure 38 presents the spatial distribution of sulfate as found by the 1986 mission. At that time, about 50% of the basin had a relatively low concentration with a value under 50 mg/L. The Wadis that were found in the region of 50 mg/L concentrations were Wadi Zahr, Wadi Hamadan, Wadi Mawrid, Wadi Shahik, and parts of Wadi Mulaikhy, Wadi Ghayman, and Wadi Sa'wan. The highest concentration appeared to be in Wadi Qasabah and Wadi Yahis with a value in the range of 250 mg/L. The desirable sulfate concentration in drinking water is 200 mg/L, while the maximum permissible limit for sulfate concentration in drinking water is 600 mg/L, according to the Yemeni water quality standards.

Figure 37 presents the spatial distribution of sulfate for the 2007 mission. Comparing the two figures shows that sulfate concentrations have gone down significantly. In more that 90% of the basin area, concentrations in 2007 did not exceed 50 mg/L. On the other hand, 2007 sulfate concentrations reach 600 mg/L at two locations: Al-Gahala in Khwalan and Bani Rassam. The sulfate concentrations increase gradually in Wadi Sa'wan from less than 100 mg/L up to 300 mg/L in the eastern part of Wadi

Al-Sirr. However, these values approach the maximum permissible limit for Yemeni Standards of drinking water quality.

2.3.3 Comparison of pH spatial distribution between 1986 and 2007 for the volcanic aquifer

Figure 40 presents the spatial distribution of pH in the volcanic aquifer within the Sana'a Basin as measured by the 1986 mission. The lowest value was found to be 7.05, while the highest value was 8.5. The high pH value of was observed in several wadis such as Wadi Qasaba, Wadi Iqbal, Wadi Hizayaz, part of Wadi Shahik, a small area of Wadi Sa'wan and Wadi Zahr, and the whole area between Al-Gahala in Khwalan and Bani Rassam. The remaining area of the volcanic aquifer ranges between pH 7.25 and pH 8.05. The lowest desirable limit, based on the Yemeni standards for drinking water, ranges from 6.5 to 8.5.

Figure 39 presents the spatial distribution of pH in the volcanic aquifer based on 2007 data. When we compare the 2007 map to the 1986 map, it can be concluded that the minimum pH value within the Wadis has increased from 7.05 to 7.65. In addition, the highest value was reduced from 8.5 to 8.25.

2.3.4 Comparison of sodium spatial distribution between 1986 and 2007 for the volcanic aquifer

Figure 42 presents the spatial distribution of sodium in the volcanic aquifer during the 1986 mission. The entire aquifer had a value between 0 and 20 mg/L, considered to be a very low value compared to the acceptable standard for drinking water, which is 200 mg/L. Figure 41 shows the spatial distribution of sodium in the 2007 mission. It can be observed that sodium concentrations have changed significantly compared to the 1986 mission. The concentration remains below 20 mg/L in Wadi Zahr at the western side of the Sana'a Basin, then starts to increase gradually until it reaches its highest value of 460mg/L at Al-Gahala in Khwalan and Bani Rassam in Wadi Al-sirr. Wadi Qasabah has a sodium concentration of 120 mg/L. The maximum permissible limit for sodium according to Yemeni standards is 400 mg/L, thus the concentrations at Al-Gahala in Khwalan and at Bani Rassam are higher than the permissible limit.

2.3.5 Comparison of magnesium spatial distribution between 1986 and 2007 for the volcanic aquifer

Figure 46 presents the spatial distribution of magnesium in the volcanic aquifer of the Sana'a Basin, based on the analysis results of the 1986 mission. In that study, magnesium concentrations in the aquifer varied from 5 mg/L to 50 mg/L. The highest desirable limit for magnesium concentration in drinking water is 30 mg/L. There were several wadis where the magnesium concentration was higher than the maximum permissible limit. These included Wadis Mawrid, Sanhan and Sa'wan. Other areas also had values lower than the permissible lowest limits. Figure 45 presents the spatial distribution of magnesium throughout the volcanic aquifer. As shown in this figure, the spatial distribution indicates that magnesium concentrations were within the permissible limits, with the exception of Al-Gahala in Khwalan at the far western side of Sana'a Basin, where concentrations were higher. (NO MENTION OF 2007 STUDY)

2.3.6 Comparison of potassium spatial distribution between 1986 and 2007 for the volcanic aquifer

Figure 44 presents the spatial distribution of potassium in the volcanic aquifer based on 1986 values. It can be seen that 80% of the aquifer had a value of about 45 mg/L. Eight wadis had a relatively high level of potassium: Wadi Qasabah, Wadi Yahis, Wadi Iqbal, Wadi Mawrid, Wadi Hizayaz, Wadi Ghyaman, and parts of Wadi Al-Sirr and Wadi Al-Foros. The permissible limit of potassium for drinking water is 12 mg/L. Figure 43 shows the spatial distribution of potassium within the volcanic aquifer found by the 2007 mission. The spatial distribution of potassium based on data from the 2007

mission indicates that potassium concentrations have been significantly reduced to below 8 mg/L for the entire aquifer. This value is lower than the permissible limit. However, one location, Al-Gahala in Khwalan, had a relatively high value, reaching 45 mg/L.

2.3.7 Comparison of bicarbonate spatial distribution between 1986 and 2007 for the volcanic aquifer

Figure 48 presents the spatial distribution of bicarbonates in the entire volcanic aquifer based on 1986 data. The entire aquifer at that time had a maximum value of 250 mg/L. The lowest desirable limit of bicarbonates for drinking water is 150 mg/L while the maximum permissible limit is 500 mg/L. Figure 47 shows the spatial distribution of bicarbonates within the volcanic aquifer in 2007. As seen in this figure, the entire volcanic aquifer has values within the level of 250 mg/L, except at Al-Gahala in Khwalan where the bicarbonate value exceeds 1100 mg/L. Thus, the bicarbonate concentration has increased significantly in the western side of the basin as compared to the status in 1986.

2.3.8 Comparison of calcium spatial distribution between 1986 and 2007 for volcanic aquifer

Figure 50 presents the spatial distribution of calcium within the volcanic basin based on 1986 data. It can be concluded from this figure that the calcium concentration at that time had a maximum value of 150 mg/L, which occurred only in Wadi Sa'wan. The lowest desirable limit for calcium based on Yemeni standards is 75 mg/L, while the maximum permissible limit is 200 mg/L. Thus, calcium concentrations throughout the volcanic aquifer in the 1986 mission were within accepted limits. Figure 49 shows calcium distribution within the volcanic aquifer based on the 2007 mission. It can be concluded that the calcium concentration is lower than that of the 1986 mission in the eastern part of the basin while, in the western part, starting at Wadi Sa'wan, Wadi Al-Foros and Wadi Al-Sirr, calcium concentrations are relatively higher. The highest values are found at Al-Gahala in Khwalan and and Bani Rassam, with values approaching 170 mg/L.

2.3.9 Comparison of chloride spatial distribution between 1986 and 2007 for the volcanic aquifer

Figure 52 presents the spatial distribution of chloride within the volcanic aquifer based on data from the 1986 mission. The highest chloride concentration discovered was in the range of 160 mg/L. The lowest desirable limit for chloride is 200 mg/L, while the maximum permissible limit is 600 mg/L. Thus, the chloride concentrations found by the 1986 mission were considered to be within acceptable limits. Figure 51 presents the spatial distribution of chloride for the 2007 mission. Compared to the 1986 mission, the chloride concentration has decreased for most of the volcanic basin except at Bani Rassam where the concentration has risen to 300 mg/L. However, this value is still within permissible limits for Yemeni drinking water.

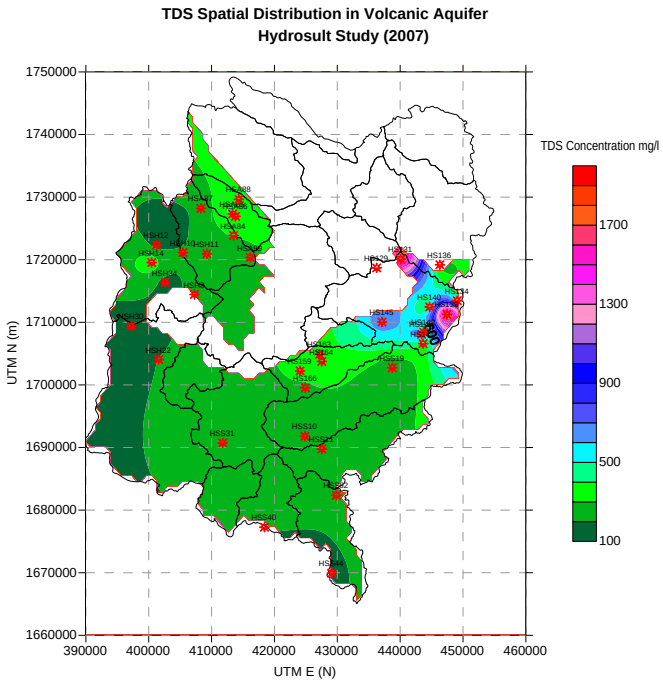

Figure 2-1 Total Dissolved Solids spatial distribution in volcanic aquifer based on Hydrosult study (2007)

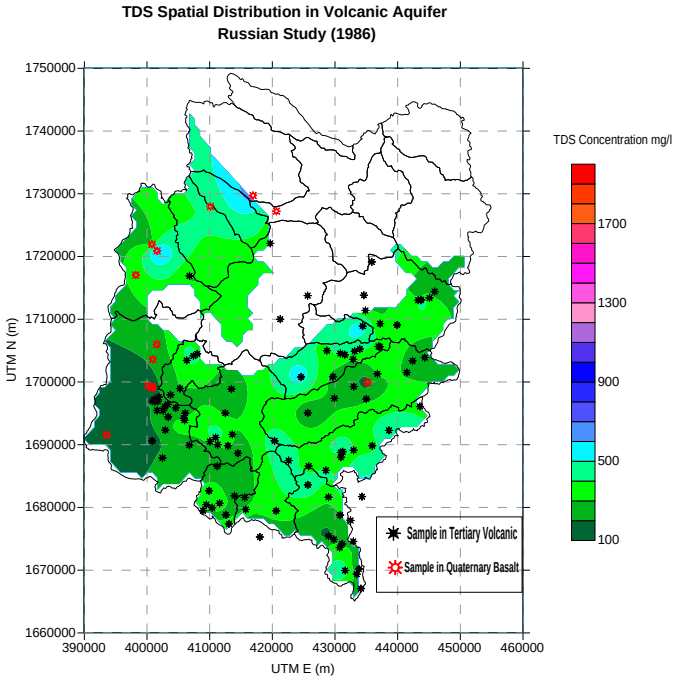

Figure 2-2 Total dissolved solids spatial distribution in volcanic aquifer based on Russian study (1986)

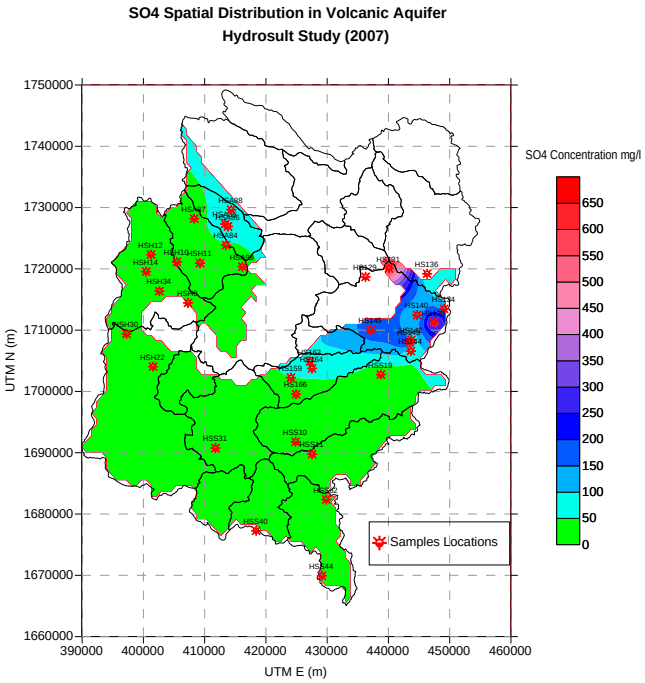

Figure 2-3 Sulfate spatial distribution in volcanic aquifer based on Hydrosult study (2007)

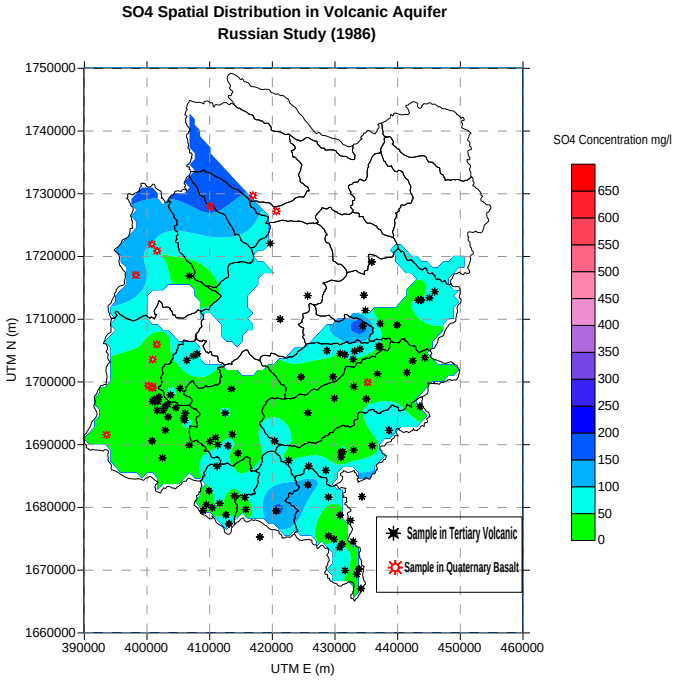

Figure 2-4 Sulfate spatial distribution in volcanic aquifer based on Russian study (1986)

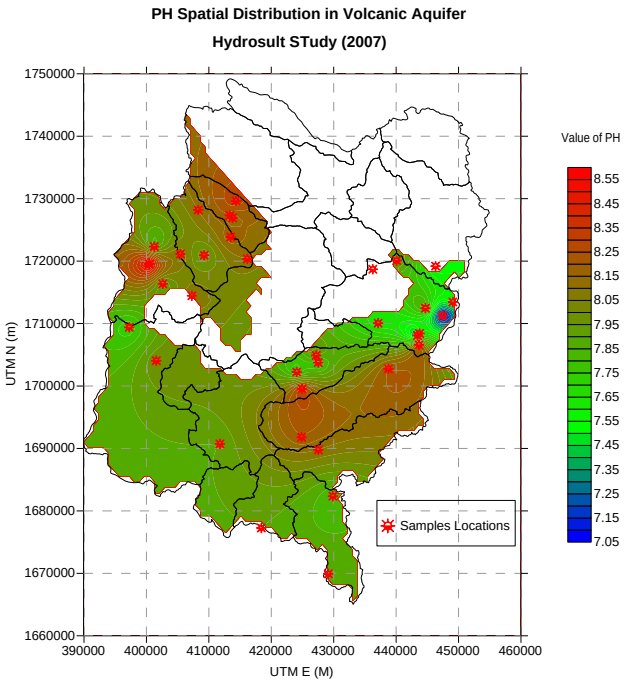

Figure 2-5 pH spatial distribution in volcanic aquifer based on Hydrosult study (2007)

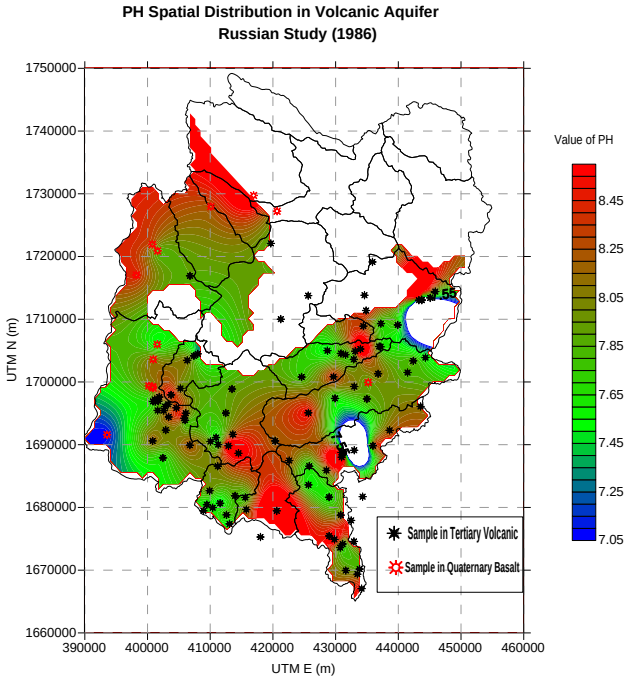

Figure 2-6 pH spatial distribution in volcanic aquifer based on Russian study (1986)

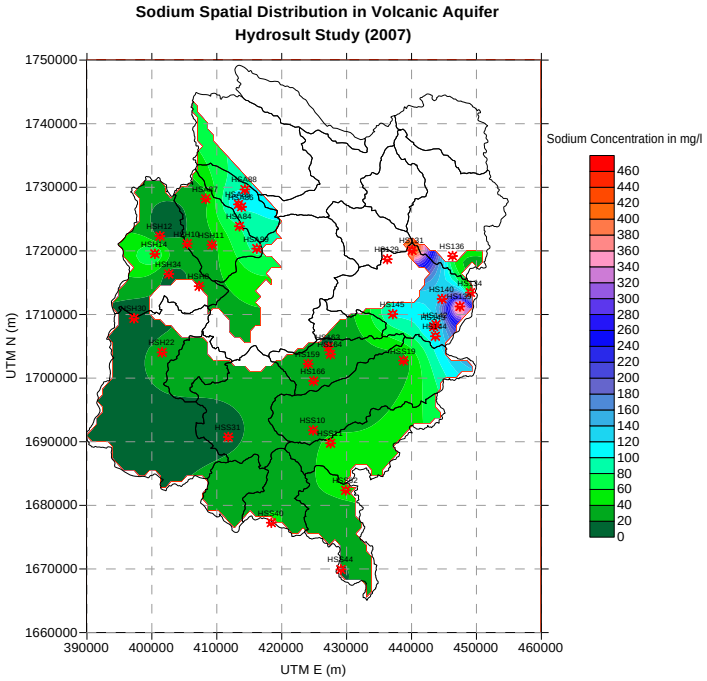

Figure 2-7 Sodium spatial distribution in volcanic aquifer based on Hydrosult study (2007)

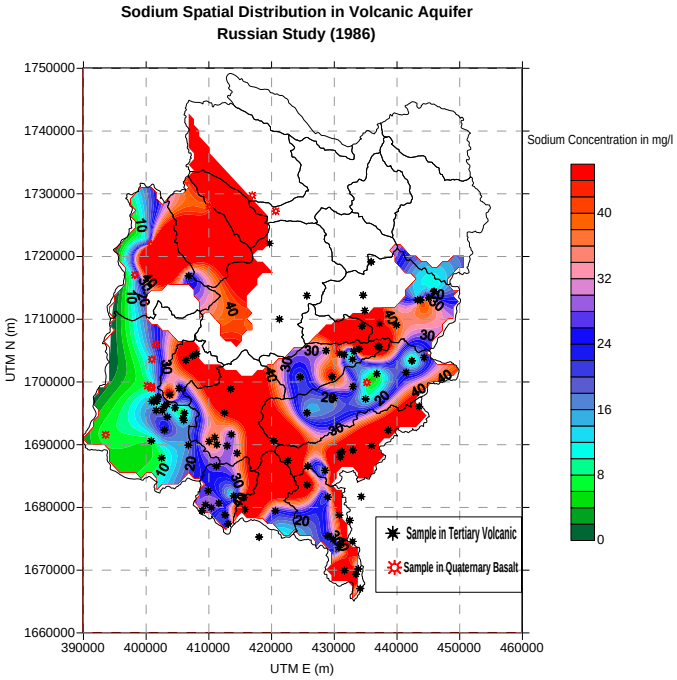

Figure 2-8 Sodium spatial distribution in volcanic aquifer based on Russian study (1986)

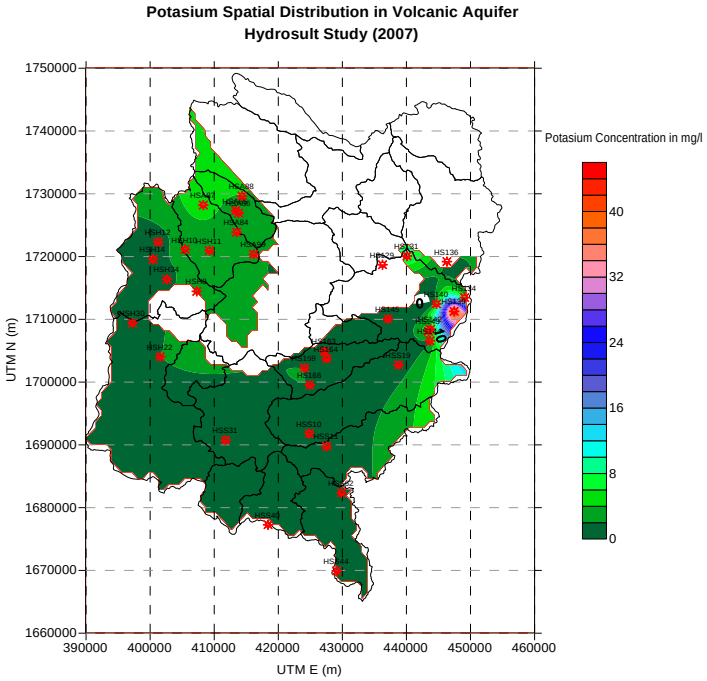

Figure 2-9 Potassium spatial distribution in volcanic aquifer based on Hydrosult study (2007)

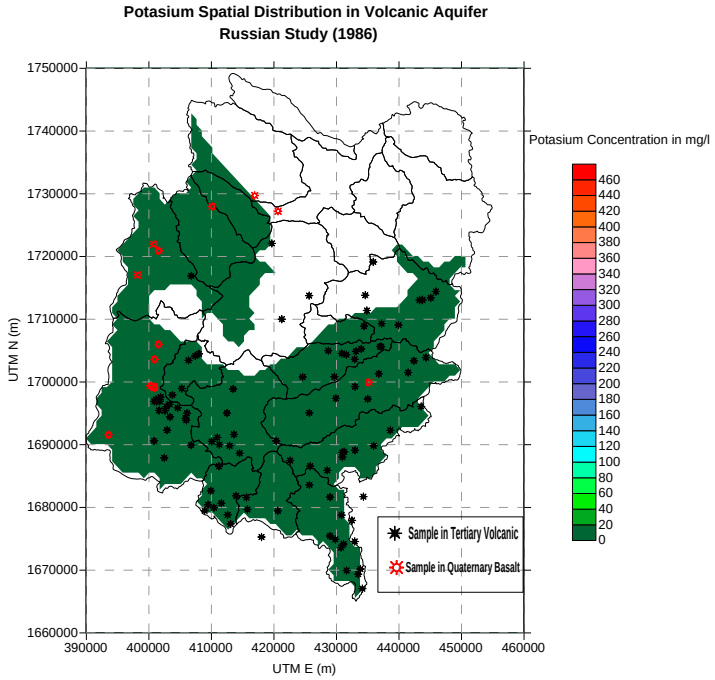

Figure 2-10 Potassium spatial distribution in volcanic aquifer based on Russian study (1986)

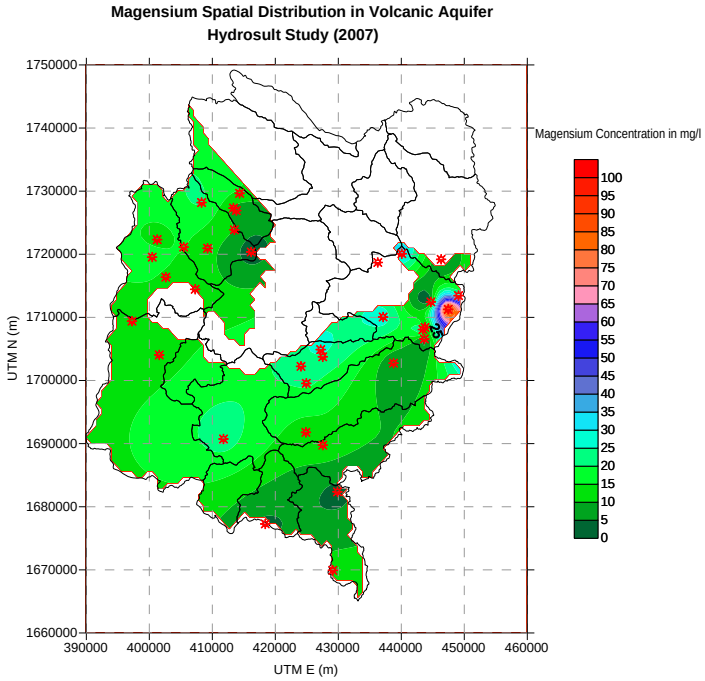

Figure 2-11 Magnesium spatial distribution in volcanic aquifer based on Hydrosult study (2007)

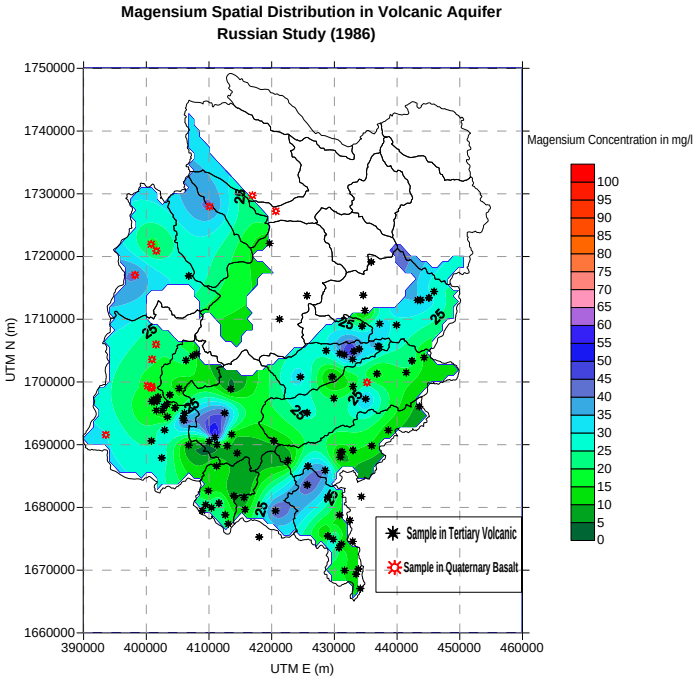

Figure 2-12 Magnesium spatial distribution in volcanic aquifer based on Russian study (1986)

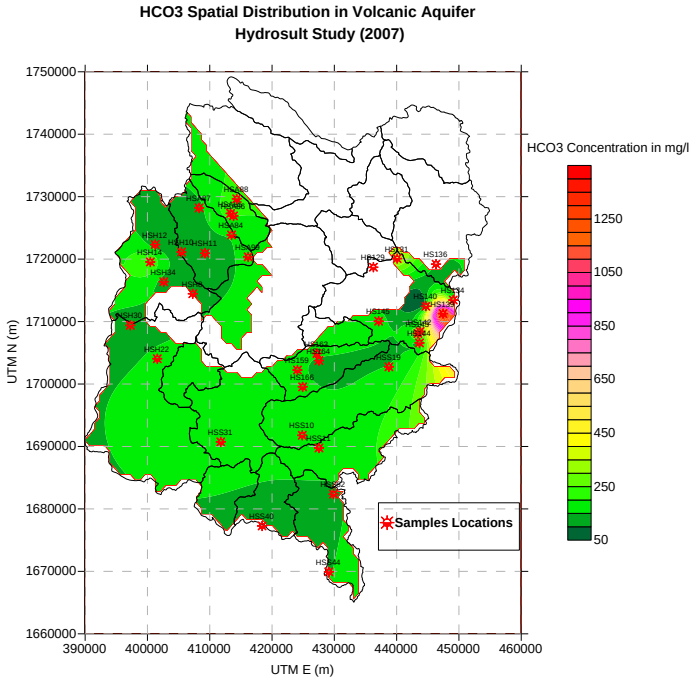

Figure 2-13 Bicarbonate spatial distribution in volcanic aquifer based on Hydrosult study (2007)

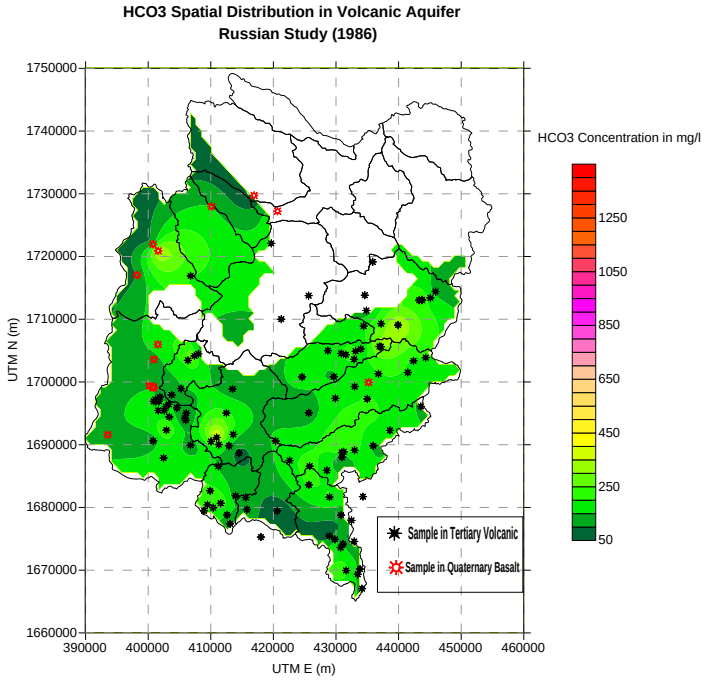

Figure 2-14 Bicarbonate spatial distribution in volcanic aquifer based on Russian study (1986)

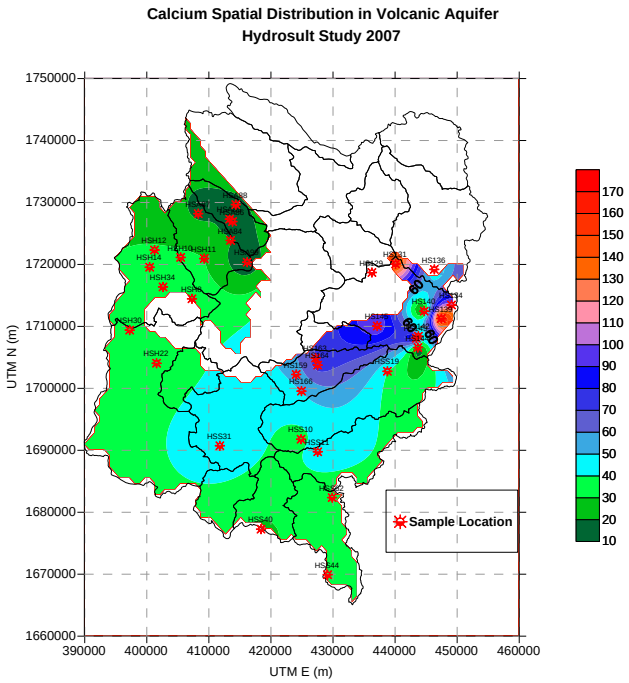

Figure 2-15 Calcium spatial distribution in volcanic aquifer based on Hydrosult study (2007)

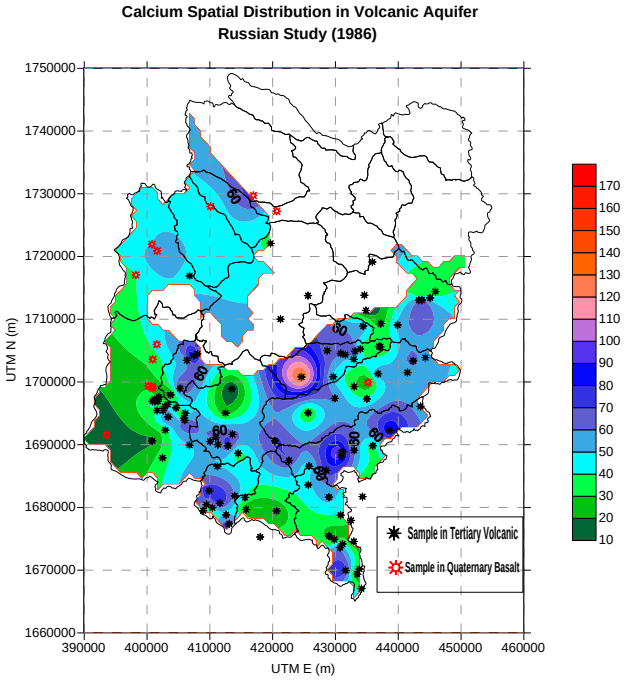

Figure 2-16 Calcium spatial distribution in volcanic aquifer based on Russian study (1986)

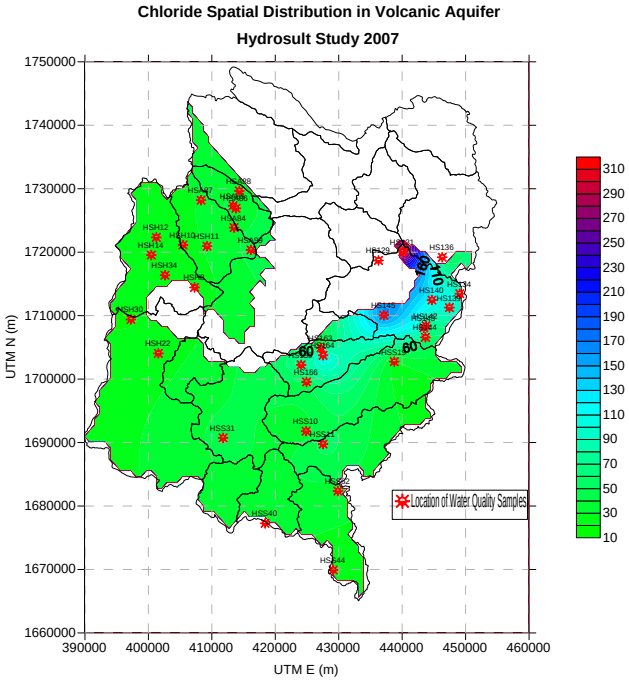

Figure 2-17 Chloride spatial distribution in volcanic aquifer based on Hydrosult study (2007)

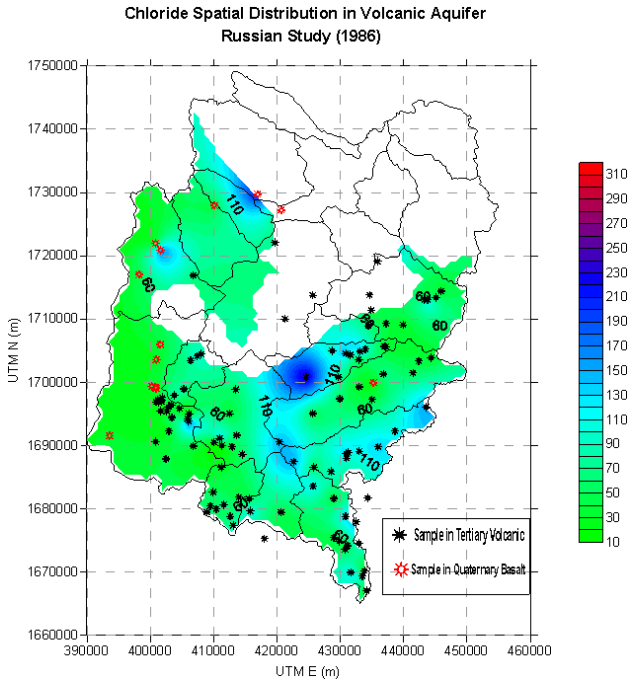

Figure 2-18 Chloride spatial distribution in volcanic aquifer based on Russian study (1986)

2.4 Comparison of Water Quality between 1986 and 2007 for the Sandstone Aquifer

2.4.1 Comparison of TDS concentration between 1986 and 2007 for the sandstone aquifer

Figure 54 and Figure 53 present the spatial distribution of total dissolved solids (in mg/L) for the 1986 study and 2007 study, respectively. In the 1986 study, the highest value of TDS was found to be in the range of 1000 mg/L at Wadi Iqbal in the north-eastern part of the Sana'a Basin and in some parts of Wadi Al-Sirr and Wadi Thomaa. TDS concentrations in the rest of the aquifer were less than 500 mg/L. The lowest values occurred at locations such as Wadi Asir, Wadi Khulaga, and the eastern part of Wadi Iqbal, with values in the range of 100 mg/L. Thus, TDS concentrations were considered relatively low and were lower than the desirable permissible limit for Yemen which is 600 mg/L in many locations.

In the 2007 study, as shown in Figure 53, the TDS concentration was relatively low for 90% of the basin area. The entire aquifer starting from Wadi Iqbal and running counterclockwise up to Wadi Asir has a relatively low value that varies between 100 mg/L and 500 mg/L. The highest TDS concentration was found to be in the range of 2000 mg/L at Bani Rassam. This high concentration is also found in Wadi Thomaa and Wadi Al-Sirr. Comparing concentration changes over the 21 years between studies shows that TDS levels have improved in the eastern part of the wadi (from 1000 mg/L to about 400 mg/L in Wadi Iqbal, for example). However, overall water quality in terms of TDS concentration has deteriorated since the high concentrations observed in 1986 have spread to a larger area in Wadi Al-Sirr and Wadi Thomaa.

2.4.2 Comparison of sulfate spatial distribution between 1986 and 2007 for the sandstone aquifer

Figure 56 presents the spatial distribution of sulfate in the 1986 mission. As shown in this Figure, about 98% of the basin had a relatively low concentration of sulfate at that time, with values less than 200 mg/L. The highest concentration was at the intersection of Wadi Zahr, Wadi Iqbal and Wadi Bani Hawat. The desirable sulfate concentration in drinking water is 200 mg/L, while the maximum permissible limit for sulfate concentration in drinking water is 600 mg/L according to the Yemeni water quality standards.

Figure 55 presents the spatial distribution of sulfate for the 2007 mission. As shown in this figure, it can be concluded that aquifer's sulfate concentration has significantly been reduced. In more that 95% of the basin area, the concentration has been reduced to less than 100 mg/L. On the other hand, sulfate concentration reaches 1100 mg/L at Bani Rassam. This value is higher than the maximum permissible limit for Yemeni drinking water.

2.4.3 Comparison of pH spatial distribution between 1986 and 2007 for the sandstone aquifer

Figure 58 presents the spatial distribution of pH in the sandstone aquifer during the 1986 mission. The lowest value of pH was found to be 7.20, while the highest value was 8.0. This elevated pH value was observed in several wadis where the sandstone is outcropped, such as Wadi Iqbal, Wadi Hamadan, Wadi Al-Foros and Wadi Mawrid. However, there are some areas in Wadi Zahr where the pH was found to be 7.7. The pH value in the eastern part of the sandstone aquifer was found to be around 7.7. The desirable pH range for Yemeni drinking water is between 6.5 and 8.5.

Figure 57 presents the spatial distribution of pH in the sandstone aquifer as found by the 2007 mission. The pH values in this case varied between 7.2 and 7.9. On the other hand, when comparing the 2007 map to the 1986 map, it can be observed that there exists considerable variation in the pH distribution found by the two missions. This variation did not however significantly affect the water quality of the sandstone aquifer. Explain?

2.4.4 Comparison of sodium spatial distribution between 1986 and 2007 for the sandstone aquifer

Figure 60 presents the spatial distribution of sodium in the sandstone aquifer based on data from the 1986 mission. The entire sandstone aquifer had a value between 20 and 105 mg/L, which is considered a relatively low value compared to the standard for drinking water, which is 200 mg/L. The highest concentrations were found in Wadi Iqbal and Wadi Zahr, and the lowest concentrations were found in Wadi Al-Sirr, Wadi Bani Hawat and Wadi Mawrid. Sodium concentration within the remaining areas of the sandstone outcrop was in the range of 50 to 80 mg/L. Figure 59 presents the spatial distribution of sodium in the 2007 mission. It can be observed that sodium concentrations have not changed significantly since the 1986 mission. The concentrations remain relatively high, from 110 mg/L in Wadi Zahr and Wadi Iqbal in the West, decreasing gradually to a value of 10 mg/L at Wadi Asir. Also, sodium concentrations reach 120 mg/L at Bani Rassam. The maximum permissible limit for sodium according to Yemeni standards is 400 mg/L, thus the concentration of the entire sandstone aquifer outcrop is lower than the permissible limit.

2.4.5 Comparison of magnesium spatial distribution between 1986 and 2007 for the sandstone aquifer

Figure 64 presents the spatial distribution of magnesium in the sandstone aquifer based on data from the 1986 mission. Magnesium concentrations varied from 5 mg/L to 50 mg/L. The desirable limit for magnesium in drinking water is 30 mg/L. In Wadi Al-Sirr the highest concentration of magnesium found was 55 mg/L. Magnesium concentrations throughout most of the sandstone outcrop were found to be below the Yemeni standards.

Figure 63 presents the spatial distribution of magnesium in the sandstone aquifer in 2007. As shown in this figure, the concentration throughout the aquifer is relatively low, in the range of 10 mg/L. Thus, comparing the spatial distribution of magnesium between the 1986 and 2007 missions indicates that magnesium concentrations have significantly decreased. The average magnesium concentration in 1986 was 50 mg/L, while in 2007 the average concentration was below 10 mg/L.

2.4.6 Comparison of potassium spatial distribution between 1986 and 2007 for the sandstone aquifer

Figure 62 presents the spatial distribution of potassium in the sandstone aquifer in 1986. Most of the aquifer had a value below 5 mg/L at that time. The highest concentration occurred at Wadi Al-Sirr, with a value of 6 mg/L. The permissible limit of potassium in drinking water is 12 mg/L.

Figure 61 shows the spatial distribution of potassium within the sandstone aquifer based on data from the 2007 mission. A comparison indicates that the potassium concentration has not changed significantly since the 1986 mission except at the intersection of Wadi Kuluqah and Wadi Thomaa in Bani Rassam, where the highest concentration occurred, with a value of 11 mg/L. Even this did not exceed the maximum limit of 12 mg/L, so it can be concluded that the entire sandstone outcrop is lower than the maximum permissible limit.

2.4.7 Comparison of bicarbonate spatial distribution between 1986 and 2007 for the sandstone aquifer

Figure 66 presents the spatial distribution of bicarbonates in the sandstone aquifer based on data from the 1986 mission. The entire aquifer had a maximum value of 330 mg/L. The lowest desirable limit of bicarbonates in drinking water quality is 150 mg/L while the maximum permissible limit is 500 mg/L. Thus, in 1986, the bicarbonate concentration was within Yemeni standards. The highest concentrations were found in some parts of Wadi Al-Sirr.

Figure 65 presents the spatial distribution of bicarbonates within the sandstone aquifer in 2007. The entire sandstone aquifer has levels below 200 mg/L, except the location at Bani Rassam where bicarbonate was in the range of 300 mg/L. Thus, it can be concluded that bicarbonate concentrations did not vary significantly between 1986 and 2007 except at Bani Rasam, where the concentration is 1.5 times higher than in 1986.

2.4.8 Comparison of calcium spatial distribution between 1986 and 2007 for the sandstone aquifer

Figure 68 presents the spatial distribution of calcium in the sandstone basin in 1986. Calcium concentrations had a maximum value of 110 mg/L, which appeared only at the intersection of Wadi Al-Sirr, Wadi Khulagah and Wadi Thomaa. The lowest desirable limit of calcium based on the Yemen standards is 75 mg/L while the maximum permissible limit is 200 mg/L. Calcium concentrations throughout the sandstone aquifer were within standard limits at the time of the 1986 mission.

Figure 67 shows calcium distribution in the sandstone basin in 2007. It can be seen that the calcium concentration in the eastern part of the basin is lower than that encountered during the 1986 mission and reaches a value of below 15 mg/L. This low concentration is found in Wadi Iqbal, Wadi Zahr, Wadi Mawrid and Wadi Bani Hawat. From the area within Wadi Al-Foros, the calcium concentration starts to increase in a counterclockwise direction until it reaches its highest value at Bani Rassam, with a value of 300 mg/L. This value is 1.5 times the maximum permissible limit of calcium allowed by Yemeni standards.

2.4.9 Comparison of chloride spatial distribution between 1986 and 2007 for the sandstone aquifer

Figure 70 presents the spatial distribution of chloride in the sandstone aquifer based on data from the 1986 mission. The highest chloride concentration was in the range of 210 mg/L, occurring at the intersection of Wadi Al-Sirr and Wadi Khulagah. The lowest desirable limit of chloride is 200 mg/L while the maximum permissible limit is 600 mg/L. Thus, the chloride concentrations found during the 1986 mission were considered to be within the acceptable limits.

Figure 69 presents the spatial distribution of chloride for the 2007 mission. Compared to the values from the 1986 mission, chloride concentrations have decreased in most of the sandstone basin. The highest value occurs at Wadi Al-Sirr, where the concentration has increased to 220 mg/L. However, this value remains within the maximum permissible limit for Yemen drinking water standards.

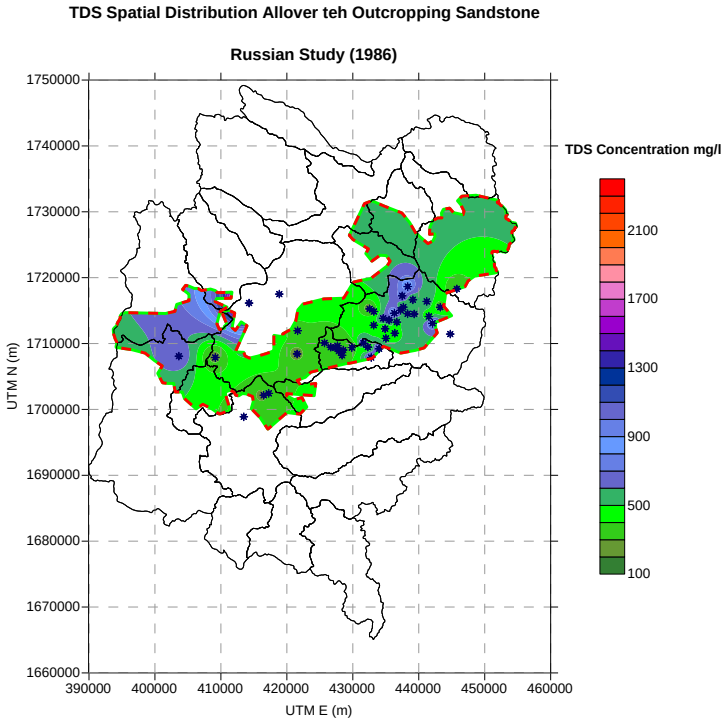

Figure 2-19 TDS spatial distribution in sandstone aquifer based on Hydrosult study (2007)

Figure 2-20 TDS spatial distribution in volcanic aquifer based on Russian study (1986)

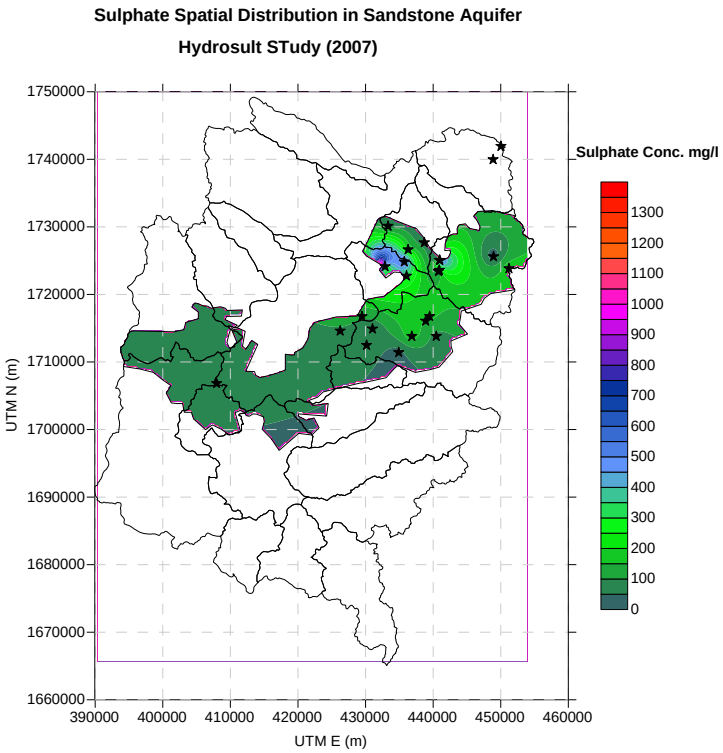

Figure 2-21 Sulfate spatial distribution in sandstone aquifer based on Hydrosult study (2007)

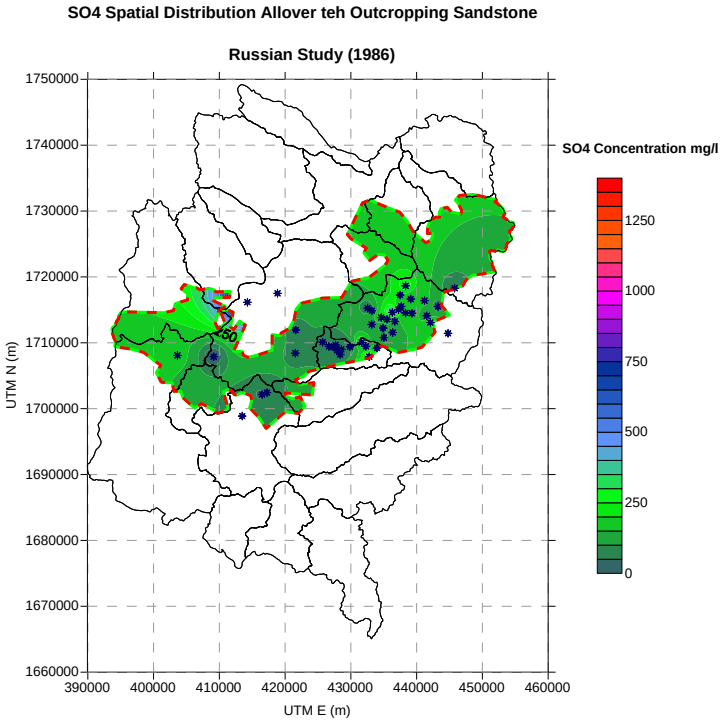

Figure 2-22 Sulfate spatial distribution in volcanic aquifer based on Russian study (1986)

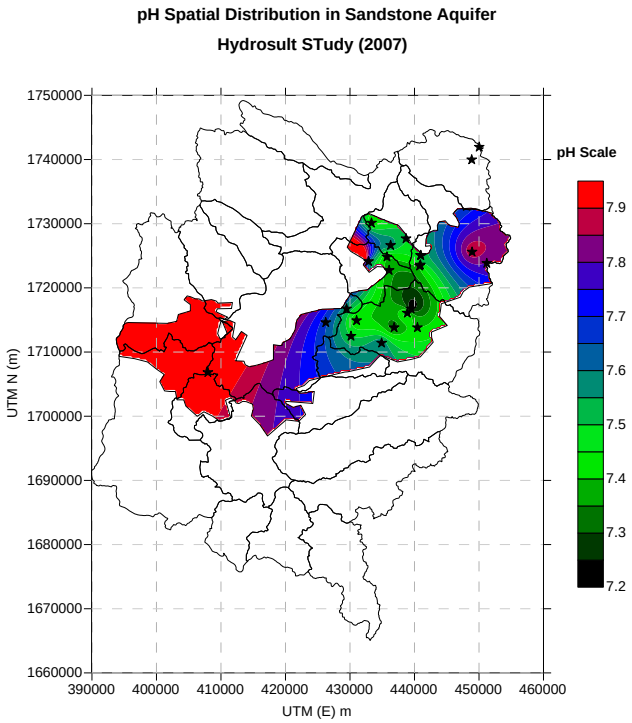

Figure 2-23 pH spatial distribution in sandstone aquifer based on Hydrosult study (2007)

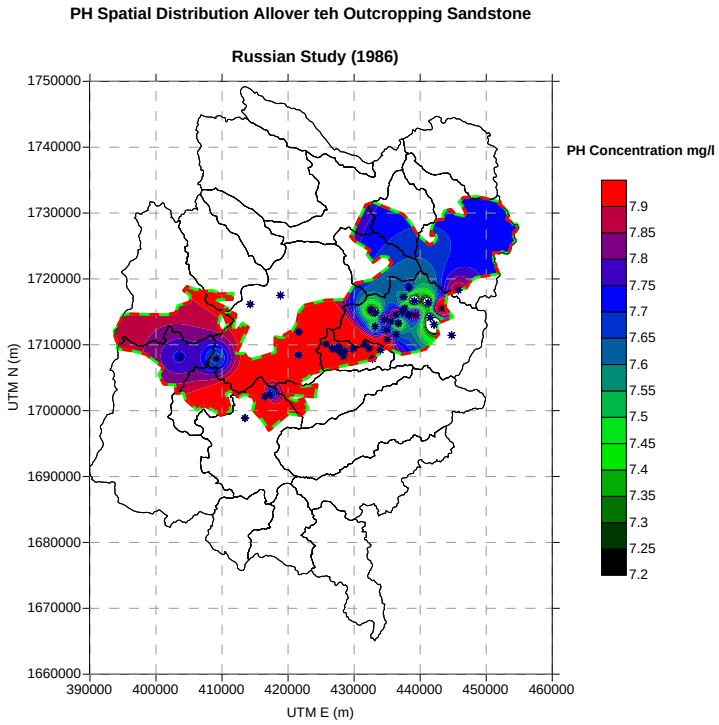

Figure 2-24 pH spatial distribution in sandstone aquifer based on Russian study (1986)

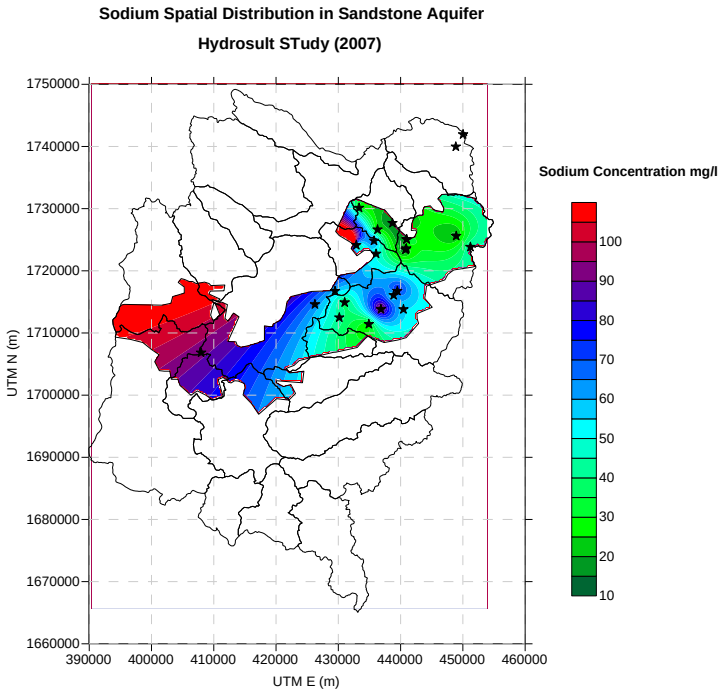

Figure 2-25 Sodium spatial distribution in sandstone aquifer based on Hydrosult study (2007)

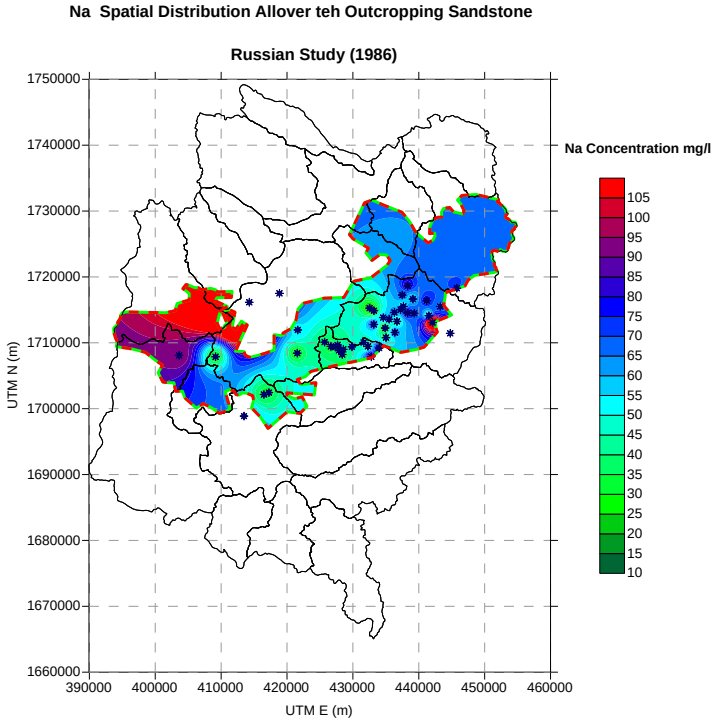

Figure 2-26 Sodium spatial distribution in sandstone aquifer based on Russian study (1986)

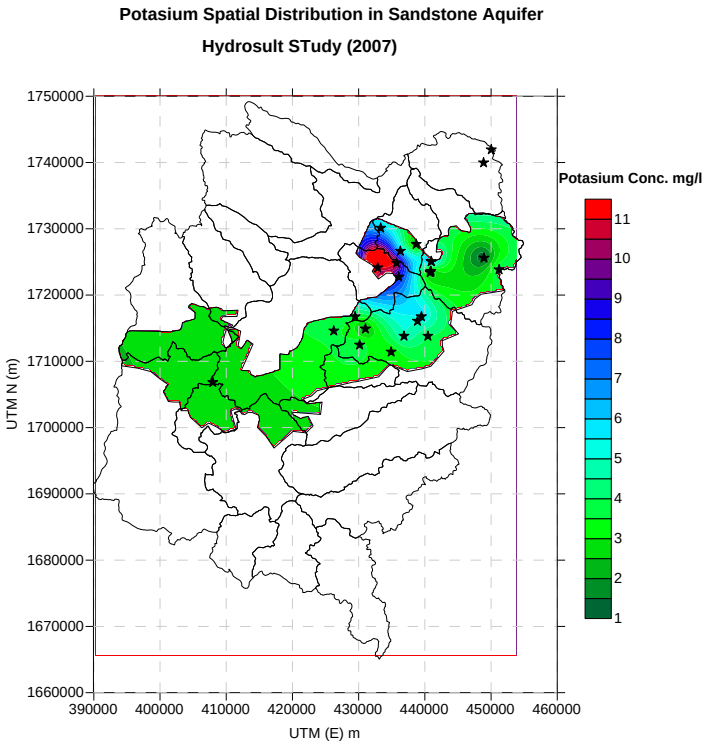

Figure 2-27 Potassium spatial distribution in sandstone aquifer based on Hydrosult study (2007)

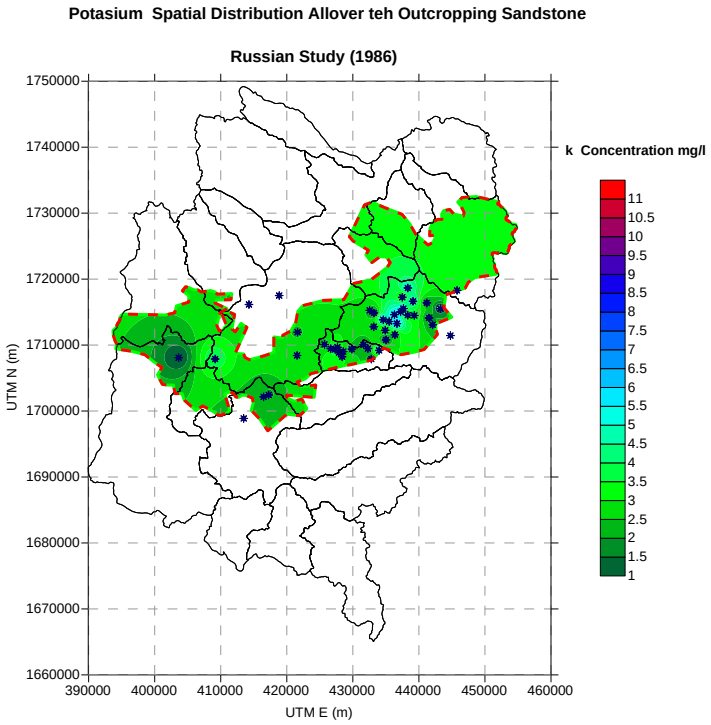

Figure 2-28 Potassium spatial distribution in sandstone aquifer based on Russian study (1986)

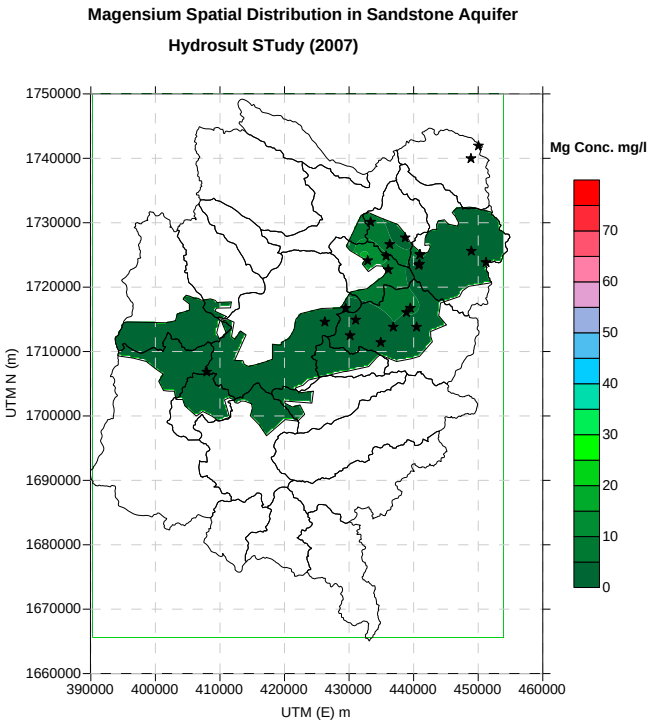

Figure 2-29 Magnesium spatial distribution in sandstone aquifer based on Hydrosult study (2007)

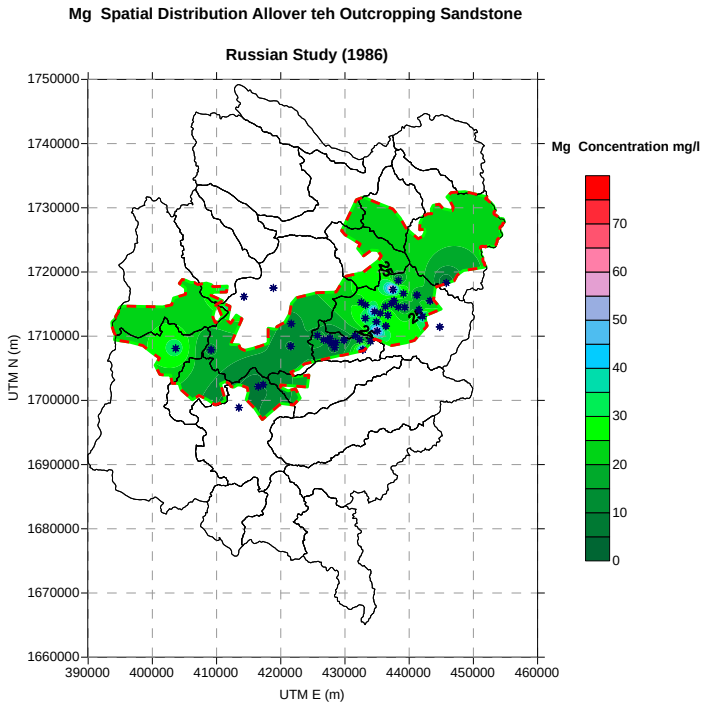

Figure 2-30 Magnesium spatial distribution in sandstone aquifer based on Russian study (1986)

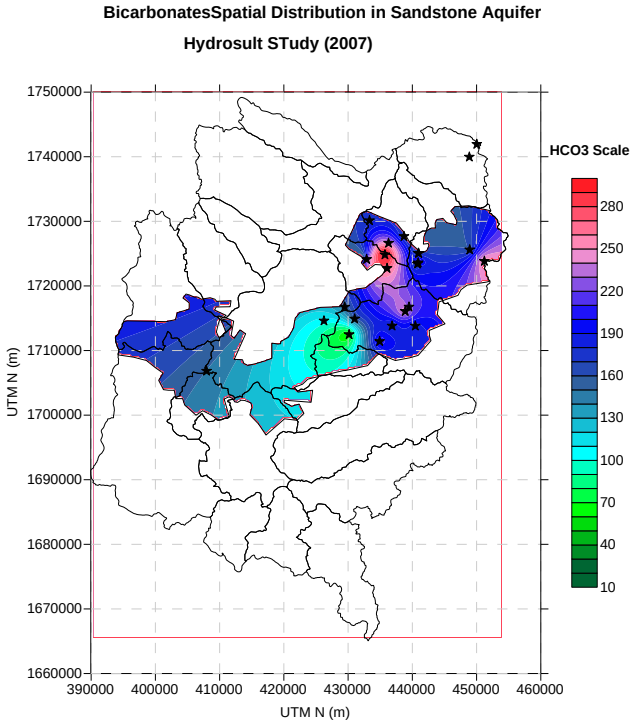

Figure 2-31 Bicarbonate spatial distribution in sandstone aquifer based on Hydrosult study (2007)

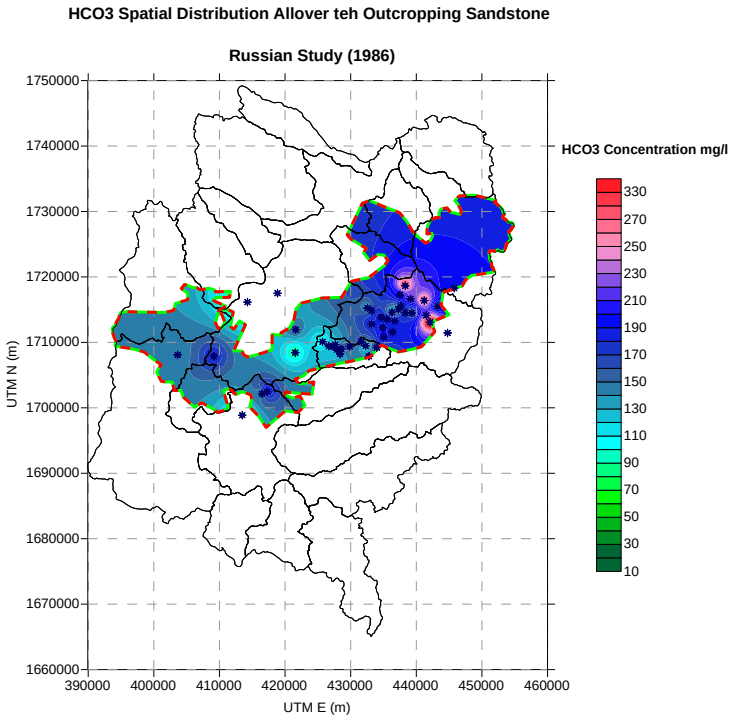

Figure 2-32 Bicarbonate spatial distribution in sandstone aquifer based on Russian study (1986)

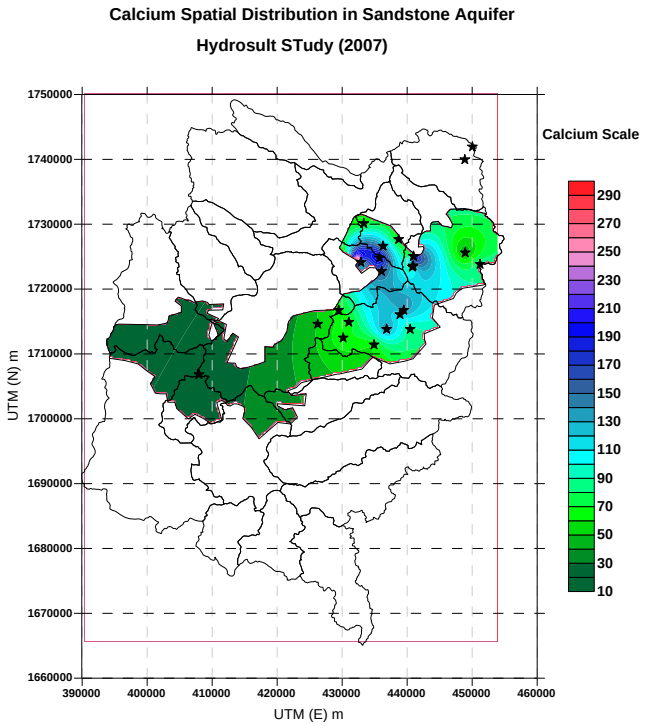

Figure 2-33 Calcium spatial distribution in sandstone aquifer based on Hydrosult study (2007)

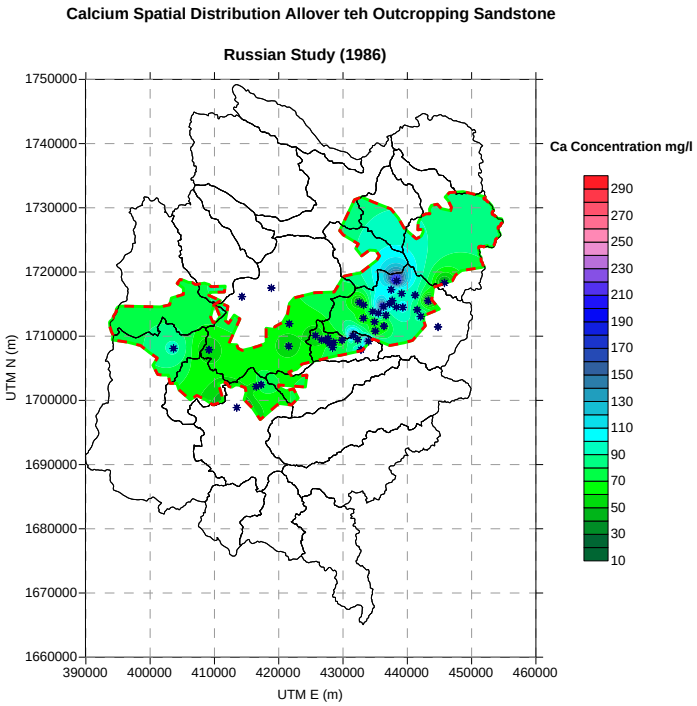

Figure 2-34 Calcium spatial distribution in sandstone aquifer based on Russian study (1986)

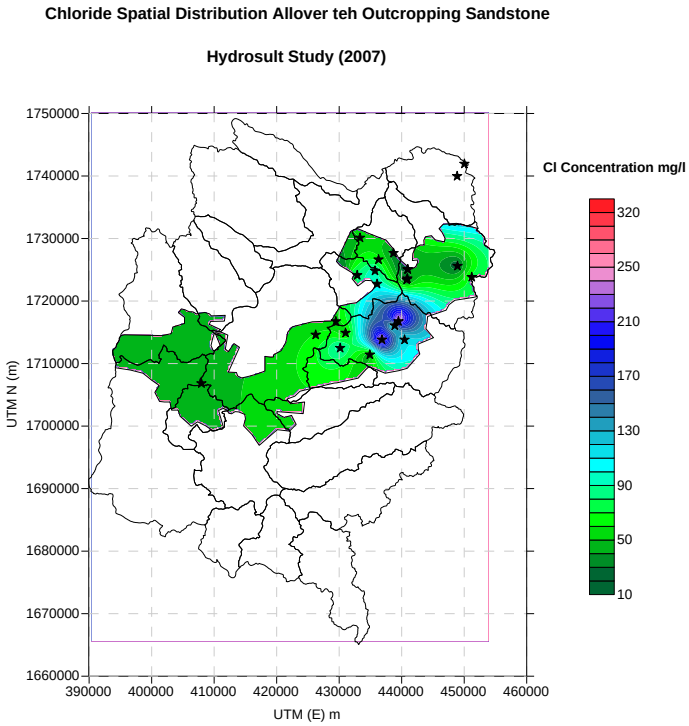

Figure 2-35 Chloride spatial distribution in sandstone aquifer based on Hydrosult study (2007)

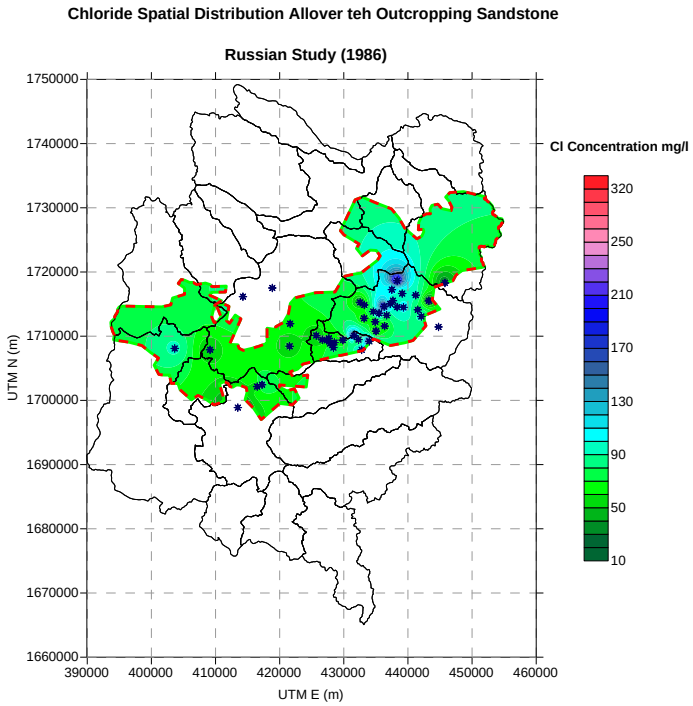

Figure 2-36 Chloride spatial distribution in sandstone aquifer based on Russian study (1986)

Chapter 3. DEVELOPMENT OF VULNERABILITY MAPS FOR THE SANA'A BASIN

3.1 Introduction

Groundwater vulnerability maps have become a standard tool for protecting groundwater resources from pollution. They are especially valuable in the decision-making process related to land use planning. Land use planners often have little experience or expertise at hand to decide which land uses and activities should be allowed in order to avoid negative impacts on the quality of groundwater resources. Also, the design of a groundwater quality network for large basins relies on the development of a vulnerability map through which the most probable locations for pollution can be determined. Groundwater vulnerability maps have been widely used over the past 30 years. There are a number of methods used worldwide (Verba and Saporozec 1994, Margane et al. 1997) but, to date, there is still no generally-accepted standard mapping method. This is mainly due to the fact that the hydrogeological conditions and the availability of data can be very different from one area to another. There are methods which require knowledge of the spatial distribution of up to ten parameters and thus depend on the availability of very detailed data. On the other hand, there are also methods which require the input of only two or three parameters. Such methods may be applied in areas where data availability is low. Many of these methods are, however, rather simple and fail to provide appropriate results.

In all these methods, the vulnerability of an aquifer is classified according to the travel time of a drop of water descending from the land surface to the aquifer (percolation time). This flow will be very different in porous rocks as compared to hard rocks, where flow preferentially follows fractures and cavities. In this respect, karst aquifers play an important role since infiltration may be highly concentrated in certain areas and travel time from the land surface to the aquifer may be extremely short.

3.2 Definition of Groundwater Vulnerability

The term, "vulnerability of groundwater to contamination" was first used by Margat (1968). The term "groundwater vulnerability" is used as the opposite of "natural protection against contamination". Although many efforts have been made to reach a common understanding of groundwater vulnerability, different authors still use it in differing senses. Foster and Hirata (1988) defined "***Aquifer Pollution Vulnerability***" as the "*intrinsic characteristics which determine the sensitivity of various parts of an aquifer to being adversely affected by an imposed contaminant load*". They describe "***Groundwater Pollution Risk***" as "*the interaction between the natural vulnerability of an aquifer, and the pollution loading that is, or will be, applied on the subsurface environment as a result of human activity*". The US EPA (1993) distinguishes between "***Aquifer Sensitivity***" and "***Groundwater Vulnerability***". Although these definitions are more closely related to agricultural activities, they should hold true for all other activities as well. The US EPA defines "Aquifer Sensitivity" as the "*relative ease with which a contaminant applied on or near the land surface can migrate to the aquifer of interest. Aquifer sensitivity is a function of the intrinsic characteristics of the geologic materials of interest, any overlying saturated materials, and the overlying unsaturated zone. Sensitivity is not dependent on agronomic practices or pesticide characteristics*". According to US EPA "***Groundwater Vulnerability***" is "*the relative ease with which a contaminant applied on or near the land surface can migrate to the aquifer of interest under a given set of agronomic management practices, pesticide characteristics and hydrogeologic sensitivity conditions*". The Committee on Techniques for Assessing Ground Water Vulnerability of the National Research Council (1993) and Verba and Zaporozec (1994) define groundwater vulnerability as *"the tendency or likelihood for contaminants to reach (a specified position in) the groundwater system after introduction at some location above the uppermost aquifer".* In addition, distinctions are made between "***Intrinsic Vulnerability***" and "***Specific Vulnerability***". For the determination of "***Intrinsic Vulnerability***" the characteristics and distinct behavior of contaminants are not taken into consideration, whereas the term "***Specific Vulnerability***" refers to a specific contaminant, class of contaminants or a certain prevailing human activity. Vowinkel et al. *(1996)* defined vulnerability as sensitivity plus intensity, where 'intensity' is a measure of the source of contamination. In this sense, groundwater vulnerability is a function, not only of the properties of the groundwater flow system (intrinsic susceptibility), but also of the proximity of contaminant sources, characteristics of the contaminant, and other factors that could potentially increase loads of specified contaminants to the aquifer and/or their eventual delivery to a groundwater resource. In general, there are two different targets for protection, as shown in Figure 71*:* the resource (aquifer) and the source (well or spring used for water supply).

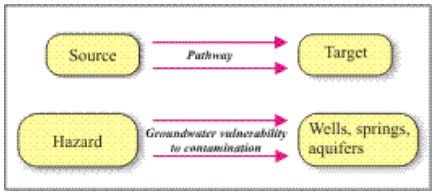

Figure 3-1 Source-Pathway-Target Model for groundwater vulnerability

The intrinsic vulnerability of groundwater is a relative, non-measurable property which is not verifiable since it depends on the attenuation and retardation properties of the sediments and rocks

overlying the aquifer, as well as on the properties of contaminants. Generally, maps of intrinsic vulnerability are closely tied to policy or management objectives, whereas specific vulnerability maps are often tied to scientific objectives and typically require additional interpretation on the part of decision makers.

3.3 Parameters determining Groundwater Vulnerability

Verba and Zaporozec (1994) list possible processes and mechanisms that could lead to an attenuation of the contaminant load in different media through which water and contaminants pass on their way to the water table (soil, unsaturated and saturated zone). The following factors determine the protective effectiveness or filtering effect of the rock and soil cover:

- mineralogical rock composition,
- rock compactness,
- degree of jointing and fracturing,
- porosity,
- content of organic matter,
- carbonate content,
- clay content,
- metal oxide content,
- pH,
- redox potential,
- cation exchange capacity (CEO),
- thickness of rock and soil cover,
- dispersion/diffusion,
- chemical complication, sorption and precipitation,
- degradation.

The behavior of chemical substances underground differs considerably from compound to compound. When assessing the specific vulnerability of a natural groundwater system, the specific behavior of each expected individual chemical substance has to be evaluated. Contaminants can be transformed by geochemical, radiological, and microbiological processes as they are transported through the various environments within the groundwater system. When mapping intrinsic vulnerability, the behavior of different pollutants is not taken into consideration. In this case, the assessment of vulnerability is based entirely on the parameters which determine the general protective effectiveness of the soil and rock cover. Such a simplification allows for the assessment of groundwater vulnerability over large areas at a relatively low cost and in a comparatively short space of time. This general assessment forms the basis of further investigations. Studies of the specific vulnerability could then be performed at a later stage in sensitive areas where groundwater pollution already exists or is expected to occur in the near future.

Soil cover often plays an important role in the attenuation process, as it leads to the retardation of contaminants and absorbable pollutants. Another factor that influences the vulnerability of groundwater resources is the way in which groundwater recharge actually takes place. This process is very much affected by different hydrogeological conditions.

3.4 Methods of Developing Vulnerability Maps

Table 4 summarizes the different approaches that can be taken for developing vulnerability maps. The COP method has been selected for developing the vulnerability maps of the Sana'a Basin,

through which useful information can be obtained in order to design a complete water quality monitoring network.

3.5 The COP method

3.5.1 Introduction to the COP method

This method was introduced by the Hydrogeology Group at the University of Malaga/Spain (VIAS et al., 2002). It is based on the following parameters:

C = Concentration of flow,

O = Overlying layers, and

P = Precipitation.

As outlined by DALY et al. (2002), the COP method may become the European approach for groundwater vulnerability mapping in karst areas, provided its application proves to be successful in the coming few years.

The COP-Index is obtained by the following equation:

$$COP - Index = (\ C\ score\ )\ x\ (\ O\ score\ )\ x\ (P\ score) \qquad \textbf{Equation 1}$$

3.5.2 Step 1: Calculation of the O Factor

The O factor takes into account the protective function of the unsaturated zone and the properties of the soil layers (Os — soil sub-factor) and unsaturated zone (OL — lithology sub-factor). Both are separately calculated and then added to obtain the O factor:

$$O = O_S + O_L \qquad \textbf{Equation 2}$$

Method	Theoretical Principle	Application	Examples
Hydrogeological Complex and Setting Methods	This group of methods assesses groundwater vulnerability by setting up classes of two or more levels of vulnerability. The classes are based on criteria found to be representative of groundwater vulnerability under certain hydrogeological conditions.	This type of mapping is mainly used for small to medium scale maps and uses basic information often available from geological, hydrogeological and topographic maps.	France, Germany
Matrix System	Matrix Systems assess groundwater vulnerability based on a selection of two or more parameters considered to be representative for a certain area. The selected parameters, such as depth to aquifer, soil leaching, groundwater recharge, or others are then grouped into classes.		

Method	Theoretical Principle	Application	Examples
Rating System	Rating Systems use many parameters and attribute fixed ranges of ratings to them according to their variation in the area. The total rating is calculated by overlaying the ratings for the different parameters and then dividing the total rating into different levels of vulnerability. The following methods can be attributed to this method:which ones?	GOD, PRZM (Pesticide Root Zone Model), GLA Method, PI-Method).	Italy, USA,
Index Methods and Analogical Relations	The index methods (IM) and analogical relations (AR) are based on mathematical standard descriptions of hydrological and hydrogeological processes (e.g. transport equations) that are analogously used to assess the groundwater vulnerability. MAGIERA (2000) describes 13 methods of this type.	N/A	N/A
Numerical Methods	Flow and transport models for the unsaturated and saturated zones are so far not being used for vulnerability mapping. Magiera (2000) describes nine examples of the application of mathematical models for specific vulnerability mapping on a medium to large scale. Those models take into account the properties of the contaminant (mostly nitrates and pesticides) and the properties of the overlying layers.	N/A	N/A
Statistical Methods	Statistical approaches provide an alternative to parametric system models and have been successfully used for specific vulnerability mapping on a small to medium scale. Statistical methods can be verified and allow for taking into account the reliability of the data.	EPIC, COP, GLA	Jordan, USA, Syria

Table 3-1 The different applied methodologies for development of vulnerability maps

Thickness and texture (mainly dependent on grain size) are used to evaluate the sub-factor Os, as shown in Figure 72. The calculation of the sub-factor OL is based on lithology and fractural (ly), thickness of each individual layer (m), and hydraulic (confined) condition (cn). The layer index is calculated by successively adding the products of the lithology and fractural values of each individual layer with its thickness:

$$Layer \quad Index = \sum l_y \; x \; m \qquad \textbf{Equation 3}$$

The corresponding value of the layer index (process IV of Figure 72) is then multiplied by the value of the hydraulic (confined) conditions to obtain sub-factor OL. The spatial distribution of the total rating for the O factor is displayed on the O map.

3.5.3 Step 2: Calculation of the C-Factor

The C-Factor represents the degree of concentration of the flow of water towards Karstic conduits that are directly connected with the saturated zone and thus indicate how the protection capacity is reduced. Differentiation is made between two distinct geological settings: the catchment area

of a swallow hole (scenario 1) and the rest of the area (scenario 2). In the first case, all water is considered to ultimately flow towards the swallow hole in the case of a Karstic system, whereas in the second case the amount of infiltration depends on the characteristics of the land surface. For scenario 1, the C-Factor is calculated based on the parameters' distance to the swallow hole (dh), distance to the sinking stream (d) and the combined effects of slope and vegetation (SV):

$$C = d_h \ x \ d_s \ x \ S_V$$ **Equation 4**

In the area where the aquifer is not recharged through a swallow hole (scenario 2), the C-Factor is calculated based on the parameters' surface features (Sf) and slope (SV) and the combined effects of slope and vegetation (SV):

$$C = S_f \ x \ S_V$$ **Equation 5**

The surface features represent geo-morphological features and the presence or absence of a protective layer that influences the character of the runoff/infiltration process. The spatial distribution of the total rating for the C-Factor is displayed on the C map.

3.5.4 Step 3: Calculation of the P Factor

This factor represents the total quantity, frequency, and duration of precipitation as well as the intensity of extreme events, which are considered to be the chief influencing factors for the quantity and rate of infiltration. The P factor is obtained by a summation of the sub-factors' quantity of precipitation (PQ) and intensity of precipitation (PI):

$$P = P_Q + P_I$$ **Equation 6**

For the evaluation of PQ, the mean precipitation of wet years with precipitation exceeding 15% of the average is used. An increasing precipitation is believed to decrease protection, arguing that the transport process in this case is more important than the dilution process. This is thought to occur up to a precipitation of 1200 mm/a, the value above which the potential contaminant becomes increasingly diluted. Calculation of the sub-factor PI is based on the assumption that higher rainfall intensity results in an increased recharge and thus a reduced protection of the groundwater resource. The "mean annual intensity" or PI is calculated from:

$$Mean\ Annual\ Intensity = \frac{Mean\ Annual\ Percipitation\ (mm)}{Mean\ Number\ of\ Rainy\ Days}$$ **Equation 7**

It is believed that intense rainfall yields more runoff to those conduits that favor concentrated infiltration and that, if rainfall intensity is low, more diffuse and slow infiltration takes place because evaporation is higher in this case. DALY et al. (2002) point out that the COP method could also be used for source protection (protection of wells/springs). In this case, the factor K is added, which describes the function of the Karstic network (similar to the K factor of EPIK).

3.5.5 Examples for Application of the COP method

The COP method was applied within the framework of the COST 620 program in the Sierra de Libar and around Torremolinos, both in the Malaga province of southern Spain (VIAS et al., 2002). Both areas represent Karstic aquifers which receive high amounts of rainfall. The Sierra de Libar area is highly Karastic, whereas the Torremolinos area is dominated by fissured limestone. A more detailed description of the method will be included in the final report of the COST 620 program, to be finalized in the first half of 2003 (personal communications, Dr. M. von Hoyer, BGR).

3.5.6 Advantages and Disadvantages of the COP method

The COP method is similar to the P1 Method with the exception that the COP method integrates the precipitation factor. The parameters needed for the COP method are relatively easy to acquire and the method is straightforward. However, due to the large number of calculation processes, the map compilation is time-consuming and requires the use of a GIS system by which these procedures can be performed. So far, there is too little experience with applications of this method to be able to judge the suitability and applicability of the method.

3.6 Development of Vulnerability Maps for the Sana'a Basin

Applying the COP method, vulnerability maps for three aquifers within the Sana'a Basin volcanic, limestone and sandstone aquifers have been developed. The following section will introduce the successive steps that were applied to develop these vulnerability maps. Because it would be too exhaustive to detail all the steps that were followed to develop each map, a brief description of each map and how it was developed will be provided as an overview. The Sana'a Basin was divided into three major groundwater aquifers: limestone, sandstone and volcanic. The alluvial aquifer vulnerability map will be added in the near future. Following the flow chart presented in Figure 3-2~~Figure 72~~, different maps were collected, analyzed and processed until the final maps were developed.

3.6.1 Process for development of the O-Factor Map (Overlying Map)

3.6.1.1 Process for development of the Os Map for Sana'a Basin

The O-Factor map is developed from two main maps: the surface soil map that describes the type and thickness of the surface soil, and the lithology map that describes the characteristics of the lithology overlying the aquifer under investigation. For development of the Os-Map, the surface soil information was collected from the Russian study conducted in 1986 as shown in Figure 73.

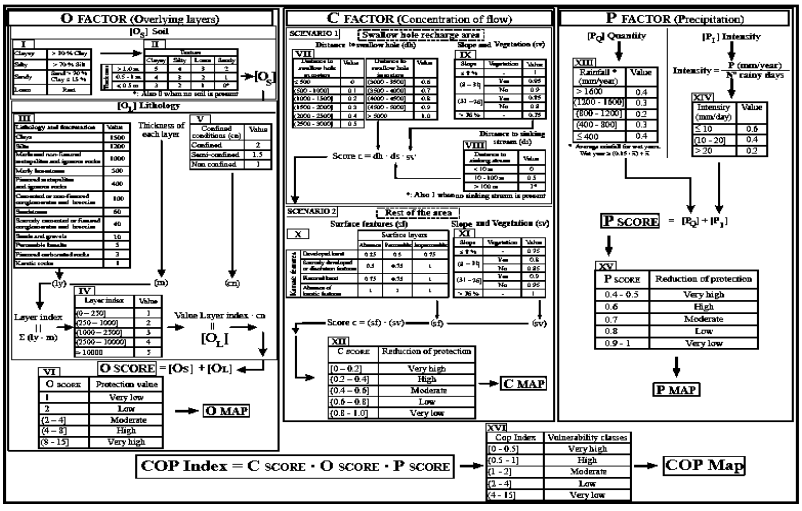

Figure 3-2 Flow Chart of the COP method (VIAS et al. 2002)

The soil column map developed by the 1986 study was also used to develop the Os map (Figure 3-4~~Figure 74~~). To make this map, soil columns were tested at different locations within the basin as

shown in Figure 3-4~~Figure 74~~. The soil samples were then analyzed to determine soil type and thickness for the first 1-1.5 meters of the surface layer. Soil column analyses at the different locations show that the surface soil mainly consists of loam or silt layers. The soil column data was then re-analyzed using GIS, and a new map that details soil layers for the entire basin was developed. Boxes I and II in the top left of Figure 3-2~~Figure 72~~ present the sequence that is followed to develop the Os map for the different aquifers.

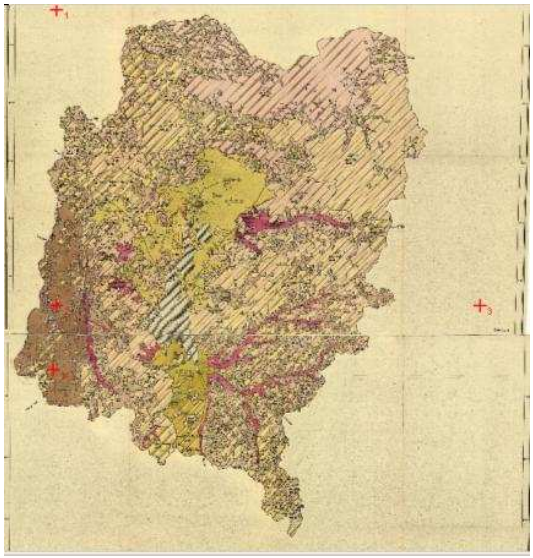

Figure 3-3 Surface soil map of the Sana'a Basin developed by the Russian study (1986)

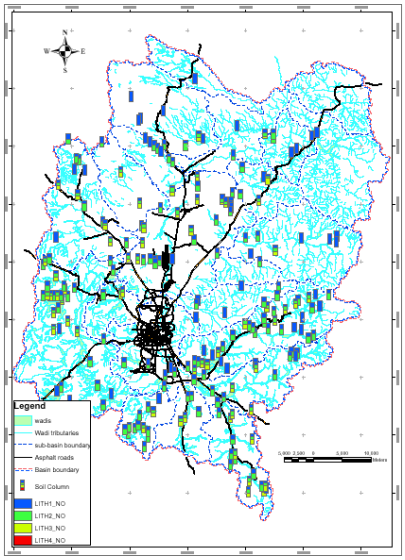

Figure 3-4 Soil column analysis within the Sana'a Basin (data was collected and analyzed by the Russian study, 1986)

3.6.1.2 Process for development of the OL Map for Sana'a Basin

Lithology analysis for the Sana'a Basin has been performed using available data from deep-well lithological analyses that were performed at different points within the Sana'a Basin. At each borehole or drilled well the successive lithological layers have been analyzed in detail to form a complete profile of the basin's lithological configuration. Figure 3-5~~Figure 75~~ introduces a sample of the available borehole data within the Sana'a Basin showing the successive layers and their thickness. The thickness of the different lithological layers was estimated from the available information for each borehole location. Numerical modeling and analysis of the available information allowed the development of a hypothetical rectangular grid of 250 meters x 250 meters for each cell. The output data were organized in GIS format, through which the successive lithology of each cell was determined by mathematical interpolation.

NAME	X_CENTER	Y_CENTER	Lyrs	ID	AV Elv	AV Dpth	LY1_LITHO	AV Frm	LY2_LITHOL	AVG2_FR	LY3_LITHOL	AVG3_FRO	LY4_LITHOL	AVG4_FROM
C20978	415125	1705375	7	2008	2229	362.5	Alluvial	62.5	Volcanic	95	Sandstone	220	Limestone	320
C35573	436125	1721875	5	1560	2244.5	16.5	Alluvial	4.8	Volcanic	10	Sandstone	3	Limestone	5.3
C38281	441625	1724875	6	1572	2162.6	28.9	Alluvial	5.9	Volcanic	25	Sandstone	14.7	Limestone	1
C39645	445375	1726375	6	1577	2151	48.8	Alluvial	5.5	Volcanic	8	Sandstone	7	Limestone	5
C41932	444375	1728875	5	1565	2102	21.5	Alluvial	8.6	Volcanic	9.5	Sandstone	8.5	Limestone	7
C42157	443875	1729125	6	1573	2098.6	30.8	Alluvial	9.7	Volcanic	30	Sandstone	40	Limestone	10
C42159	444375	1729125	6	1579	2109.2	59	Alluvial	6.7	Volcanic	3	Sandstone	13	Limestone	15
C42383	443625	1729375	6	1581	2088.9	62.8	Alluvial	9.7	Volcanic	3	Sandstone	10	Limestone	12
C42606	443875	1729625	6	1580	2103.2	62.3	Alluvial	8.3	Volcanic	0	Sandstone	4	Limestone	11
C42835	445375	1729875	6	1638	2128	150.3	Alluvial	9.2	Volcanic	8	Sandstone	37	Limestone	45
C43053	445375	1730125	5	1578	2121.9	51.8	Alluvial	8.7	Volcanic	16	Sandstone	10	Limestone	7.3
C44269	446875	1731625	6	1570	2185	25	Alluvial	5	Volcanic	3	Sandstone	12	Limestone	20
C44270	447125	1731625	7	1595	2190.7	118.8	Alluvial	10	Volcanic	20	Sandstone	25	Limestone	35
C50526	449625	1740625	6	1569	2182.7	25	Alluvial	5	Volcanic	15	Sandstone	15	Limestone	5
C50662	449625	1740875	6	1568	2180.3	24.4	Alluvial	3.5	Volcanic	4	Sandstone	6	Limestone	5
C51650	445875	1742875	5	1588	2211	99.5	Alluvial	3	Volcanic	0	Sandstone	50	Limestone	3
C20770	415125	1705125	5	538	2251.8	408.3	Alluvial	100	Sandstone	220	Limestone	320		0
C27792	423875	1713125	5	533	2212	320	Alluvial	70	Sandstone	247	Limestone	317		0
C28248	426375	1713625	5	539	2203.8	418.9	Alluvial	9	Sandstone	334	Limestone	340		0
C28468	426125	1713875	5	534	2204.5	333.3	Alluvial	22.5	Sandstone	330	Limestone	350		0
C28705	430125	1714125	5	531	2239	306.7	Alluvial	12	Sandstone	367	Limestone	367		0
C28914	427125	1714375	5	535	2211	340	Alluvial	24	Sandstone	316	Limestone	340		0
C29193	441875	1714625	5	6708	2380.8	400	Volcanic	250	Sandstone	100	Limestone	350		0
C29350	426125	1714875	5	528	2200	250	Alluvial	19	Sandstone	221	Limestone	240		0
C29568	425875	1715125	5	525	1649.3	200	Alluvial	13	Sandstone	219	Limestone	239		0
C29577	428125	1715125	5	530	2263.3	299.8	Alluvial	10.5	Sandstone	301	Limestone	310		0
C29786	425875	1715375	5	527	2199	250	Alluvial	20	Sandstone	220	Limestone	240		0

Figure 3-5 Methodology for lithological analysis of the Sana'a Basin

3.6.1.3 Process for development of the O-Map for Sana'a Basin

The value of the layer index OL can be determined from boxes numbered III, IV and V of Figure 72. From box VI, the value of the O-score can be obtained for each cell and thus a complete map for the basin (the O***score*** map) can be developed for any spatial area. The protection index value for the cell can then be calculated.

3.6.2 Process for development of the C-Factor Map (Concentration of Flow Map)

To develop the C-Factor Map, three major maps should be analyzed: the fracture density map, the vegetation cover map and the terrain slope map. The following section will present a brief description of the development process for each map.

3.6.2.1 Development of the Surface Feature Map (Sf -Map)

A fracture density map was developed based on the WEC (2002) and ItalConsult (1973) project maps for the Sana'a Basin. The map is presented in Figure 3-6~~Figure 76~~. It can be observed that, close to the basin boundaries, lineaments are present in high density relative to the middle zone. It is also clear that the northern and eastern zones have more fractures than the other areas of the basin. For the current study, the map shown in Figure 3-6~~Figure 76~~ was converted to GIS format and broken down into 250 meter x 250 meter rectangular grids. For each cell, the fracture density is calculated based on lineament lengths. Thus, the value of the Sf coefficient can be determined from box X in Figure 3-2~~Figure 72~~, according to the characteristics of the cell under investigation.

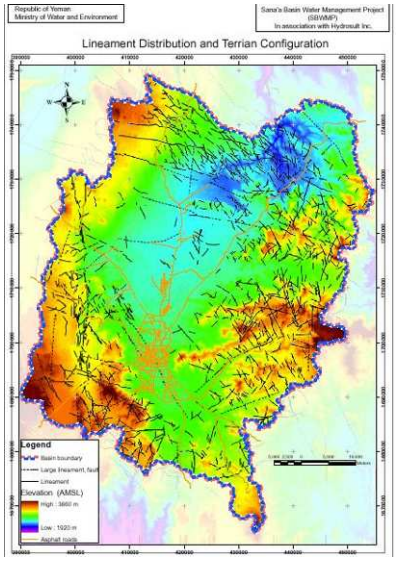

Figure 3-6 Fracture identification map for the Sana'a Basin

3.6.2.2 Development of the Slope and Vegetation Map (Sv-Map)

A terrain slope map for the entire Sana'a Basin was developed from the digital elevation map (DEM-Map) formulated by the **Shuttle Radar Topography Mission (SRTM).** The original DEM-Map was developed based on a rectangular grid of 90 meter x 90 meter cells, with an average elevation at the middle of each cell. To develop the terrain slope map, the DEM-Map was modeled on the GIS platform and the slope of each 90 m x 90 m cell was calculated. Figure 3-7~~Figure 77~~ shows the DEM-Map for the entire basin.

The second map in this category is the vegetation cover map. Based on satellite image analysis, the vegetation cover was estimated based on 250 meter x 250 meter rectangular cells. Figure 3-8~~Figure 78~~ shows a general satellite image for the entire Sana'a Basin. Based on the map shown in Figure 3-10~~Figure 80~~, the cultivated area within the 250 m x 250 m rectangular cells was calculated to estimate the vegetation cover of the entire basin. Following the flow chart presented in Figure 3-2~~Figure 72~~, the value of Sv for each cell can then be calculated. Next, the value of the C-Map coefficient can be determined (flow chart box XII) for each cell and a C-map can be developed for the entire basin.

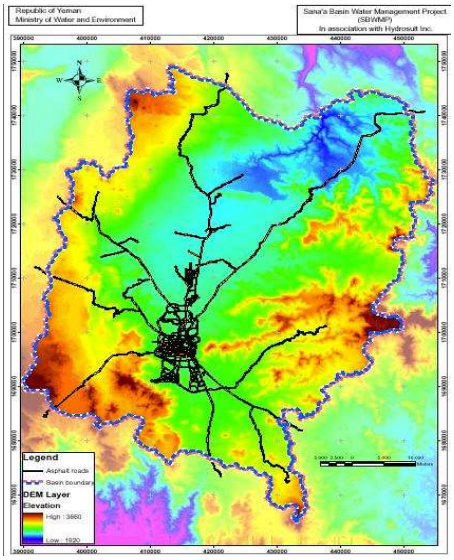

Figure 3-7 Digital elevation map for the entire Sana'a Basin. High elevations are shown in dark red while low elevations are dark blue

3.6.3 Development of the P-Factor Map (P-Map)

A map of average yearly rain intensity was developed for the Sana'a Basin based on historical data from available rainfall stations. Table 3-2~~Table 4~~ introduces a data summary for all the rainfall stations in the basin. The table also shows the period of reliable data collection for each station. The minimum continuous reading period for a station was two years, and the maximum was 23 years. An intensive analysis of the data from each station was performed in order to select the most reliable data set from which the overall average yearly rainfall can be calculated. Results showed that the minimum value for the yearly rainfall intensity within the Sana'a Basin is 180.2 mm/year while the maximum value is 424.8 mm/year. Figure 3-11~~Figure 81~~ shows a contour map indicating the average yearly rainfall intensity at different locations within the Sana'a Basin.

The number of rainy days experienced annually in the basin is also essential for the development of a P-Map. Thus, the number of rain-days at different locations within the basin was extracted from the historical data of each of the reliable rain stations listed in Table 6. Table 3-4~~Table 6~~ and Table 3-5~~Table 7~~ present the raw data from which the rain-days were calculated. Figure 3-12~~Figure 82~~ presents the rain-days contour map developed for the basin. It can be seen that the number of rainy days varies from 13 days in the eastern part of the basin to 50 days in the south-western part.

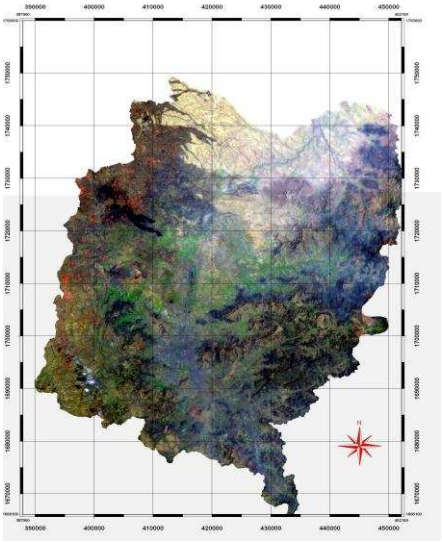

Figure 3-8 Satellite Image of the Sana'a Basin showing geological outcropping

The PQ and PI factors can be calculated based on the previously developed maps of average rainfall and number of rain-days throughout the basin. From the information presented in boxes XIII and XIV respectively, as presented in Figure 3-9 MISSING Location of the currently Operating Rainfall Stations within Sana'a Basin (stations inside the basin boundaries are marked by the red arrow)

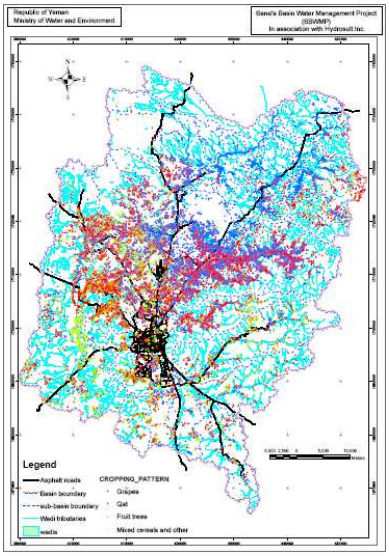

Figure 3-10 Cropping patterns within the Sana'a Basin, extracted from the satellite image (blue=grape, red=qat, green=fruit trees, yellow=cereal)

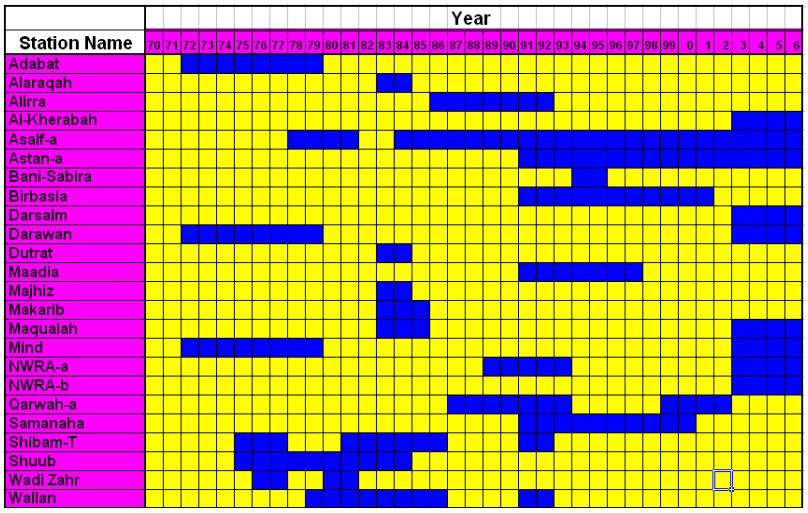

Table 3-2 Data from rainfall stations within the Sana'a Basin from 1970 to 2006 showing the recording period for each station

Ser. no.	Station Name	UTM E (m)	UTM N (m)	Average yearly rainfall (mm/year)
1	Adabat	432250	1698700	209.5
2	Asalf-a	385800	1683400	424.8
3	Astan-a	427550	1743027	221.3
4	Birbasla	444000	1729284	220.8
5	Darawan	402126	1718733	193.1
6	Maadia	442250	1737750	187.7
7	Mind	399550	1690005	279.4
8	Qarwah-a	447785	1689375	132.1
9	Samanaha	426650	1730085	180.2
10	Sana-Cama	416700	1711150	236.5
11	Shibam-T	383807	1715787	416.4
12	Shuub	417500	1701000	223.3
13	Wallan	421199	1671381	249.3
14	Sanaa Airport	410000	1710000	234.1
15	NWRA Old	414581	1701935	226.6

Table 3-3 Average yearly rainfall at the reliable rainfall stations for the period of 1970 to 2006

Station	Year	Month	Days														
			1	2	3	4	5	6	7	8	9	10	11	12	13	14	15
NWRA Branch	2002	MAY	0	0	0	0	0	0	0	0	0	0	0	0	0	0	0
NWRA Branch	2002	JUN	0	0	0	0	0	0	0	0	0	0	0	0	0	0	0
NWRA Branch	2002	JUL	0	0	0	0	0	0	0	0	0	0	0	0	0	0	0
NWRA Branch	2002	AUG	15	0	0	0	0	0	0	0.25	0.5	0	0	0	0	0	0
NWRA Branch	2002	SEP	5.5	10.8	3.5	1.25	0	0	0	0	0	0	0	0	0	0.25	0
NWRA Branch	2002	OCT	0	0	0	0	1.5	0	0	0	0	0	0	0	0	0	0
NWRA Branch	2002	NOV	0	0	0	0	0	0	0	0	0	0	0	0	0	0	0
NWRA Branch	2002	DEC	0	0	0	0	0	0	0	0	0	0	0	0	0	0	0
NWRA Branch	2003	JAN	0	0	0	0	0	0	0	0	0	0	0	0	0	0	0
NWRA Branch	2003	FEB	0	0	0	0	0	0	0	0	0	0	0	0	0	0	0
NWRA Branch	2003	MAR	0	0	0	0	0	0	0	0	0	0	0	0	0	0	0
NWRA Branch	2003	APR	0	5	5	5.25	4.75	19	4	0.5	1.25	3	0	0	7.75	12.5	9
NWRA Branch	2003	MAY	0	0	0	0	0	0	0	0	0	0	0	0	0	0	0
NWRA Branch	2003	JUN	0	0	0	0	0	0	0	0	0	0	0	0	0	0	0
NWRA Branch	2003	JUL	0	0	0	0	0	0	0	0	0	0	0	0	2	0.25	0.25
NWRA Branch	2003	AUG	0	0	0	0.25	1.25	27.8	45.5	6.75	1.25	2	21.3	1.75	0.5	1	0
NWRA Branch	2003	SEP	0	0	0	0	0	0	0	0	0	0	0	0	0	0	0
NWRA Branch	2003	OCT	0	0	0	0	0	0	0	0	0	0	0	0	0	0	0
NWRA Branch	2003	NOV	0	0	0	0	0	0	0	0	0	0	0	0	0	0	0

Table 3-4 Count of rain-days (red fill), at NWRA-Branch station from May 2002 to November 2003 for the first 15 days of each month

Station	Year	Month	Days														
			16	17	18	19	20	21	22	23	24	25	26	27	28	29	30	31
NWRA Branch	2002	MAY	0	0	0	0	0	0	0	0	0	0	0	0	0	0	0	0
NWRA Branch	2002	JUN	0	0	0	0	0	0	0	0	0	0	0	0	0	0	0	
NWRA Branch	2002	JUL	0	0	0	0	0	0	0	0	0	0	0	0	0	0	0	7.75
NWRA Branch	2002	AUG	0	0	0	0	0	0	0	1.25	0.5	0	0	0.5	1	0	0.5	0.25
NWRA Branch	2002	SEP	0	0	0	0	0	0	0	0	0	0	0	0	0.5	0	0	
NWRA Branch	2002	OCT	0	0	0	0	0	0	0	0	0	0	0	0	0	0	0	0
NWRA Branch	2002	NOV	0	0	0	0	0	0	0	0	0	0	0	0	0	0	0	
NWRA Branch	2002	DEC	0	0	0	0.25	0.5	0	0	0	0.25	0	0	0	0	0	0	0
NWRA Branch	2003	JAN	0	0	0	0	0	0	0	0.75	0	0	0	0	0	0.25	3.75	0
NWRA Branch	2003	FEB	0	0	0	0	0	2	0	5.75	7.5	0	6.5	0.25	2.25			
NWRA Branch	2003	MAR	0	0	0	0	0	0	6.75	0	0	0.75	0.75	2.25	0.25	4.5	0	0.5
NWRA Branch	2003	APR	3.25	0	1.75	0.25	0	0.25	2	21.3	0	0	0	0	0	0	0	
NWRA Branch	2003	MAY	0	0	0	0	0	0	0	0	0	0	0	0	0	0	0	0
NWRA Branch	2003	JUN	0.25	0	0	0.75	6	1.5	1	0	0	0	0	0	0	0	0.25	
NWRA Branch	2003	JUL	3	0	0	0	0	0	0	0	0	0	0	0	0	0	1.5	1.5
NWRA Branch	2003	AUG	0	0	0	4	3.5	0	0.75	6	0.25	0	0	0	0	0	0	0
NWRA Branch	2003	SEP	0	0	0	0	0	0	0	0	0	0	0	0	0	0	0	
NWRA Branch	2003	OCT	0	0	0	0	0	0	0	0	0	0	0	0	0	0	0	0
NWRA Branch	2003	NOV	0	0	0	0	0	0	0	0	0	0	0	0	0	0	0	

Table 3-5 Count of rainy-days (red fill), at NWRA-Branch station from May 2002 to November 2003 for the last 15 days of each month

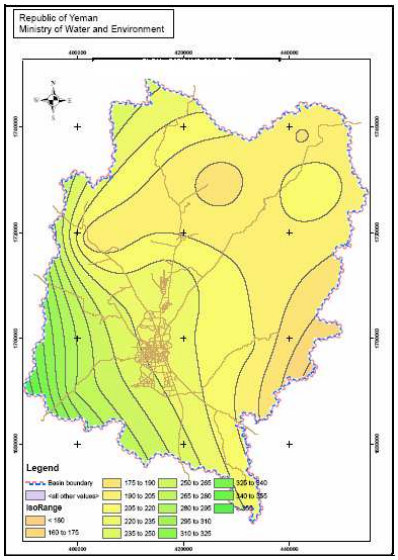

Figure 3-11 A contour map shows the average yearly rainfall intensity within the Sana'a Basin - calculated based on data from 1970 to 2006

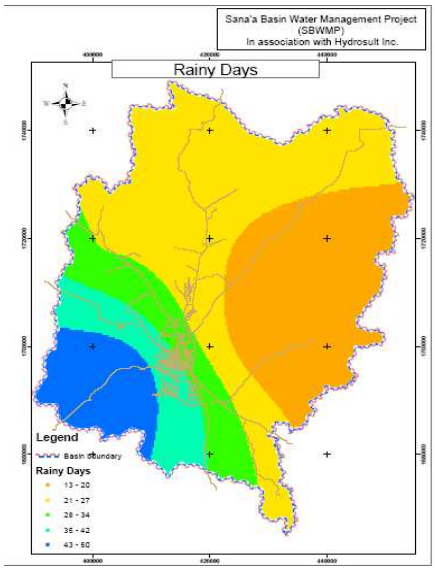

Figure 3-12 Contour map shows the average number of rain-days in the Sana'a Basin

3.6.4 Vulnerability Maps for the Sana'a Basin

Sana'a Basin consists of four groundwater aquifers: limestone, sandstone, volcanic and alluvial. Figure 3-13~~Figure 83~~ presents the geological outcropping map for the Sana'a Basin. The limestone aquifer outcropping is located in the northern and north-eastern parts of the Basin while the sandstone is formed in the eastern part of the basin and extends to the west part in a crescent pattern. The sandstone aquifer runs underneath the alluvial and volcanic aquifers from the midpoint of the crescent up to the eastern part of the basin. In some scattered areas, the sandstone aquifer appears as it is presented in Figure 3-13~~Figure 83~~. The alluvial aquifer expands in the lower elevation areas and is found mainly in the centre regions where the Sana'a plain is located. The volcanic aquifer, on the other hand, extends from the southern region and extends northward, covering large swaths of the basin. In the current study, each aquifer is treated separately and a vulnerability map for each has been developed based on the previously described methodologies. The following section presents the O-maps, C-maps, P-maps and final vulnerability maps for the limestone, sandstone and volcanic aquifers (Figures 83 through 123).

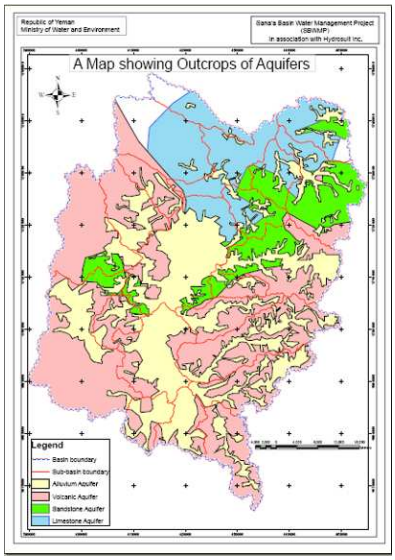

Figure 3-13 Map showing the outcropping of the different aquifers within the Sana'a Basin

3.6.4.1 Vulnerability Maps for the Limestone Aquifer

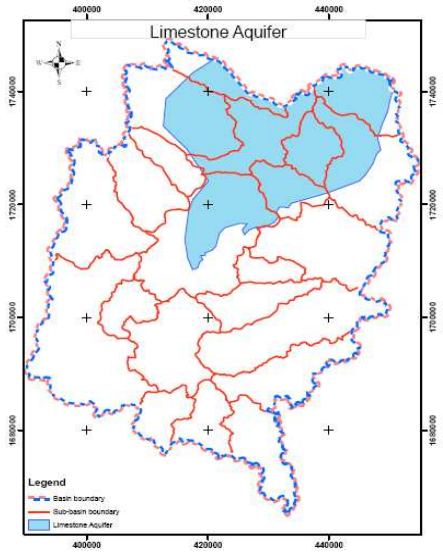

Figure 3-14 Boundaries of the limestone aquifer within the Sana'a Basin (determined by borehole analysis)

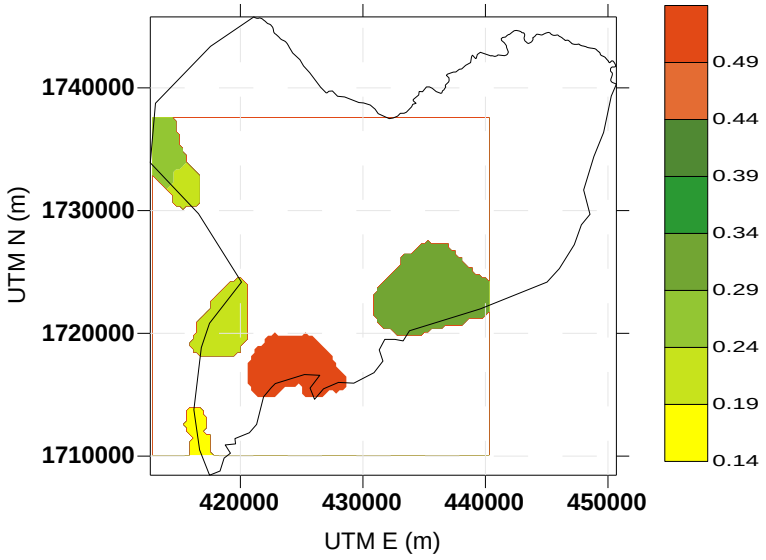

Figure 3-15 Map showing the locations and depth of silt (in m) within the limestone aquifer

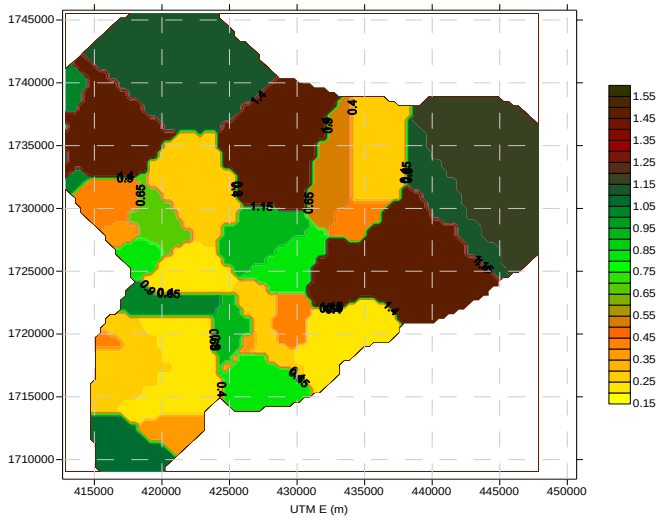

Figure 3-16 Map showing the locations and depth of loam (in m) within the limestone aquifer

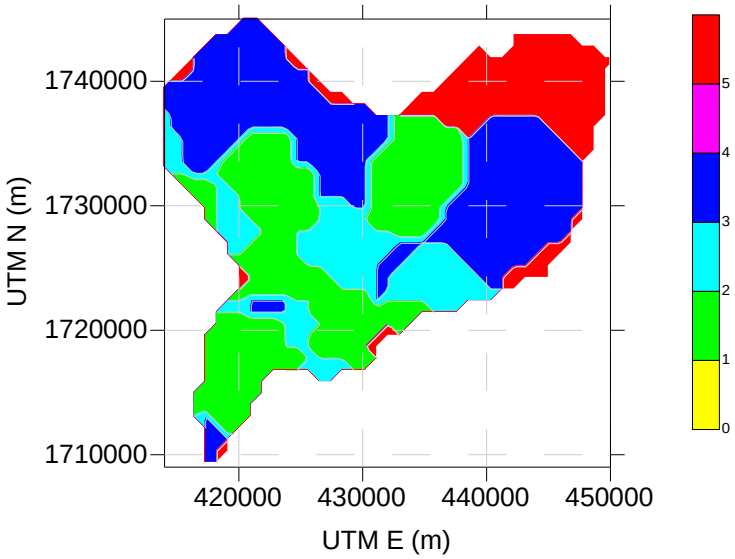

Figure 3-17 Map showing the Os value for the limestone aquifer

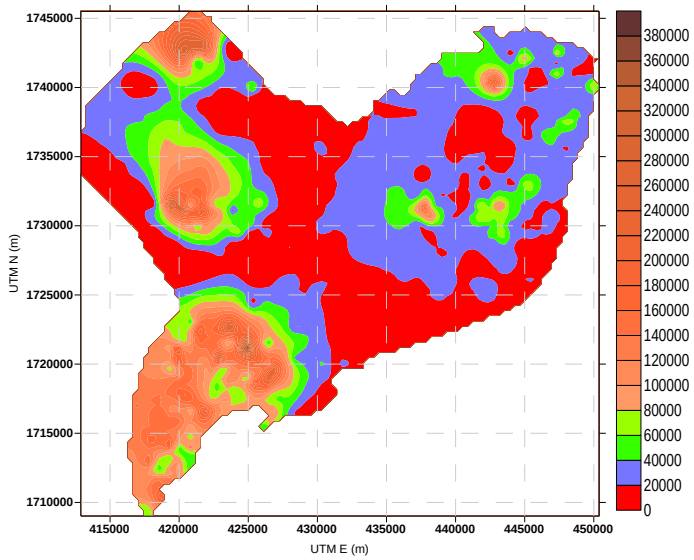

Figure 3-18 Map showing the lithology layer index for the limestone aquifer

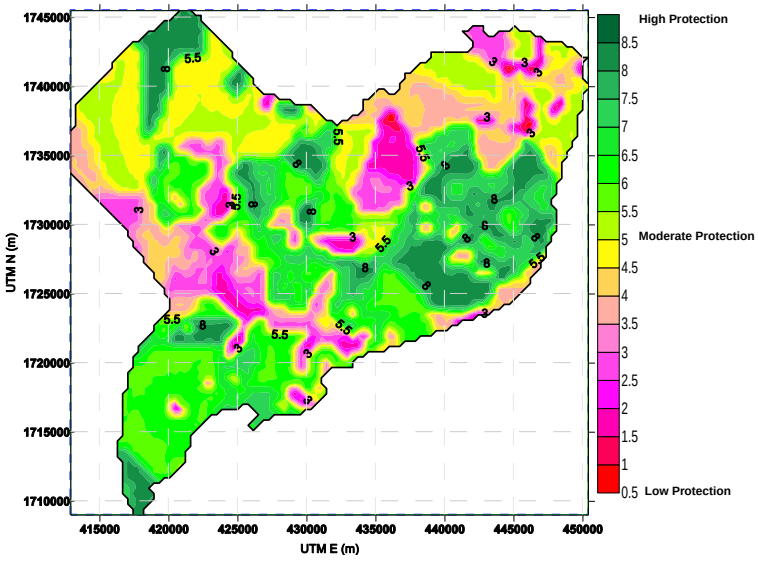

Figure 3-19 O-Factor map (Overlying Layer Map) for the limestone aquifer

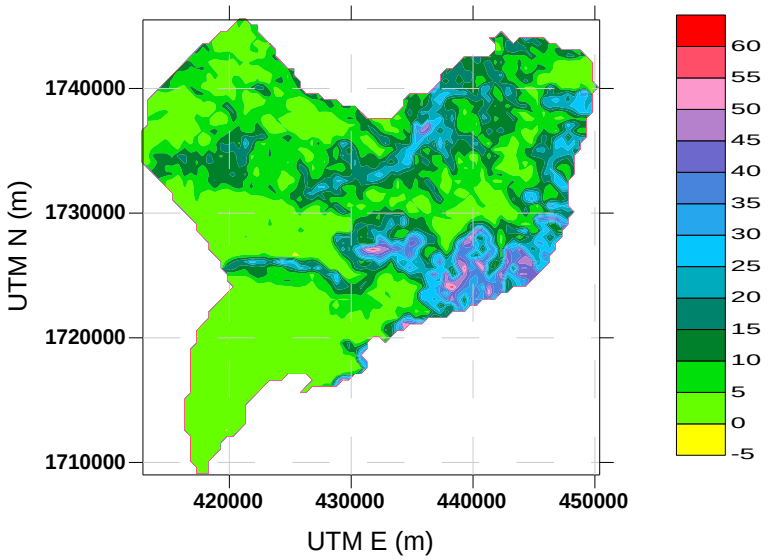

Figure 3-20 Map showing the values of terrain slope (percentage) within the limestone aquifer boundaries

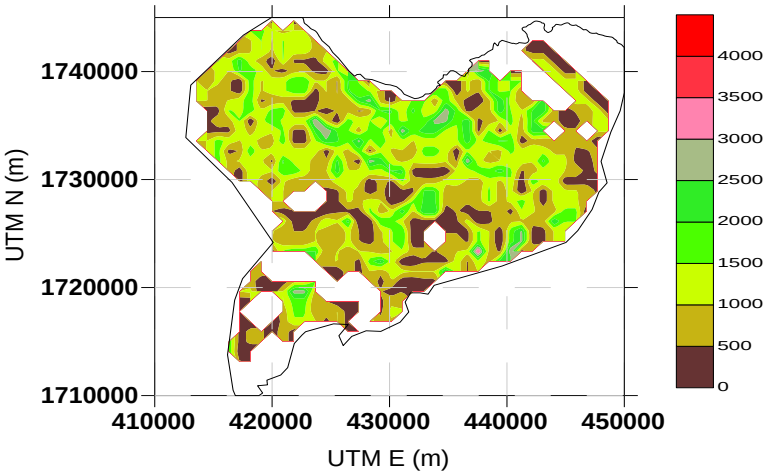

Figure 3-21 Fracture density map in length (m) for the limestone area, developed from the lineament map

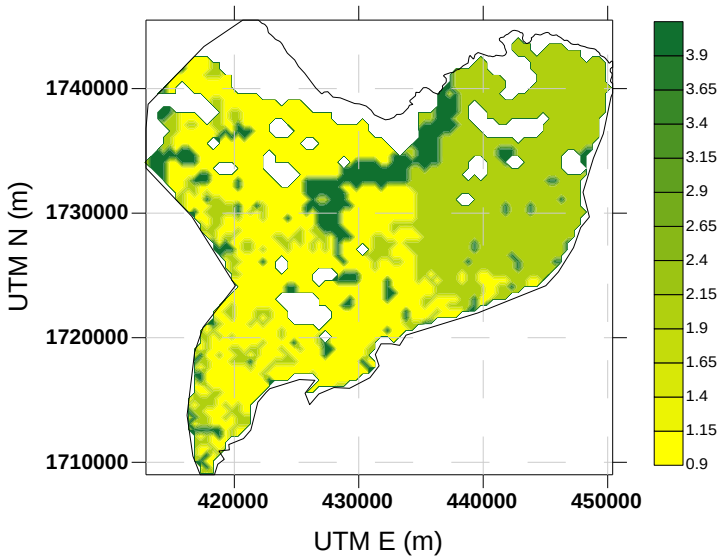

Figure 3-22 Vegetation density within the limestone area

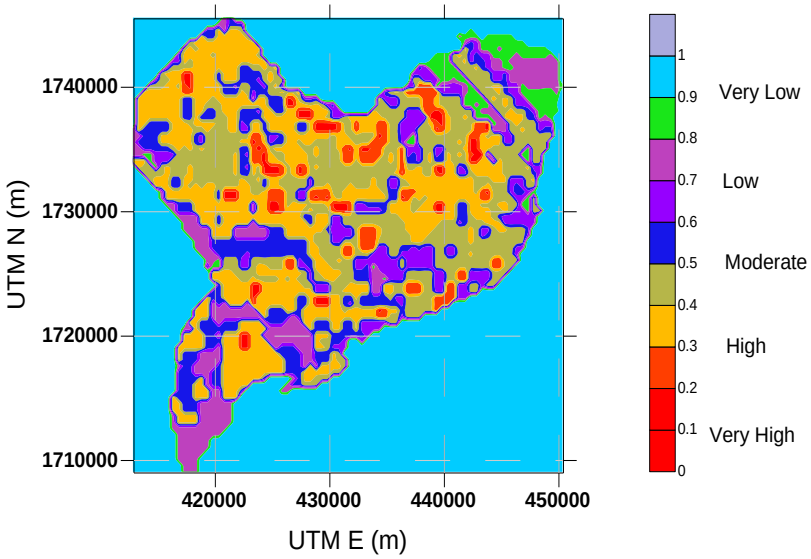

Figure 3-23 Map showing the reduction of protection as indicated by C-Factor (concentration of flow) for the limestone area

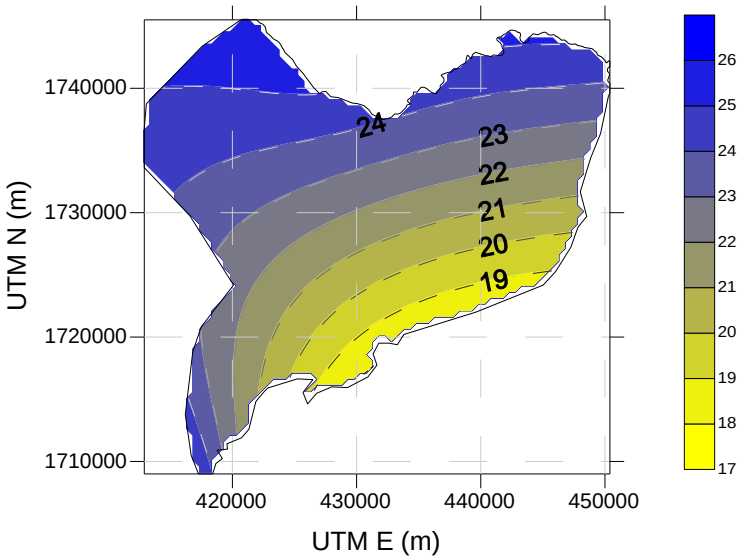

Figure 3-24 Map showing the rainfall days within the boundaries of the limestone aquifer

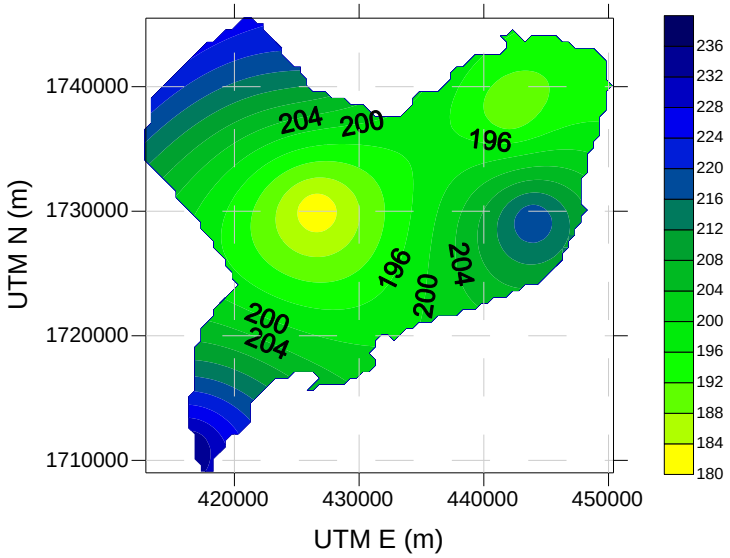

Figure 3-25 Map showing rainfall intensity within the limestone boundaries

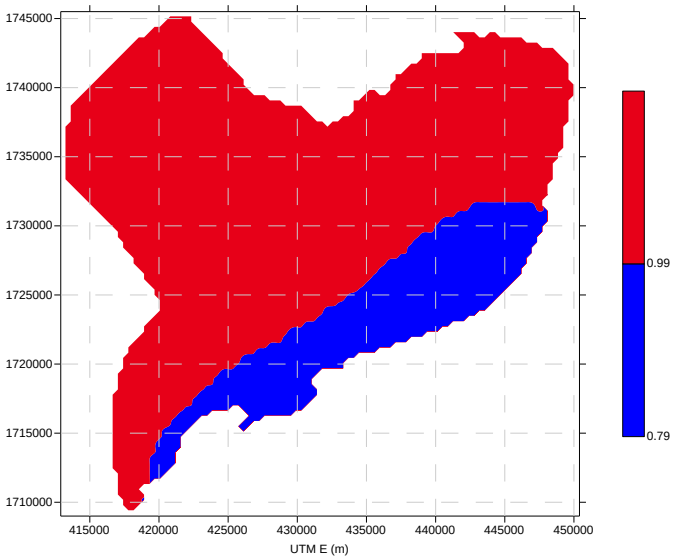

Figure 3-26 P-Score Map for the limestone aquifer

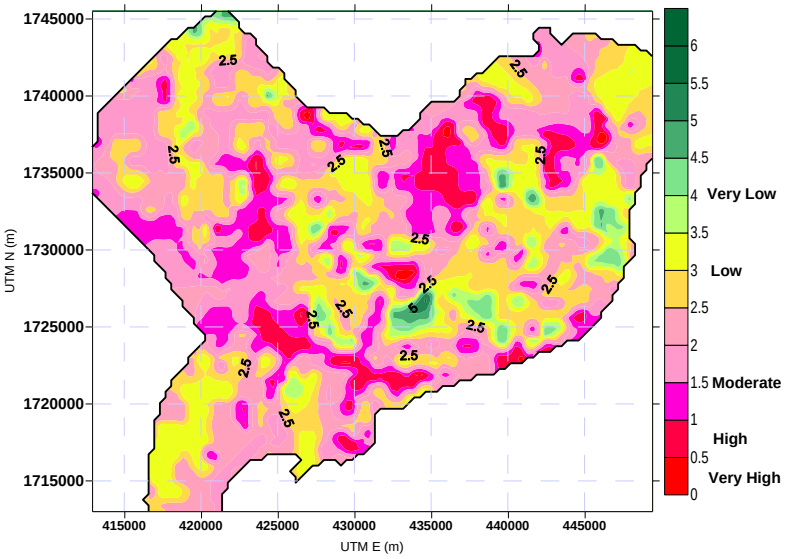

Figure 3-27 Final vulnerability map for the limestone area of the Sana'a Basin

3.6.4.2 Vulnerability Map for the sandstone aquifer

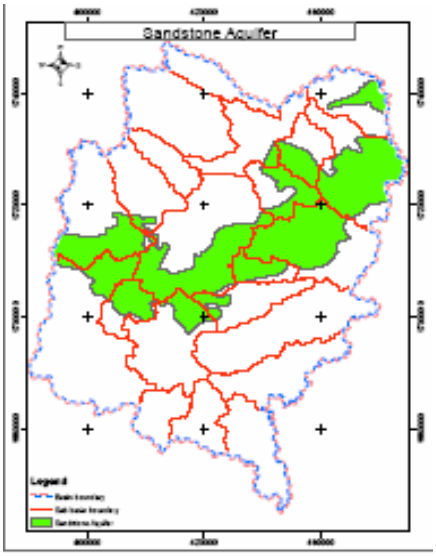

Figure 3-28 Boundaries of the sandstone aquifer within the Sana'a Basin (determined by borehole analysis)

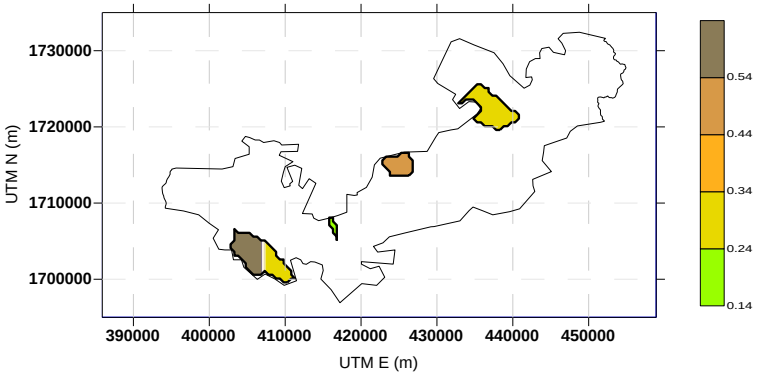

Figure 3-29 Silt thickness within the sandstone aquifer of the Sana'a Basin

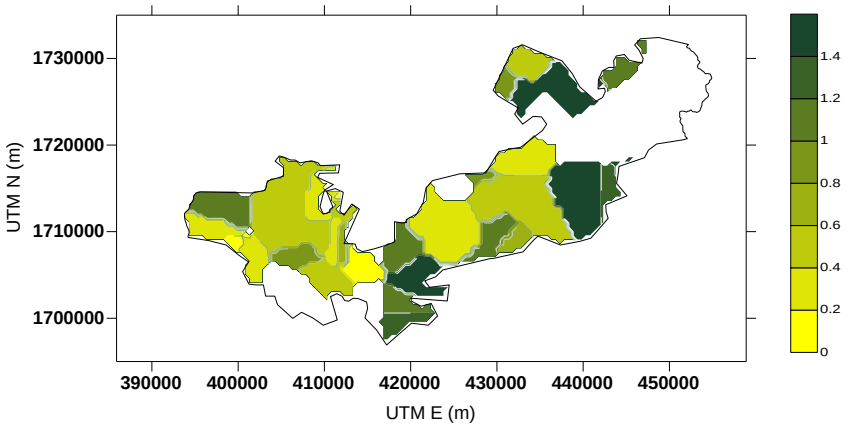

Figure 3-30 Loam thickness within the sandstone aquifer of the Sana'a Basin

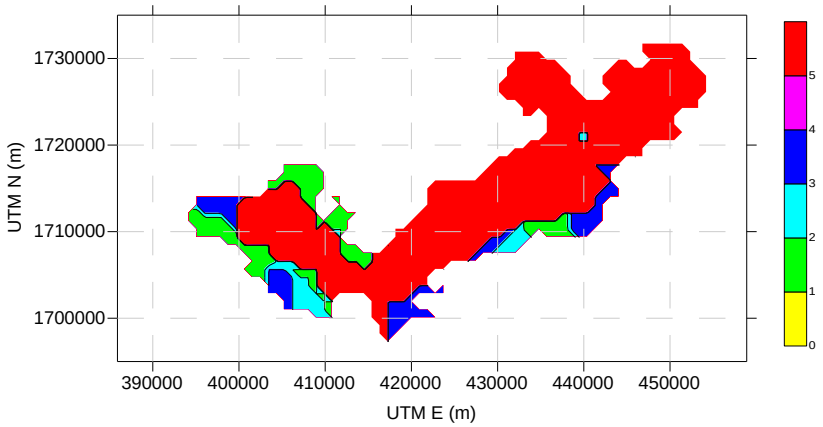

Figure 100a Overlaying map (Os – Map) within sandstone area

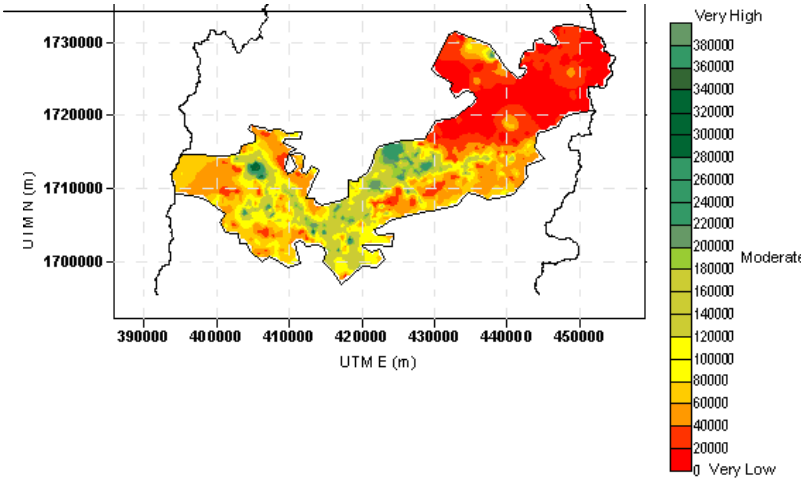

Figure 3-31 Map showing the lithology layer index for the sandstone aquifer

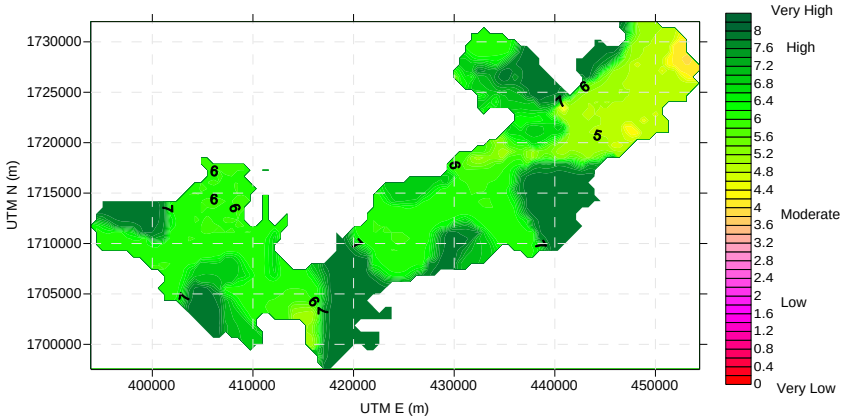

Figure 3-32 Final O-Factor map (Overlying Layer Map) for the sandstone aquifer

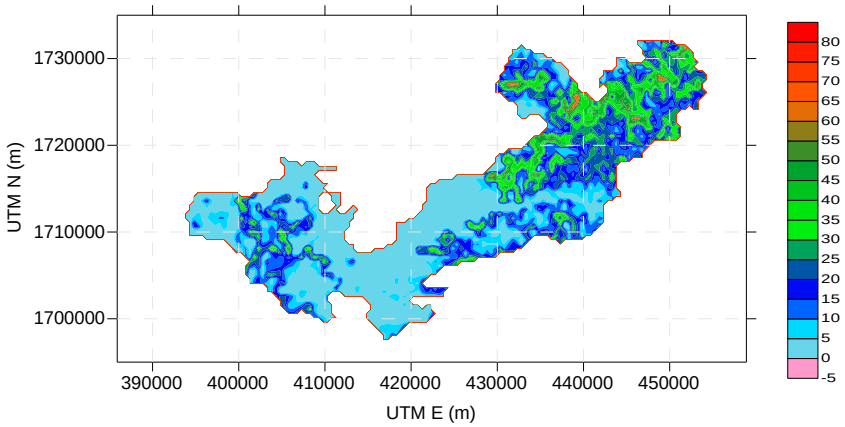

Figure 3-33 Map showing the values of terrain slope (percentage) within the sandstone aquifer boundaries

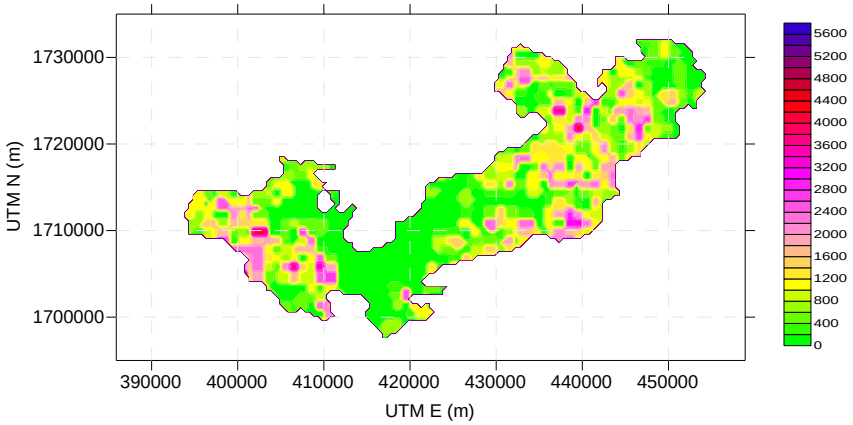

Figure 3-34 Fracture density map in length (m) for the sandstone area, developed from lineament map

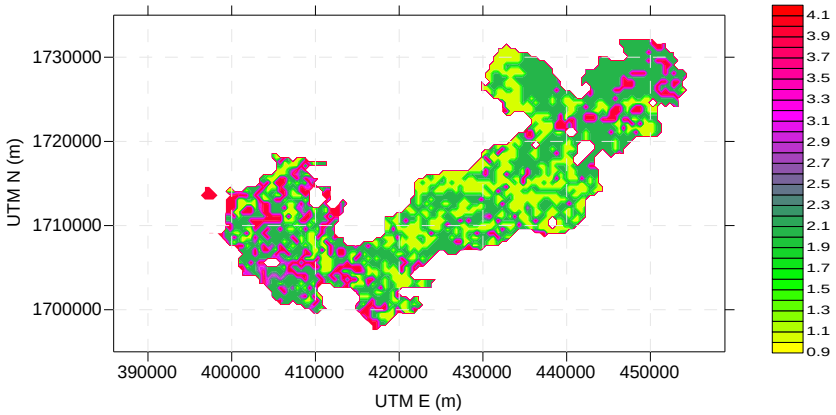

Figure 3-35 Vegetation densities within the sandstone area

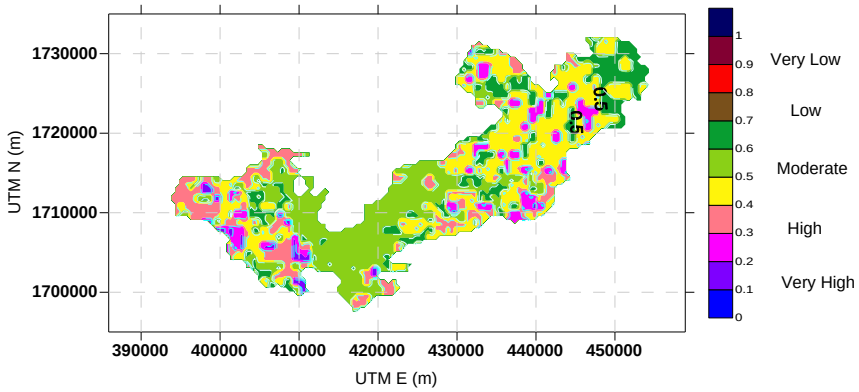

Figure 3-36 Map showing the reduction of protection as indicated by C-Factor (concentration of flow) for the sandstone area

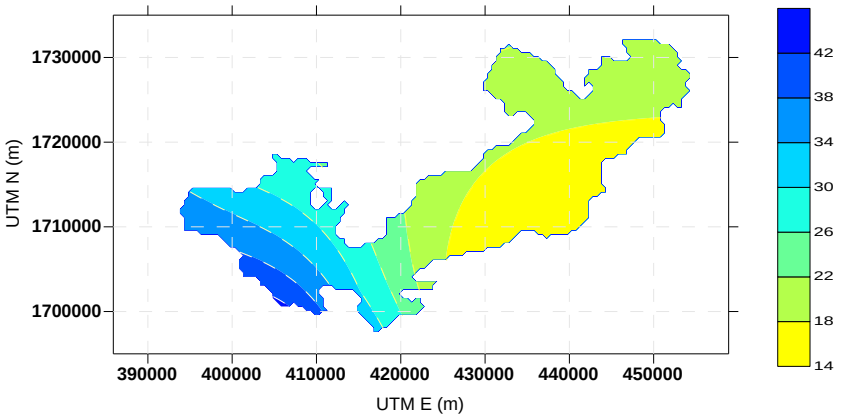

Figure 3-37 Rainfall days within the boundaries of the sandstone aquifer

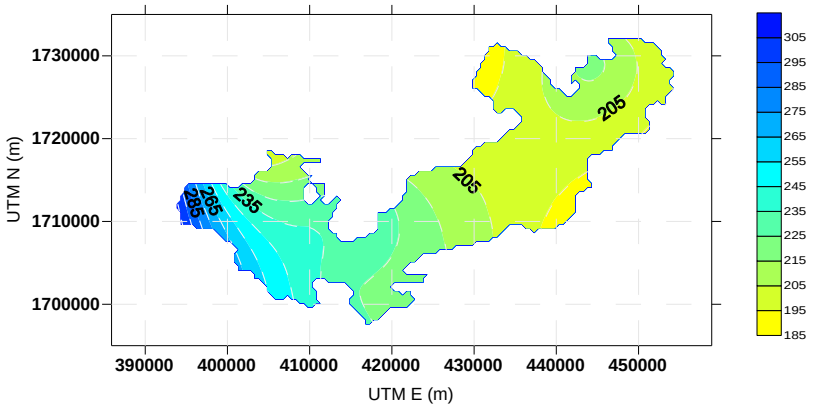

Figure 3-38 Map showing rainfall intensity within the sandstone boundaries

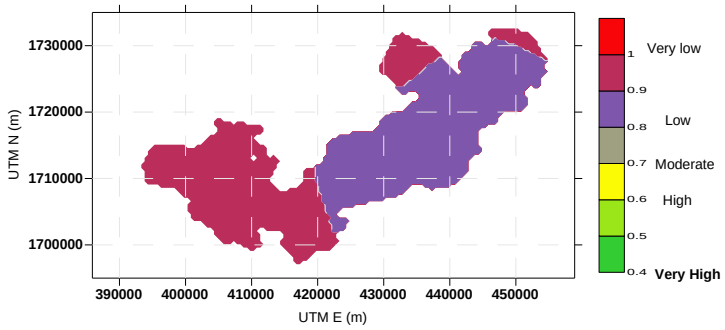

Figure 3-39 Reduction of protection factor for precipitation (P-Score)

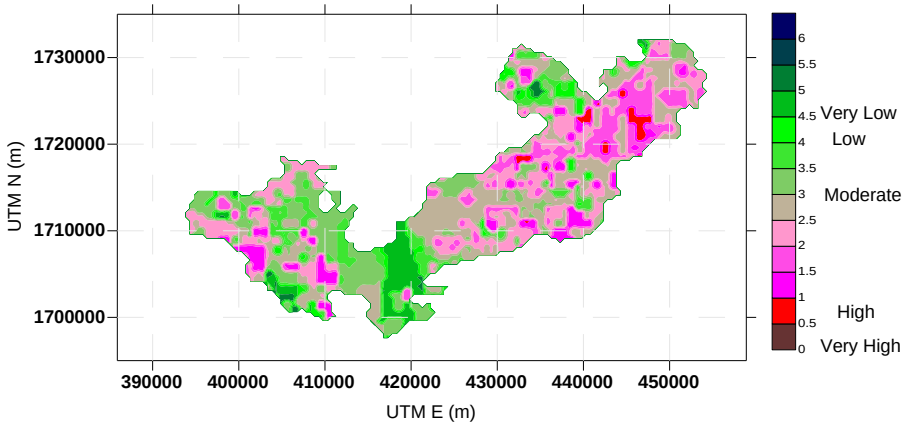

Figure 3-40 Final vulnerability map for the sandstone aquifer

3.6.4.3 Vulnerability Map for the volcanic aquifer

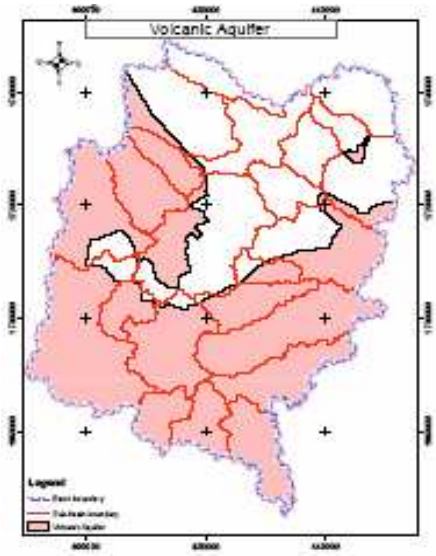

Figure 3-41 Boundaries of the volcanic aquifer within the Sana'a Basin (determined by borehole analysis)

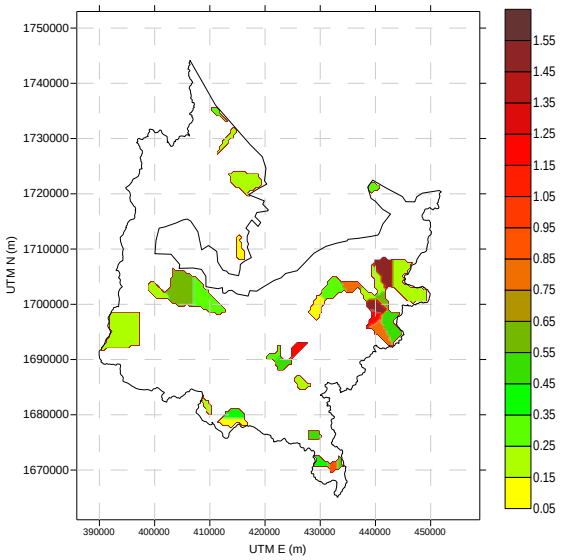

Figure 3-42 Silt thickness within the volcanic aquifer of the Sana'a Basin

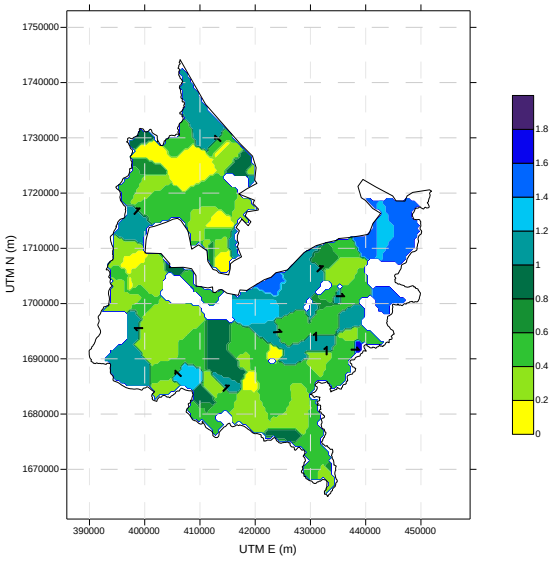

Figure 3-43 Loam thickness within the volcanic aquifer of the Sana'a Basin

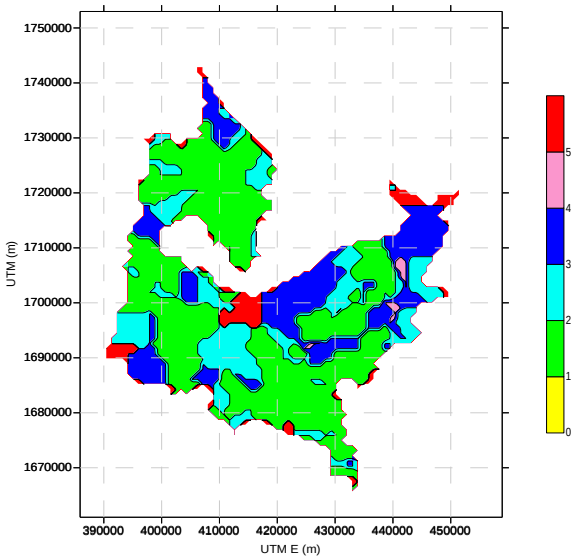

Figure 113a Overlaying map (Os – Map) within volcanic area

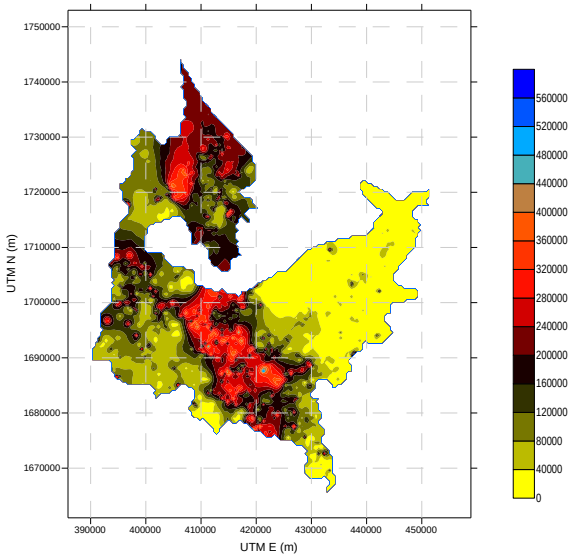

Figure 3-44 Map showing the lithology layer index for the volcanic aquifer

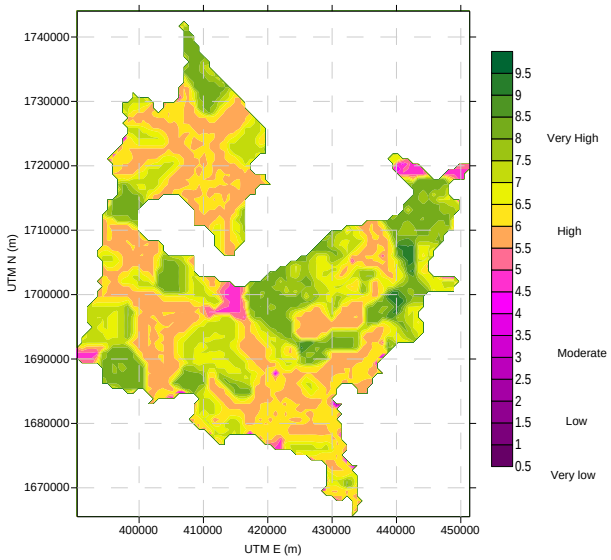

Figure 3-45 O-Factor (Overlying Layer Map) for volcanic aquifer

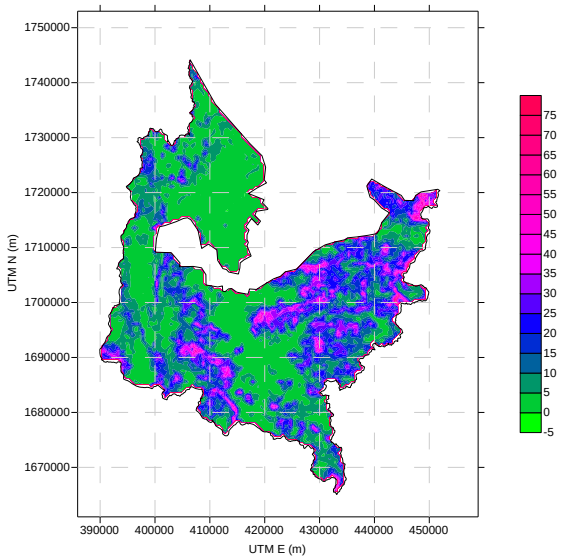

Figure 3-46 Map showing the values of terrain slope (percentage) within the volcanic aquifer boundaries

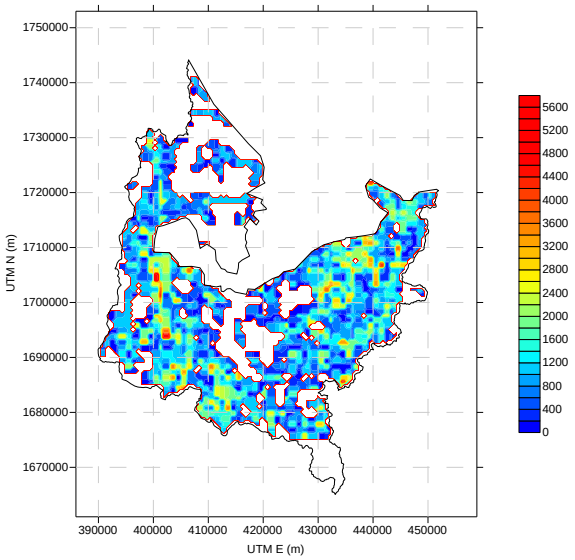

Figure 3-47 Fracture density map in length (m) for volcanic area, developed from the lineament map

Figure 3-48 Vegetation densities within the volcanic area

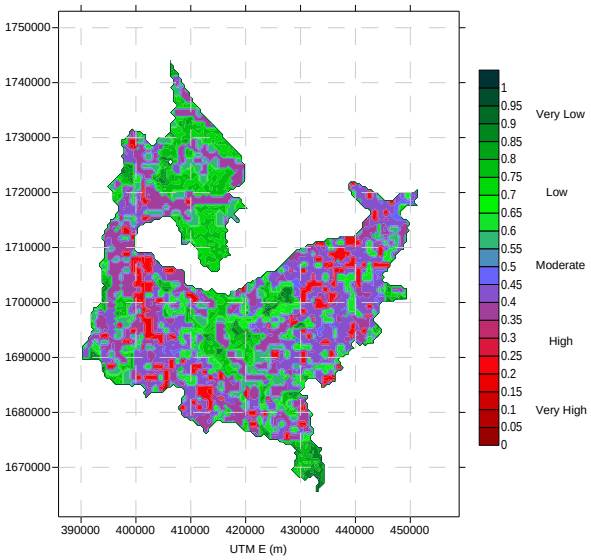

Figure 3-49 Map showing the reduction of protection as indicated by C-Factor (concentration of flow) for the volcanic area

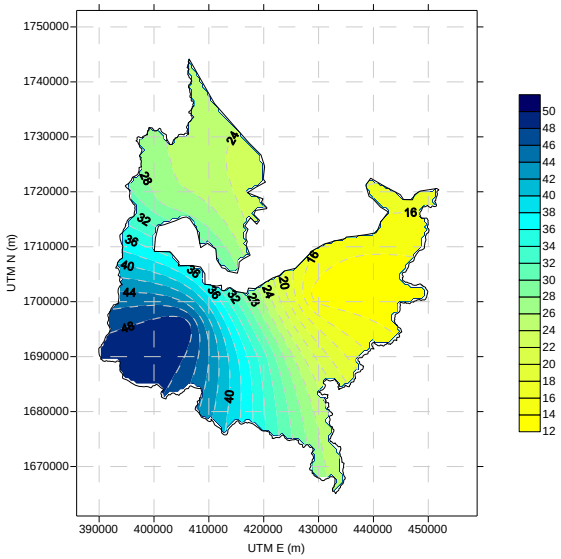

Figure 3-50 Rainfall days within the boundaries of volcanic aquifer

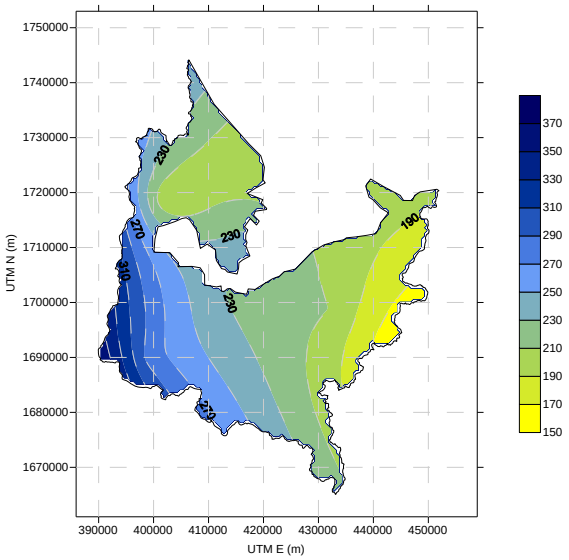

Figure 3-51 Map showing rainfall intensity within the volcanic aquifer boundaries

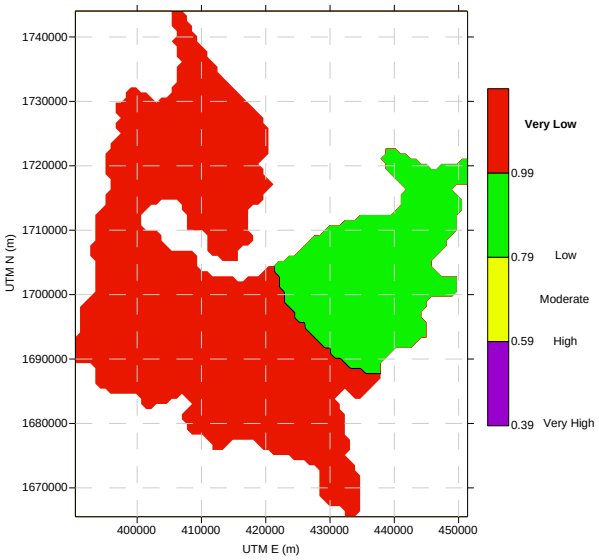

Figure 3-52 The reduction of protection factor for precipitation (P-Score) within the volcanic aquifer

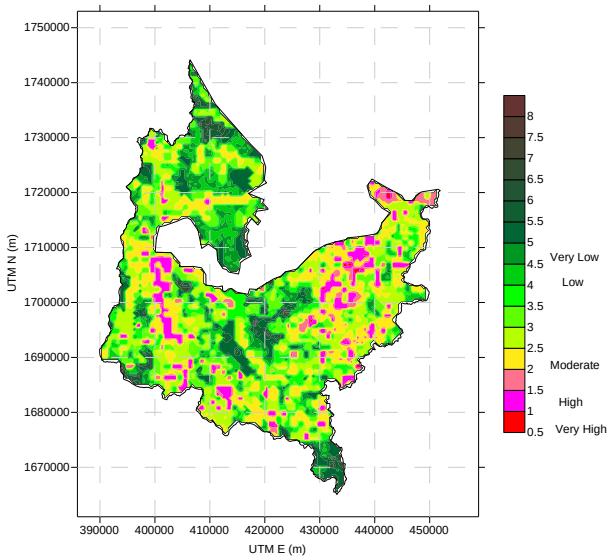

Figure 3-53 Final vulnerability map for the volcanic aquifer

Chapter 4. GROUNDWATER QUALITY IN THE VICINITY OF THE TREATED WASTEWATER PASSAGE IN SANA'A BASIN

4.1 Introduction

Sewage passage in Sana'a Basin starts at the outlet of the Sana'a City wastewater treatment plant at the northern edge of the Sana'a Basin. The passage runs across the basin for about 20 km until it reaches the main stream of Wadi Al-Kharid. Along the passage there are three dams: Al-Mosyreka Dam, Al-Masham Dam and Al-Samena Dam. The passage runs across very critical geological features, including major faults, and encounters significant geological variation, including volcanic and limestone outcrops. Figure 124 presents a Google Earth image showing the passage marked by a black line. The difference in rock color on the east and West sides is very clear. A volcanic rock outcrop is found on the west side while, on the east side, the rock is limestone. Because the treated wastewater traverses sensitive areas, it is important to study the groundwater quality in the vicinity of the passage.

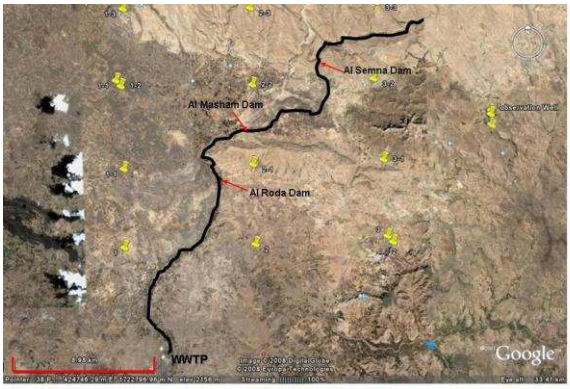

Figure 4-1 A Google Earth image of the wastewater route showing the infrastructures along the passage

4.2 Objectives of the Current Study

The objectives of the current study can be listed as follows:

- Study the impact of the passage on the different aquifers;
- Study the impact of the passage on different water depths;
- Study the lateral diffusion of the passage's water;
- Perform basic water quality analyses (including cation and anion testing) for collected samples;
- Perform microbiological analyses of the different collected samples to evaluate the microbiological status of groundwater aquifers within the vicinity of the passage.

4.3 Collected Water Samples

35 water samples were collected from the area under investigation. Table 9 presents the well ID, well location, well coordinates, well rim elevation, depth of water and tipping aquifer of each sampling point. As shown in this table, the selected wells represent the volcanic, alluvial and limestone aquifers. Water samples were collected at different depths, ranging from 21 m to 450 m. Well rim elevations ranged from 2001 m to 2506 m.

4.4 Results of Water Quality Analysis

The following Figures 125 through 141 show maps developed based on water quality analyses in the vicinity of the treated wastewater passage within the boundaries of the Sana'a Basin.

ID	Well ID	Locality	UTM N (m)	UTM E (m)	Elev. AMSL	Water Depth (m)	Aquifer
1	HSA84	Al-jahman / baraman / ARHAB	413496	1723877	2239	300	Volcanic
2	HSA85	Al-Asmad/Hzam / ARHAB	413350	1727319	2281	450	Volcanic

ID	Well ID	Locality	UTM N (m)	UTM E (m)	Elev. AMSL	Water Depth (m)	Aquifer
3	HSA86	Al-Asmad/ ARHAB	413814	1726919	2268	352	Volcanic
4	HSA87	Hotban/ ARHAB	408295	1728198	2506	437	Volcanic
5	HSA88	Bait Dafa'a/ ARHAB	414334	1729656	2303	380	Volcanic
6	HSA90	Gader Al asfal/Bani Al harth	412671	1709899	2201	105	Alluvial
7	HSH8	Al Hawry / Hamdan	407277	1714451	2248	280	Volcanic
8	HSH10	Bait Al Rafik /Hamdan	405457	1721136	2248	350	Volcanic
9	HS152	Shibam //Bani Husheish	426243	1714598	2087	240	Sandstone
10	HS55	Zijan //Bani Husheish	429466	1716736	2239	42	Sandstone
11	HS27	Bit Al anz /NIHM	432478	1724413	2127	40	Limestone
12	HS28	Bit Al anz /NIHM	430758	1724836	2127	35	Limestone
13	HSA91	Shira'a /ARHAB	429370	1725365	2066	400	Limestone
14	HSA92	Bani Jarmoz /ARHAB	426167	1726223	2086	150	Limestone
15	HSA93	Al Ajar /Bani Al harith	419134	1716018	2186	250	Volcanic
16	HSA94	Bani Aseam Bani Alharith	424535	1716871	2190	230	Volcanic
17	HSA95	Bit Duqhish /Bani Al harith	423296	1721513	2165	150	Volcanic
18	HSA96	Al Safra /ARHAB	418236	1725785	2171	300	Volcanic
19	HSA97	Aomarah /ARHAB	417010	1726772	2207	230	Limestone
20	HSA98	Al mamar/Bani Al harith	412395	1718404	2195	250	Alluviam
21	HSH11	Al Hokah /Hamdan	409246	1720948	2253	250	Volcanic
22	HSA99	Bit Al Thib Al A'alah /Bani Al harith	416163	1720363	2182	240	Volcanic
23	HSA16	Bit Rasam /Bani Al harith	417248	1717731	2186	300	Volcanic
24	HSA100	Al Awzari Al a'alah /Bani Al harith	417243	1719087	2198	300	Volcanic
25	HSA101	Bit AlWishah /Bani Al harith	418561	1720651	2175	300	Volcanic
26	HSA102	Bit Al Euthari /Bani Al harith	419534	1723364	2167	172	Limestone

Formatted: Dutch (Netherlands)

Formatted: Dutch (Netherlands)

Formatted: Dutch (Netherlands)

ID	Well ID	Locality	UTM N (m)	UTM E (m)	Elev. AMSL	Water Depth (m)	Aquifer
27	HSA103	Bit Duqaish /Bani Al harith	419477	1720943	2166	230	Limestone
28	HSA7	Bit athrwb /Bani Al harith	421957	1719694	2161	120	Alluviam
29	HSA104	BitAl Rashid /Bani Al harith	422559	1717798	2175	190	Alluviam
30	HSA105	Bab Al Rawdah /ARHAB	419380	1725310	2156	200	Limestone
31	HSA106	Al baglan /ARHAB	419567	1730016	2156	300	Limestone
32	HSA74	Simnah /ARHAB	426751	1729981	2031	21	Alluviam
33	HSA107	Bit Swdi /ARHAB	430467	1729702	2074	30	Limestone
34	HSA108	Markan /ARHAB	430695	1730438	2105	50	Limestone
35	HSA109	Bani Al Hakam /ARHAB	430402	1732830	2001	150	Limestone
36	HSA110	Harat el osta'a /Bani Al harith	418279	1712455	2197	250	Volcanic

Table 4-1 Water sampling points in the vicinity of the wastewater passage

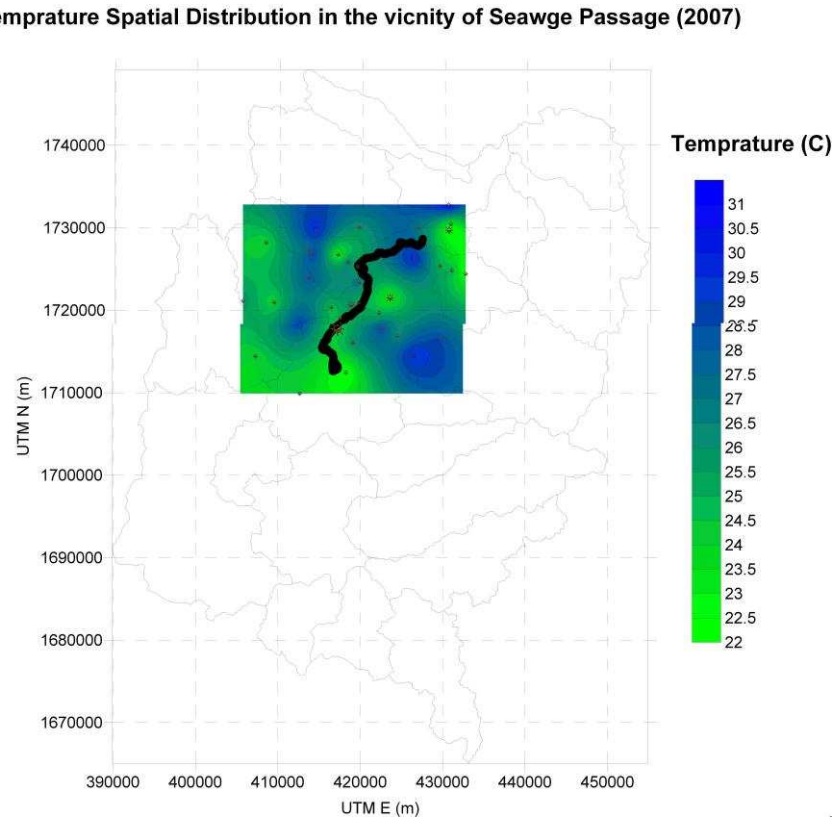

Figure 4-2 Spatial distribution of temperature in the vicinity of the wastewater passage

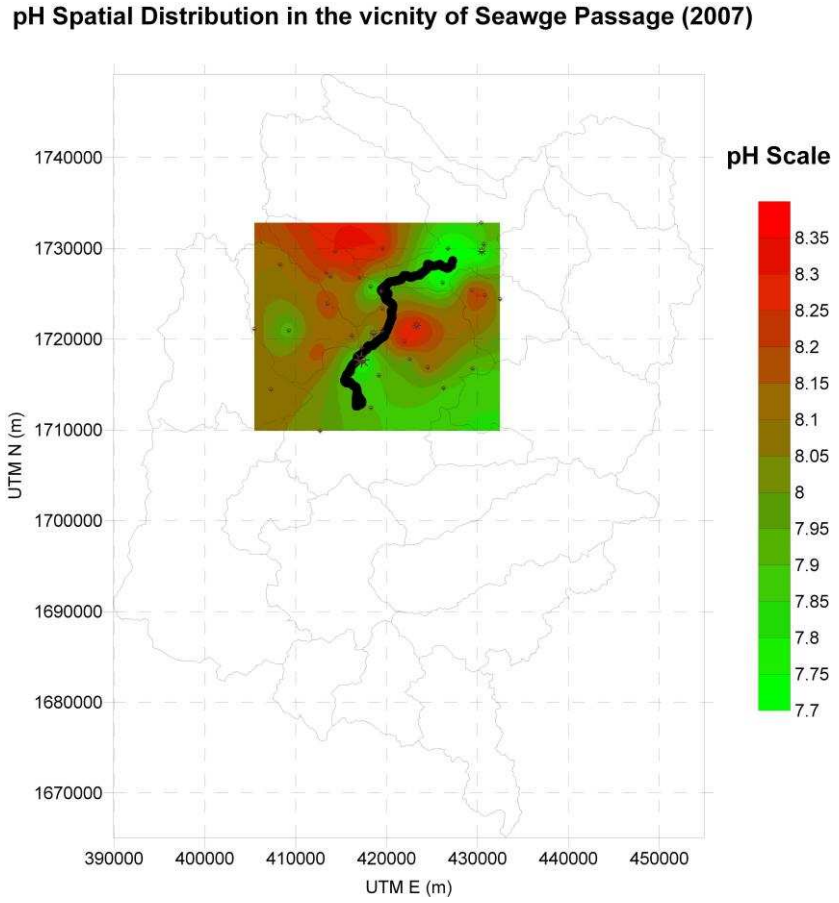

Figure 4-3 Spatial distribution of pH in the vicinity of the wastewater passage

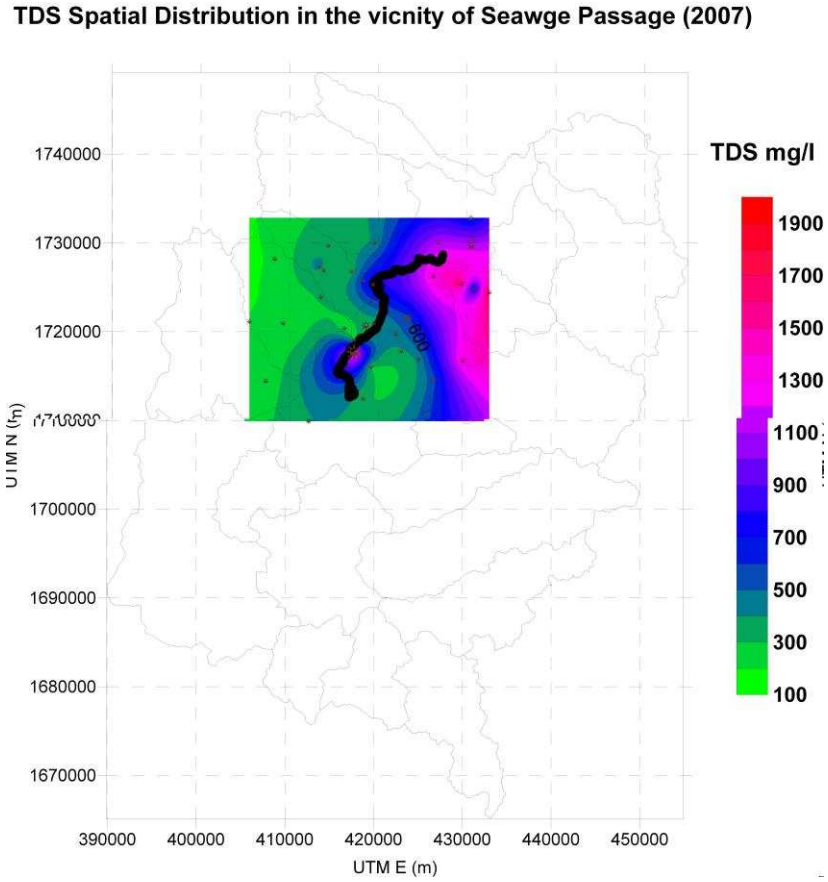

Figure 4-4 Spatial distribution of TDS in the vicinity of the wastewater passage

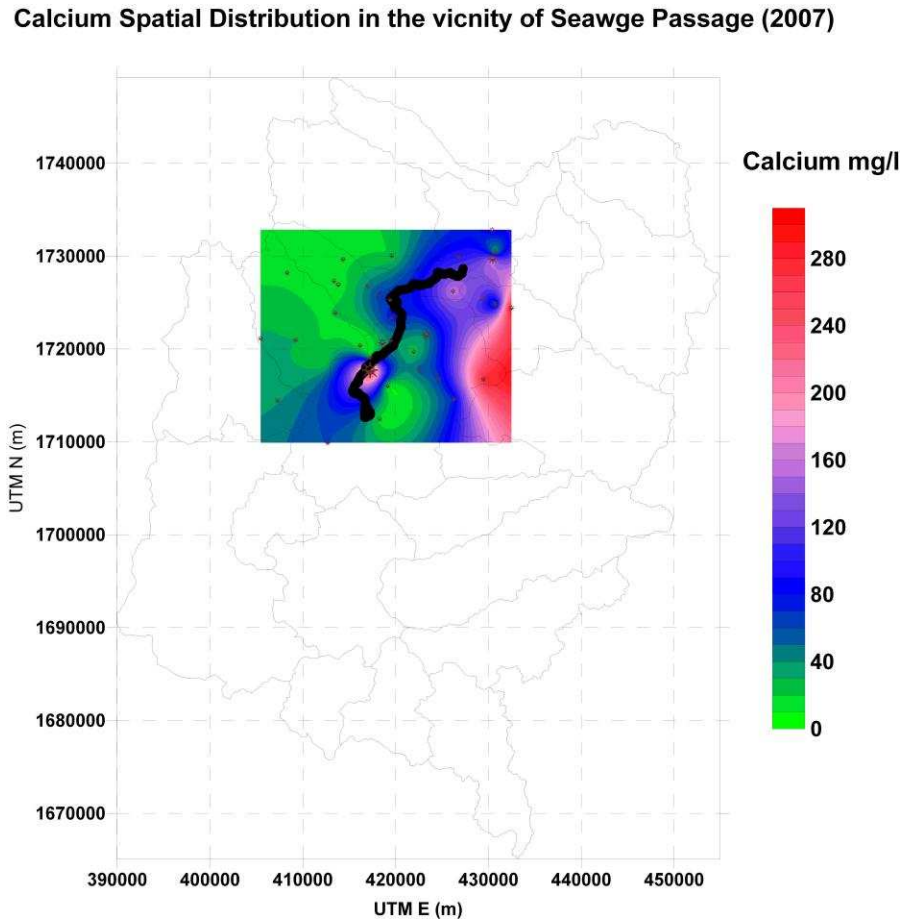

Figure 4-5 Spatial distribution of calcium in the vicinity of the wastewater passage

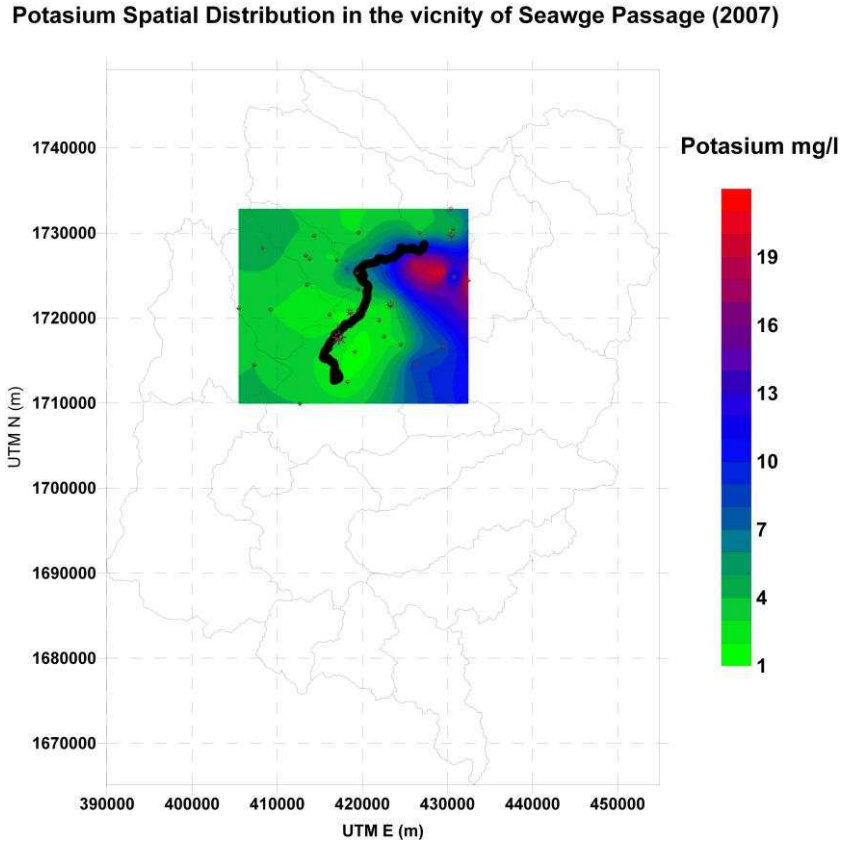

Figure 4-6 Spatial distribution of potassium in the vicinity of the wastewater passage

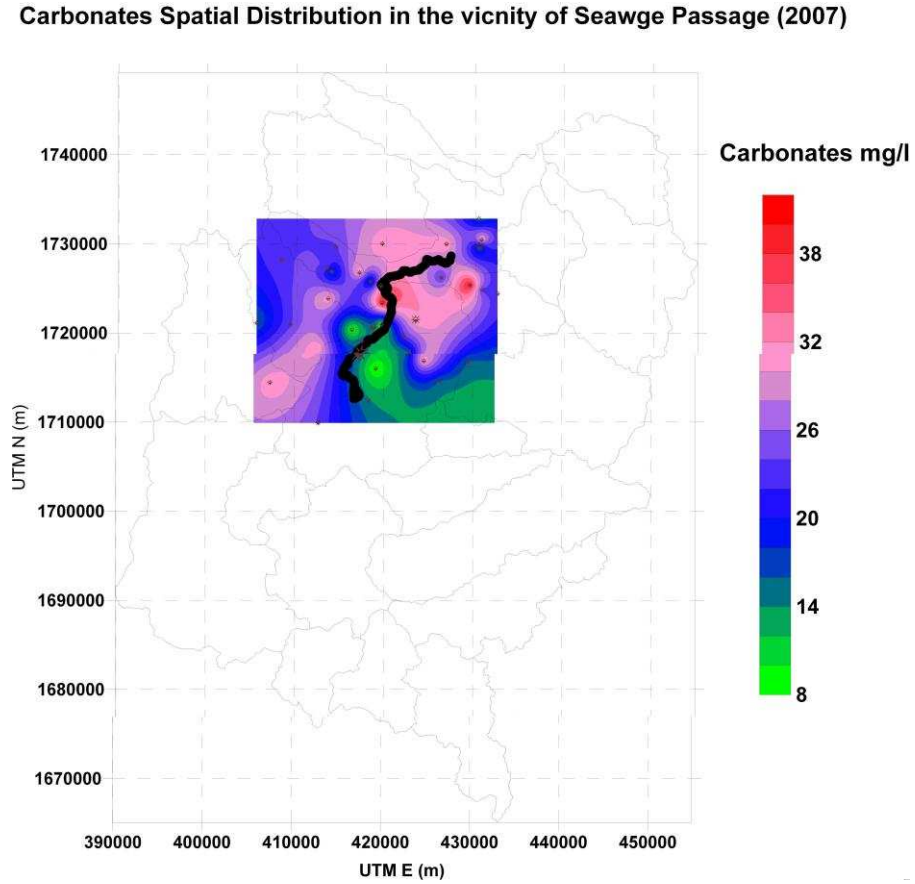

Figure 4-7 Spatial distribution of carbonates in the vicinity of the wastewater passage

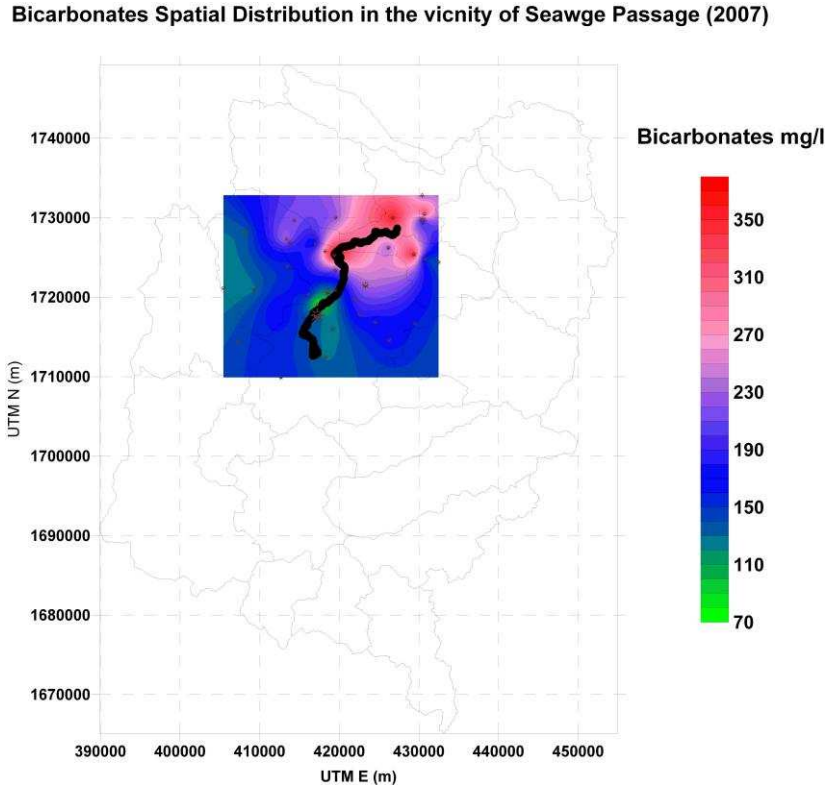

Figure 4-8 Spatial distribution of bicarbonates in the vicinity of the wastewater passage

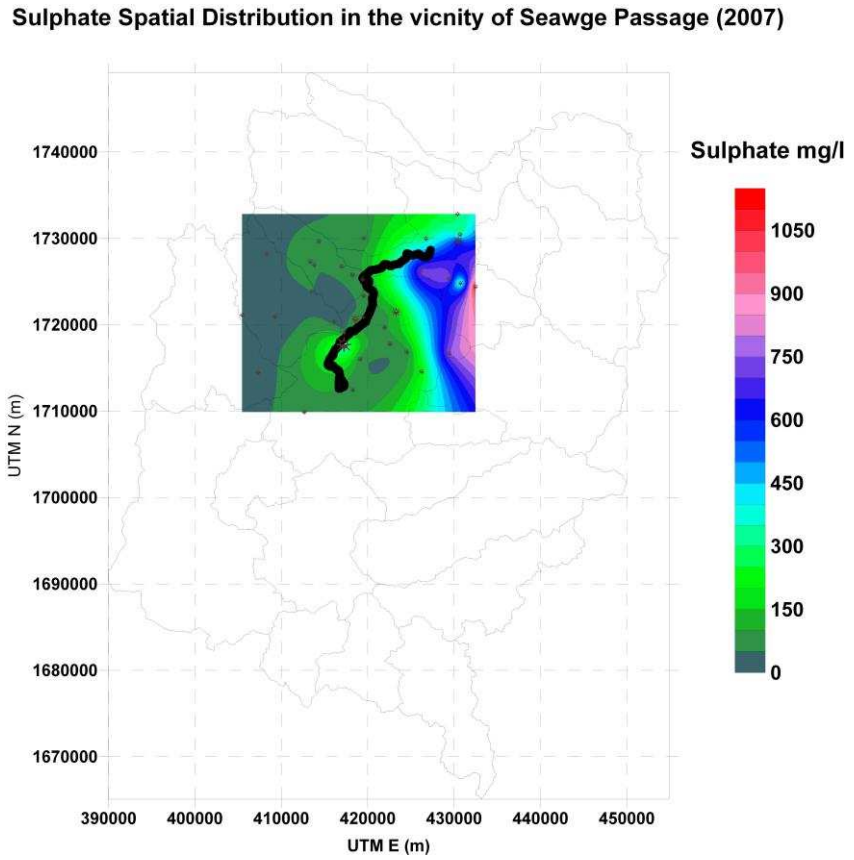

Figure 4-9 Spatial distribution of sulfate in the vicinity of the wastewater passage

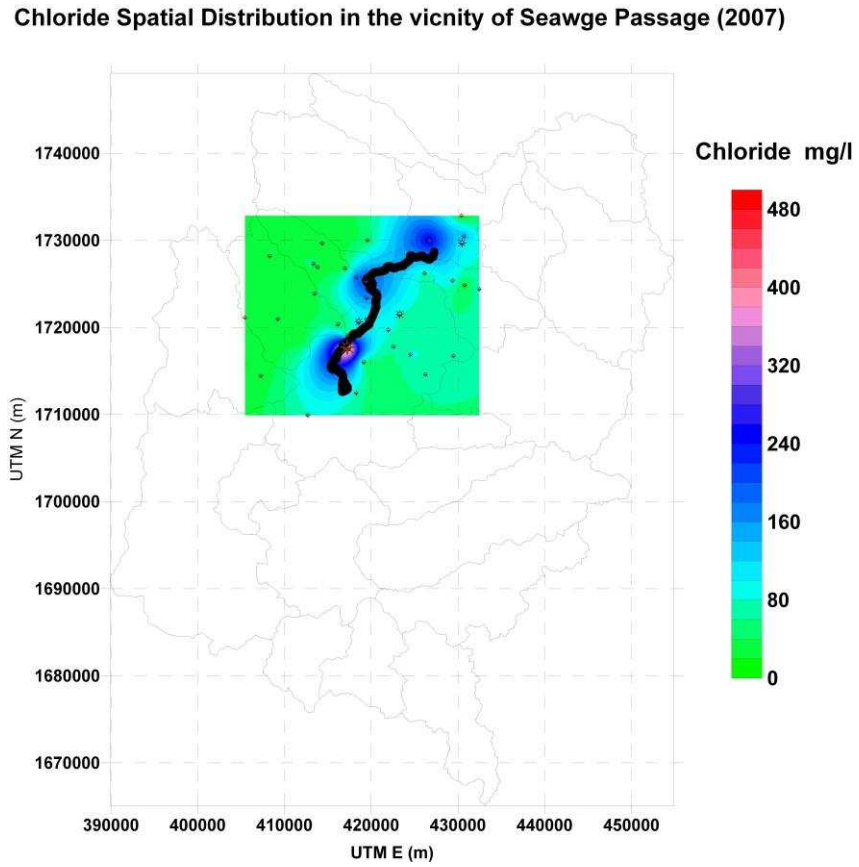

Figure 4-10 Spatial distribution of chloride in the vicinity of the wastewater passage

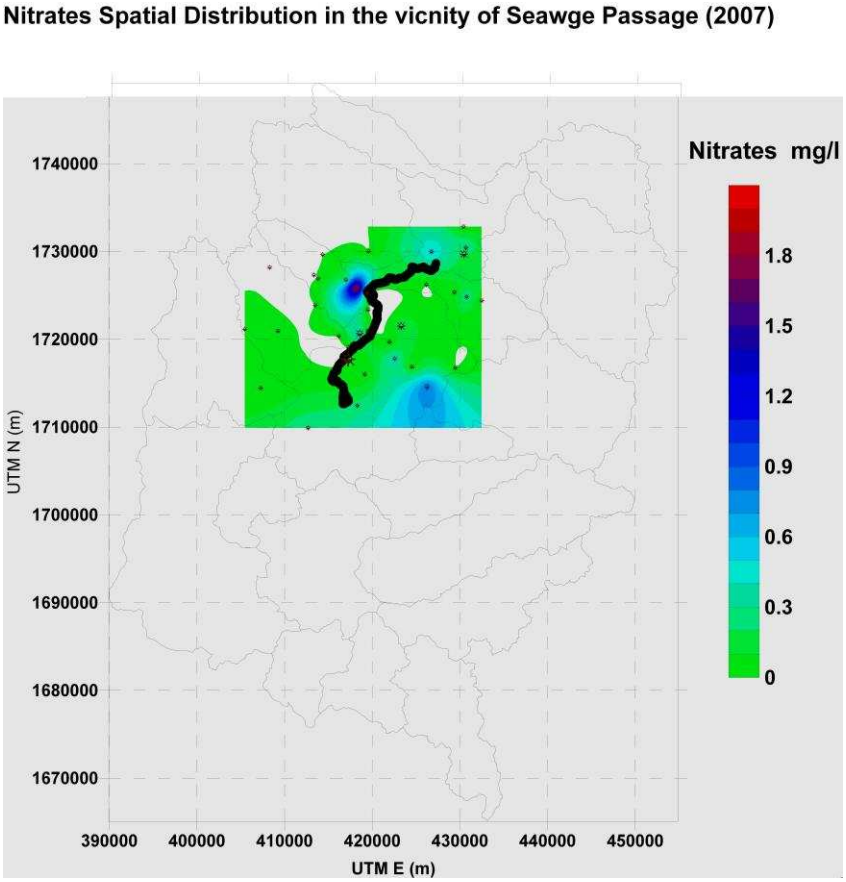

Figure 4-11 Spatial distribution of nitrates in the vicinity of the wastewater passage

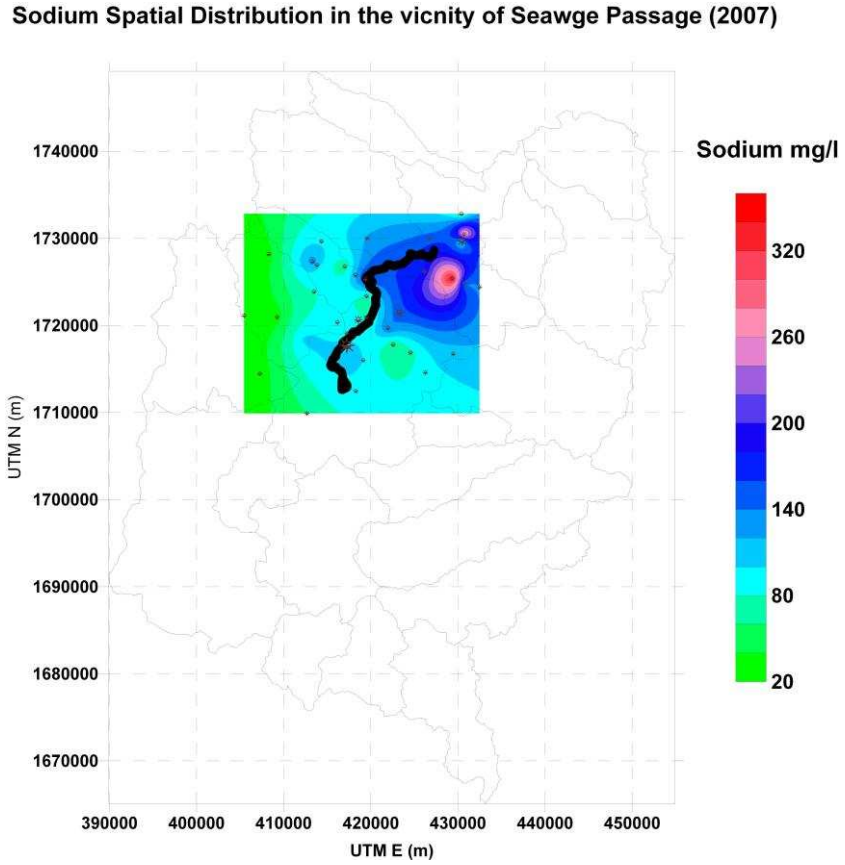

Figure 4-12 Spatial distribution of sodium in the vicinity of the wastewater passage

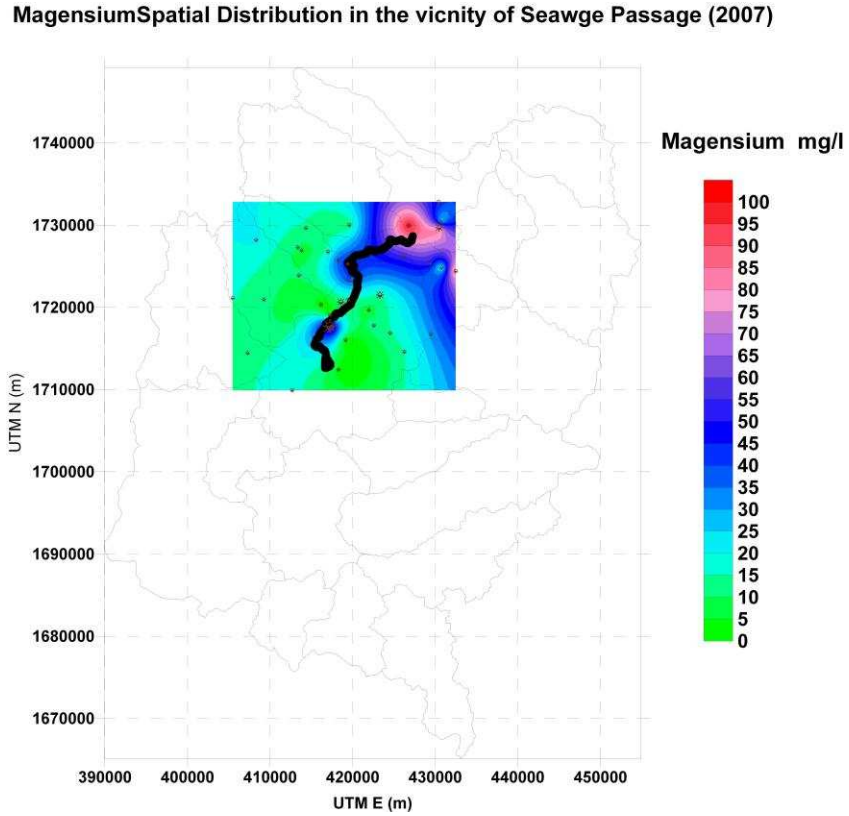

Figure 4-13 Spatial distribution of magnesium in the vicinity of the wastewater passage

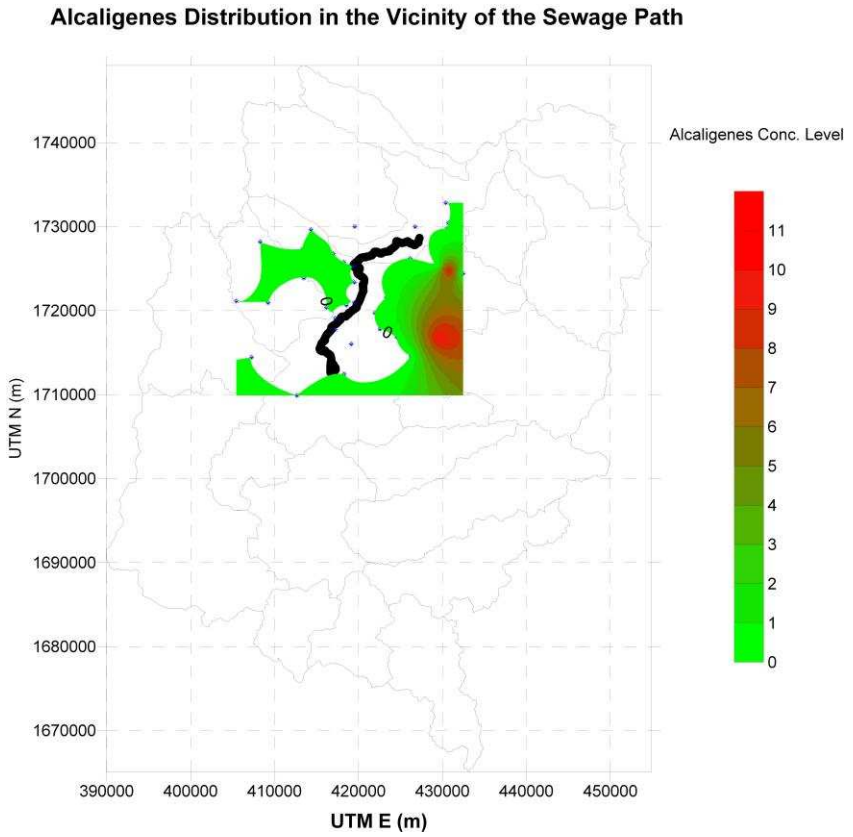

Figure 4-14 Spatial distribution of alcaligenes in the vicinity of the wastewater passage

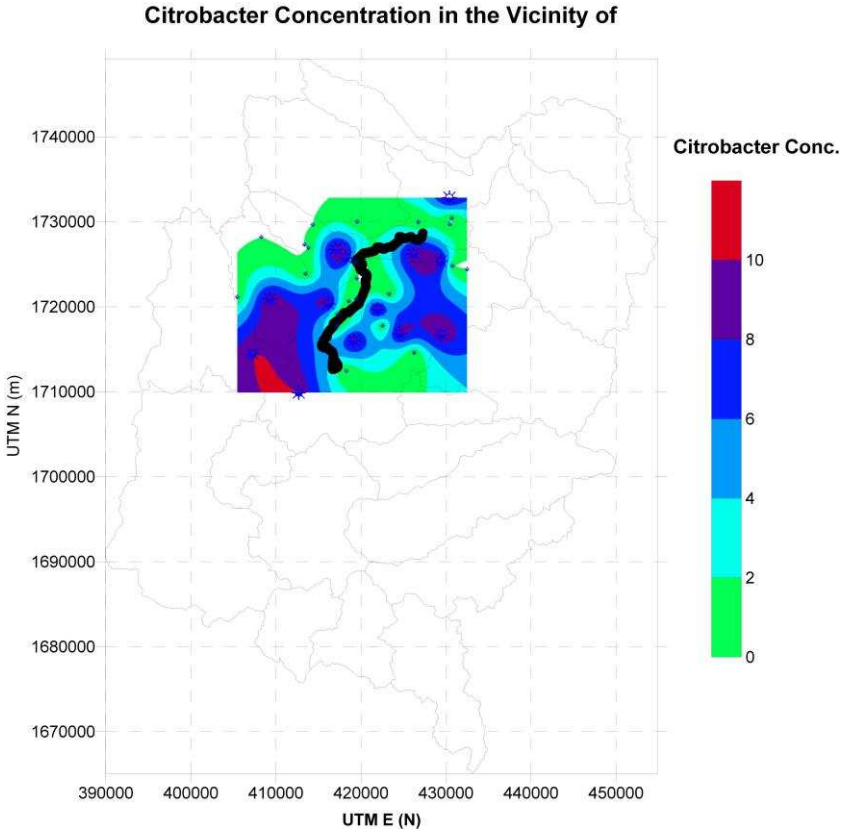

Figure 4-15 Spatial distribution of citrobacter in the vicinity of the wastewater passage

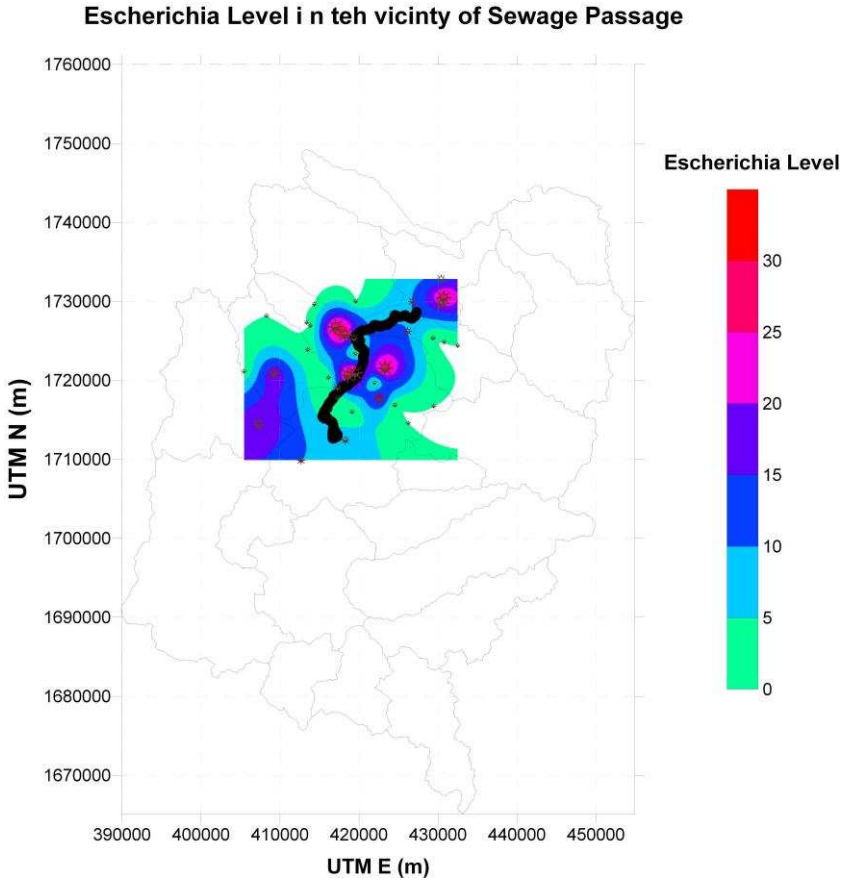

Figure 4-16 Spatial distribution of escherichia coli in the vicinity of the wastewater passage

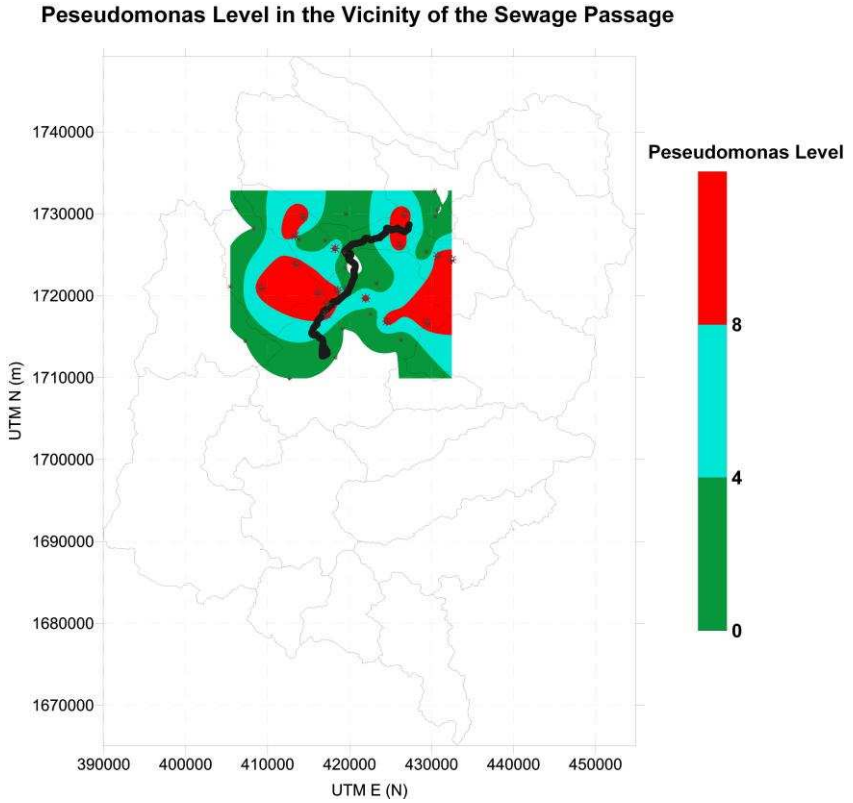

Figure 4-17 Spatial distribution of pseudomonas in the vicinity of the wastewater passage

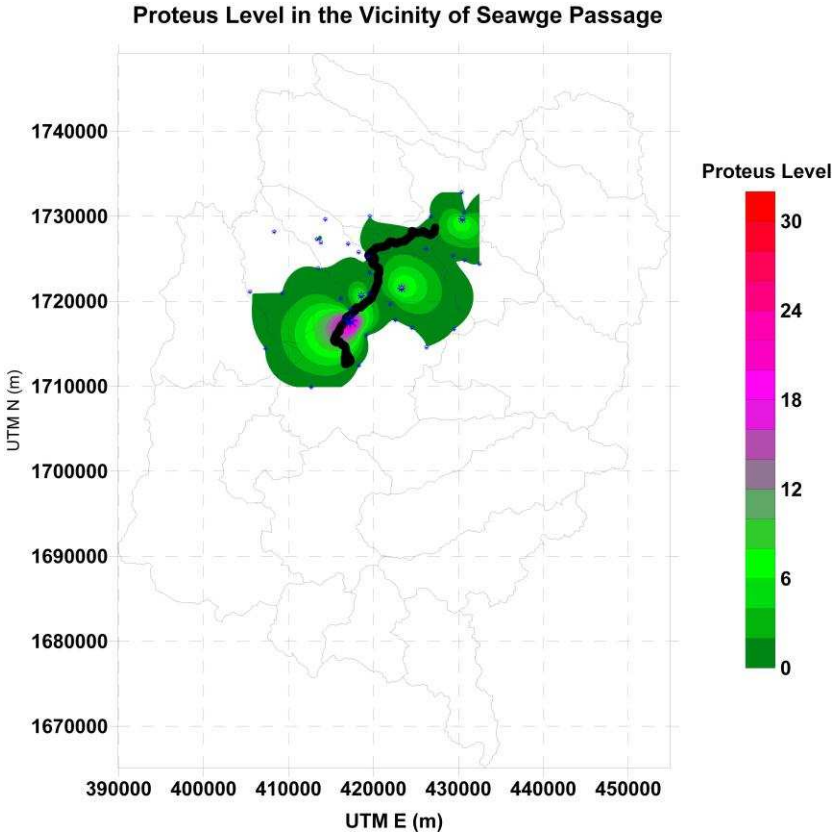

Figure 4-18 Spatial distribution of proteus in the vicinity of the wastewater passage

4.5 Analysis of Results

As shown in Figures 137 through 141, the impact of the wastewater treatment passage is not significant, except in the case of chloride. Looking at the map presented in Figure 133, chloride concentrations appear to be more elevated along the sewage passage. This phenomenon was not observed in any other parameters. Thus, it can be concluded that the wastewater passage does not have a significant impact on the groundwater quality at different levels and aquifers within its vicinity.

The microbiological water quality analyses gave the following results:

- **Alcaligene microorganisms**: Results show that high concentrations of these organisms occur only far to the south-east of the passage. Groundwater pollution with alcaligenes does not appear to be caused by the wastewater passage.
- **Citrobacter microorganisms**: Results show that there are regions of high citrobacter concentrations that coincide with the sewage passage. Another location with high concentrations can be seen in the south-west zone. Looking at the land-use map, it becomes clear that the Al-Azrakein landfill is located in this area. So this may be the main reason for the high concentration of Citrobacter. However, more studies are needed to verify this conclusion.

- **Escherichia coli microorganisms**: Results show that there are regions of high concentration along the sewage passage. Another location with high concentrations can be found in the south-west zone. Looking at the land-use map, it becomes clear that the Al-Azrakein landfill is located in this area. So this may be the main reason for the high concentration of Escherichia, (this does not appear to be true, cut/copied from above by mistake?) however more studies are needed to verify this conclusion;
- **Pseudomonas microorganisms**: Results show that there are incidences of high concentration along the sewage passage.
- **Proteus microorganisms**: Results show that this microorganism is not significantly present along the passage or in its vicinity.

Chapter 5. EVALUATION OF SANA'A BASIN WATER QUALITY FOR DIFFERENT INTENDED USES

5.1 Introduction Caution: this section seems to be directly taken out of a manual and is not referenced as such...

An integral part of any environmental monitoring program is the reporting of results to both managers and the general public. This poses a particular problem in the case of water quality monitoring because of the complexity associated with analyzing a large number of measured variables. The traditional practice has been to produce reports describing trends and compliance with official guidelines or other objectives on a variable-by-variable basis. The advantage of this approach is that it provides a wealth of data and information; however, in many cases, managers and the general public have neither the inclination nor the training to study these reports in detail. Rather, they require statements concerning the general health or status of the system of concern. One possible solution to this problem is to reduce the multivariate nature of water quality data by employing an index that will mathematically combine all water quality measures and provide a general and readily understood description of water. In this way, the index can be used to assess water quality relative to its desirable state (as defined by water quality objectives) and to provide insight into the degree to which water quality is affected by human activity. An index is a useful tool for describing the state of the water column, sediments and aquatic life and for ranking the suitability of water for use by humans, aquatic life, wildlife, etc.

A water quality index provides a convenient means of summarizing complex water quality data and facilitating its communication to a general audience. The CCME Water Quality Index (1.0) is based on a formula developed by the British Columbia Ministry of Environment, Lands and Parks and modified by Alberta Environment. The Index incorporates three elements: scope (the number of variables not meeting water quality objectives); frequency (the number of times these objectives are not met); and amplitude (the amount by which the objectives are not met). The index produces a number between 0 (worst water quality) and 100 (best water quality). These numbers are divided into 5 descriptive categories to simplify presentation.

The specific variables, objectives, and periods used in the index are not specified and indeed could vary from region to region, depending on local conditions and issues. It is recommended that a minimum of four variables, sampled at least four times, be used in the calculation of index values. It is also expected that the variables and objectives chosen will provide relevant information about a particular site. The index can be used both for tracking changes at one site over time, and for drawing comparisons among sites. If used for the latter purpose, care should be taken to ensure that there is a valid basis for comparison. Sites can be compared directly only if the same variables and objectives are used; otherwise, a comparison of the sites' ability to meet relevant objectives must be made in terms of the category obtained.

5.2 CCME Water Quality Index

An index can be used to reflect the overall and ongoing condition of the water. As with most monitoring programs, an index will not usually show the effect of spills and other such random and transient events, unless these are relatively frequent or long-lasting. The index is based on a combination of three factors: the number of variables whose objectives are not met (Scope), the frequency with which the objectives are not met (Frequency), and the amount by which the objectives are not met (Amplitude). These are combined to produce a single value (between 0 and 100) that describes water quality. Unlike some earlier indices, the basic BC formulation captures all key components of water quality, is easily calculated, and is sufficiently flexible that it can be applied in a variety of situations. The index can be very useful in tracking water quality changes at a given site over time and can also be used to compare directly among sites that employ the same variables and objectives. However, if the variables and objectives that feed into the index vary across sites, comparing among sites can be complicated. In these cases, it is best to compare sites only as to their ability to meet relevant objectives. For example, in calculating the index for a mountain stream and a prairie river, one might employ different nutrient objectives, but the sites could still be compared as to their rank (e.g. both sites are ranked as "Good" under the index). In January 1997, the Canadian Council of Ministers of the Environment (CCME) Water Quality Guidelines Task Group, in cooperation with the CCME State of the Environment Task Group, formed a technical subcommittee. The task of the subcommittee was to examine and, if necessary, modify the BC index with a view to creating a CCME Water Quality Index (CCME WQI) that could be adopted by all provinces and territories in Canada. This subcommittee examined, modified and tested the CCME WQI on artificial and "real world" data sets from a number of provinces. The final formulation of the CCME WQI, although based on the BC index, incorporates modifications developed by the province of Alberta; and closely resembles the Alberta Agricultural Water Quality Index, or AAWQI (Wright et al. 1999).

5.3 General Description of the Index

The CCME Water Quality Index relies on measures of the scope, frequency and amplitude of diversion from objectives. The index value can range from 0-100. Thus, in the CCME WQI, a value of 100 is the best possible index score and a value of 0 is the worst possible. Once the CCME WQI value has been determined, water quality is ranked by relating it to one of the following categories:

- **Excellent:** (CCME WQI Value 95-100) – water quality is protected with a virtual absence of threat or impairment; conditions very close to natural or pristine levels.
- **Good:** (CCME WQI Value 80-94) – water quality is protected with only a minor degree of threat or impairment; conditions rarely depart from natural or desirable levels.
- **Fair:** (CCME WQI Value 65-79) – water quality is usually protected but occasionally threatened or impaired; conditions sometimes depart from natural or desirable levels.
- **Marginal:** (CCME WQI Value 45-64) – water quality is frequently threatened or impaired; conditions often depart from natural or desirable levels.
- **Poor:** (CCME WQI Value 0-44) – water quality is almost always threatened or impaired; conditions usually depart from natural or desirable levels.

The assignment of CCME WQI values to these categories is termed "categorization" and represents a critical but somewhat subjective process. The categorization is based on the best available information, expert judgment, and the general public's expectations of water quality.

5.4 Data for Index Calculation

The CCME WQI provides a mathematical framework for assessing ambient water quality conditions relative to water quality objectives. It is flexible with respect to the type and number of water quality variables to be tested, the period of application, and the type of water body (stream, river reach,

lake, etc.) tested. These decisions are left to the user. Therefore, before the index is calculated, the water body, time period, variables, and appropriate objectives need to be defined.

The body of water to which the index will apply can be defined by one station (e.g. a monitoring site on a particular river reach) or by a number of different stations (e.g. sites throughout a lake). Individual stations work well, but only if there are enough data available for them. The more stations that are combined, the more general the conclusions will be.

The time period chosen will depend on the amount of data available and the reporting requirements of the user. A minimum period of one year is often used because data are usually collected to reflect this period (monthly or quarterly monitoring data). Data from different years may be combined, especially when monitoring in certain years is incomplete, but, as with combining stations, some degree of variability will be lost.

The calculation of the CCME WQI requires that at least four variables, sampled a minimum of four times, be used. However, a maximum number of variables or samples is not specified. The selection of appropriate water quality variables for a particular region is necessary for the index to yield meaningful results. Clearly, choosing a small number of variables for which the objectives are not met will provide a different picture than if a large number of variables are considered, only some of which do not meet objectives. It is up to the professional judgment of the user to determine which and how many variables should be included in the CCME WQI to most adequately summarize water quality in a particular region.

5.5 Calculation of the index

After the body of water, the period of time, and the variables and objectives have been defined, each of the three factors that make up the index must be calculated. The calculation of F1 and F2 is relatively straightforward; F3 requires some additional steps.

F1 (Scope) represents the percentage of variables that do not meet their objectives at least once during the time period under consideration ("failed variables"), relative to the total number of variables measured:

$$F_1 = \left[\frac{Number\ of\ Failed\ Variables}{Total\ Number\ of\ Variables} \right] \times 100$$

F2 (Frequency) represents the percentage of individual tests that do not meet objectives ("failed tests"):

$$F_2 = \left\{ \frac{Number\ of\ Failed\ Tests}{Total\ Number\ of\ Tests} \right\} \times 100$$

F3 (Amplitude) represents the amount by which failed test values do not meet their objectives. F3 is calculated in three steps.

The number of times by which an individual concentration is greater than (or less than, when the objective is a minimum) the objective is termed an "excursion" and is expressed as follows. When the test value must not exceed the objective:

$$excrusion_i = \left\{ \frac{Failed\ Test\ Value_i}{Objective_j} \right\} - 1.0$$

For the cases in which the test value must not fall below the objectives:

$$excursion_i = \left\{ \frac{Objective_j}{Failed\ Test\ Value_i} \right\} - 1.0$$

ii) The collective amount by which individual tests are out of compliance is calculated by summing the excursions of individual tests from their objectives and objectives and dividing by the total number of tests (both those meeting objectives and those not meeting objectives). This variable, referred to as the normalized sum of excursions or nse, is calculated as:

$$nse = \frac{\sum_{i=1}^{n} excursion_i}{Number\ of\ Tests}$$

iii) F3 is then calculated by an asymptotic function that scales the normalized sum of the excursions from objectives (*nse*) to yield a range between 0 and 100

$$F_3 = \left(\frac{nse}{0.01\, nse + 0.01} \right)$$

Once the factors have been obtained, the index itself can be calculated by summing the three factors as if they were vectors. The sum of the squares of each factor is therefore equal to the square of the index. This approach treats the index as a three-dimensional space defined by each factor along one axis. With this model, the index changes in direct proportion to changes in all three factors.

CCME Water Quality Index

$$CCMEWQ = 100 - \left\{ \frac{\sqrt{F_1^2 + F_2^2 + F_3^2}}{1.732} \right\}$$

The divisor 1.732 normalizes the resultant values to a range between 0 and 100, where 0 represents the "worst" water quality and 100 represents the "best" water quality.

5.6 Water Quality Index for the Sana'a Basin

Water quality samples that were collected from the Sana'a Basin and analyzed in chapter 13 were used to determine the water quality index of the entire Sana'a Basin. The CCME water quality index was used for this application following the steps presented above. The water quality index for drinking water, irrigation and livestock was calculated and the output results are presented in the following Figures 142 through 144).

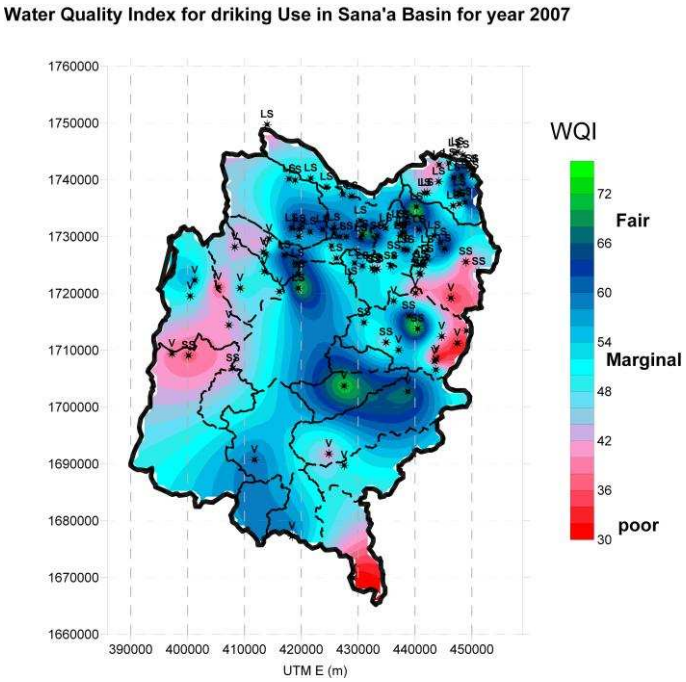

Figure 5-1 Water quality index for Sana'a basin water - suitability for drinking (using CCME index approach)

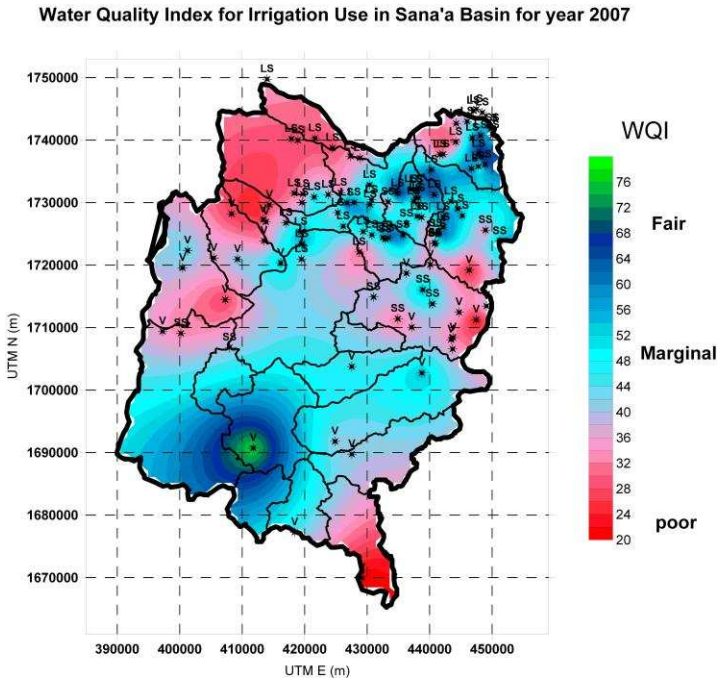

Figure 5-2 Water quality index for Sana'a Basin water - suitability for irrigation (using CCME index approach)

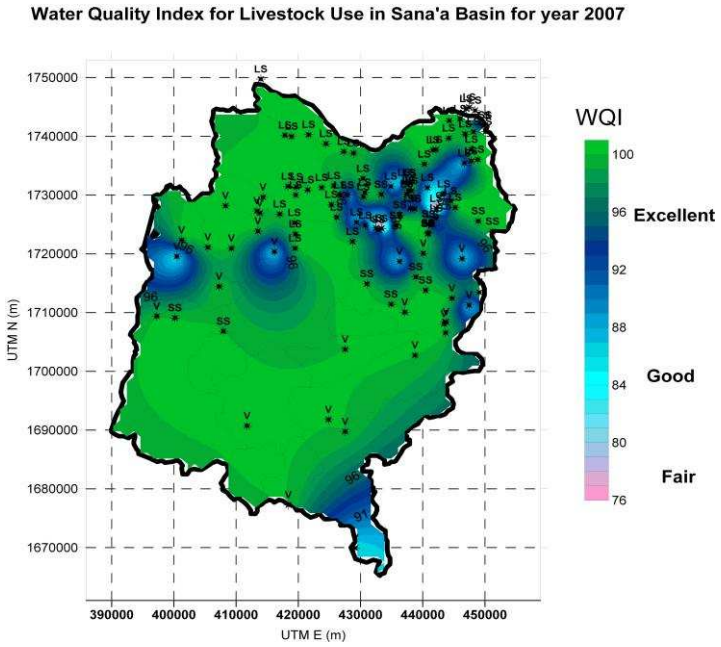

Figure 5-3 Water quality index for Sana'a Basin water - suitability for livestock (using CCME index approach)

5.7 Interpretation of Water Quality Index Maps

From the water index map of drinking water (Figure 142), it can be concluded that water quality in most of the basin area is ranked in the range of marginal to fair based on the CCME index. However, in some locations, water quality is evaluated as poor. In general, this index value does not mean that water is dangerous for human health. The index level instead indicates that there are some parameters that are either below minimum values or exceeding maximum permissible values under Yemeni standards. The worst occurrences of water quality are: Wadi Sanhan in the southern part of the basin, the area between Wadi Zahr and Wadi Iqbal on the western side of the basin, and the area between Wadi Al-Sirr and Wadi Asir on the eastern side of the basin. From the water index spatial distribution map for irrigation water (Figure 143), it can be concluded that there are many locations where the water quality is evaluated to be poor for irrigation use. The areas where the 'poor' water quality index for irrigation purposes occurs are in the following wadis:

- Wadi Sanhan, in the southern part of the basin;
- Starting from Wadi Iqbal on the east side of the basin and all the wadis located north of Wadi Iqbal on the west side (as shown by the red and light red colors in the figure);
- Wadi Al- Sirr on the east side of the basin;
- Wadi Al-Maadi in the north part of the basin.

From the water index spatial distribution map for livestock water (Figure 144), it can be concluded that the water quality for livestock is considered "excellent" for the entire basin, with the exception of some scattered locations where the index indicates the "good" level.

Chapter 6. WATER TYPE ANALYSIS FOR THE SANA'A BASIN

6.1 Introduction

In the current section, the output results for the analysis of the water quality samples using Aquachem Software will be presented in tables and figures. Figures 145 through 172 show the outputs of the Aquachem software, and tables 10 through 13 present the water type results in tabulated format for the alluvial, limestone, sandstone and volcanic aquifers. Interpretations for these data will be presented in the Activity 1 project report.

SampleID	StationID	Water Type	Water Type
106	HSA16	Ca-Mg-Cl-SO4	2
125	HS161	Ca-Mg-HCO3-SO4	1
82	HS150	Ca-Na-HCO3-Cl	3
72	HS69	Ca-Na-HCO3-Cl	3
99	HSA94	Ca-Na-HCO3-Cl	1
112	HSA104	Ca-Na-HCO3-Cl-SO4	1
89	HSA90	Ca-Na-HCO3-Cl-SO4	1
115	HSA74	Mg-Na-Ca-Cl-SO4-HCO3	2
107	HSA100	Na-Ca-Cl-HCO3-SO4	2
108	HSA101	Na-Ca-Cl-HCO3-SO4	2
100	HSA95	Na-Ca-HCO3-SO4-Cl	4
119	HSA110	Na-HCO3-Cl-SO4	2
111	HSA7	Na-HCO3-Cl-SO4	4
98	HSA93	Na-HCO3-Cl-SO4	4
103	HSA98	Na-HCO3-SO4	4

Table 6-1 Water type for alluvial aquifer water samples

SampleID	StationID	Water Type	Water Type
33	HS95	Ca-HCO3	1
52	HS115	Ca-Mg-Cl-SO4-HCO3	1

SampleID	StationID	Water Type	Water Type
39	HS102	Ca-Mg-HCO3	1
40	HS104	Ca-Mg-HCO3	1
35	HS99	Ca-Mg-HCO3	1
1	HSA63	Ca-Mg-HCO3	1
2	HSA65	Ca-Mg-HCO3	1
3	HSA66	Ca-Mg-HCO3	1
20	HSA77	Ca-Mg-HCO3	1
21	HSA80	Ca-Mg-HCO3	1
22	HSA83	Ca-Mg-HCO3	1
15	HS78	Ca-Mg-HCO3-SO4	1
25	HS84	Ca-Mg-HCO3-SO4	1
6	HSA69	Ca-Mg-HCO3-SO4	1
7	HSA70	Ca-Mg-HCO3-SO4	1
8	HSA71	Ca-Mg-HCO3-SO4	1
10	HSA73	Ca-Mg-HCO3-SO4	1
14	HS77	Ca-Mg-HCO3-SO4-Cl	1
19	HS82	Ca-Mg-HCO3-SO4-Cl	1
109	HSA102	Ca-Mg-Na-Cl-HCO3	1
23	HS83	Ca-Mg-Na-Cl-HCO3-SO4	1
38	HS101	Ca-Mg-Na-HCO3	1
11	HSA74	Ca-Mg-Na-HCO3-Cl-SO4	1
9	HSA72	Ca-Mg-Na-HCO3-SO4	1
28	HS88	Ca-Mg-Na-HCO3-SO4-Cl	1
94	HS27	Ca-Mg-Na-SO4	2
116	HSA107	Ca-Mg-Na-SO4	2

SampleID	StationID	Water Type	Water Type
56	HS121	Ca-Mg-Na-SO4-HCO3	2
118	HSA109	Ca-Mg-Na-SO4-HCO3	1
55	HS120	Ca-Mg-SO4	2
48	HS24	Ca-Mg-SO4	2
34	HS96	Ca-Mg-SO4	2
54	HS119	Ca-Mg-SO4-Cl	2
16	HS79	Ca-Mg-SO4-Cl	1
32	HS93	Ca-Na-HCO3-Cl	1
36	HS34	Ca-Na-Mg-Cl-HCO3-SO4	2
29	HS89	Ca-Na-Mg-Cl-HCO3-SO4	1
57	HS122	Ca-Na-Mg-SO4	2
97	HSA92	Ca-Na-Mg-SO4	2
49	HS112	Ca-Na-Mg-SO4-HCO3	2
12	HSA75	Mg-Ca-Na-Cl-SO4-HCO3	1
43	HS106	Mg-Ca-Na-SO4-Cl	2
110	HSA103	Na-Ca-Cl-HCO3	2
53	HS117	Na-Ca-Cl-HCO3-SO4	2
37	HS100	Na-Ca-Mg-Cl-HCO3-SO4	2
30	HS90	Na-Ca-Mg-HCO3-Cl	4
102	HSA97	Na-Ca-Mg-HCO3-SO4	4
44	HS107	Na-Ca-Mg-HCO3-SO4-Cl	4
95	HS28	Na-Ca-SO4-HCO3	2
96	HSA91	Na-Ca-SO4-HCO3	2
26	HS85	Na-Cl-SO4	2
114	HSA106	Na-HCO3	4

SampleID	StationID	Water Type	Water Type
5	HSA68	Na-HCO3	3
4	HSA67	Na-HCO3-Cl	4
13	HSA76	Na-HCO3-SO4	4
31	HS91	Na-Mg-Ca-Cl-SO4-HCO3	2
113	HSA105	Na-Mg-Ca-HCO3-Cl	2
17	HS80	Na-Mg-Ca-HCO3-SO4	1
18	HS81	Na-Mg-Ca-SO4-HCO3	2
45	HS108	Na-Mg-HCO3-SO4-Cl	4
117	HSA108	Na-SO4-HCO3-Cl	4
96	HSA91	Na-Ca-SO4-HCO3	2

Table 6-2 Water type for limestone aquifer water samples

StationID	SampleID	Water Type	Water Type
HS25	41	Ca-HCO3-SO4	1
HS110	46	Ca-Mg-HCO3-Cl	1
HS113	50	Ca-Mg-HCO3-Cl	1
HS120	55	Ca-Mg-HCO3-Cl	1
HS102	39	Ca-Mg-HCO3-SO4	1
HS104	40	Ca-Mg-HCO3-SO4	1
HS34	36	Ca-Mg-HCO3-SO4	1
HS106	43	Ca-Mg-Na-Cl-HCO3-SO4	2
HS95	33	Ca-Mg-Na-Cl-SO4	2
HS100	37	Ca-Mg-Na-HCO3	1
HS107	44	Ca-Mg-Na-HCO3-SO4-Cl	1
HS121	56	Ca-Mg-SO4	2

StationID	SampleID	Water Type	Water Type
HS90	30	Ca-Mg-SO4	1
HS91	31	Ca-Mg-SO4-HCO3	1
HS99	35	Ca-Mg-SO4-HCO3	1
HS108	45	Ca-Na-Cl-HCO3-SO4	1
HS112	49	Ca-Na-Cl-SO4-HCO3	2
HS24	48	Ca-Na-HCO3-Cl	1
HS31	47	Ca-Na-Mg-Cl-SO4	2
HS96	34	Ca-Na-Mg-HCO3-SO4-Cl	1
HS115	52	Ca-Na-SO4	2
HS105	42	Ca-SO4-HCO3	1
HS119	54	Mg-Ca-HCO3-Cl	1
HS101	38	Mg-Ca-HCO3-SO4	1
HS18	51	Na-Ca-SO4-HCO3-Cl	2

Table 6-3 Water type for sandstone aquifer water samples

SampleID	StationID	Water Type	Water Type
64	HS129	Ca-HCO3-Cl-SO4	1
65	HS164	Ca-Mg-Cl-HCO3	1
68	HS134	Ca-Mg-Cl-HCO3-SO4	1
69	HSH12	Ca-Mg-HCO3	1
70	HSH30	Ca-Mg-HCO3	1
71	HSS31	Ca-Mg-HCO3-Cl	1
73	HSH10	Ca-Mg-Na-HCO3	4
74	HSS44	Ca-Mg-Na-HCO3	1
75	HS145	Ca-Na-Cl-SO4-HCO3	2

SampleID	StationID	Water Type	Water Type
77	HSS19	Ca-Na-HCO3-Cl	3
127	HSH11	Ca-Na-Mg-HCO3-Cl	3
84	HSS10	Ca-Na-Mg-HCO3-Cl	3
85	HSS11	Ca-Na-Mg-HCO3-Cl	1
86	HSH8	Ca-Na-Mg-HCO3-CO3	1
87	HSA87	Mg-Na-Ca-HCO3-Cl	1
88	HS142	Na-Ca-Cl-HCO3-SO4	2
105	HS136	Na-Ca-HCO3-Cl	3
91	HSS40	Na-Ca-HCO3-Cl	3
104	HS143	Na-Ca-HCO3-SO4-Cl	2
129	HSH14	Na-Ca-Mg-HCO3	3
130	HS131	Na-Ca-SO4-Cl-HCO3	2
140	HS140	Na-Cl-SO4	4
90	HSA84	Na-HCO3	4
135	HSA86	Na-HCO3	4
136	HSA99	Na-HCO3-Cl	4
137	HS144	Na-HCO3-Cl-SO4	4
141	HSA85	Na-HCO3-SO4	1
142	HSA88	Na-HCO3-SO4	4
143	HS139	Na-Mg-Ca-HCO3-SO4	3

Table 6-4 Water type for volcanic aquifer water samples

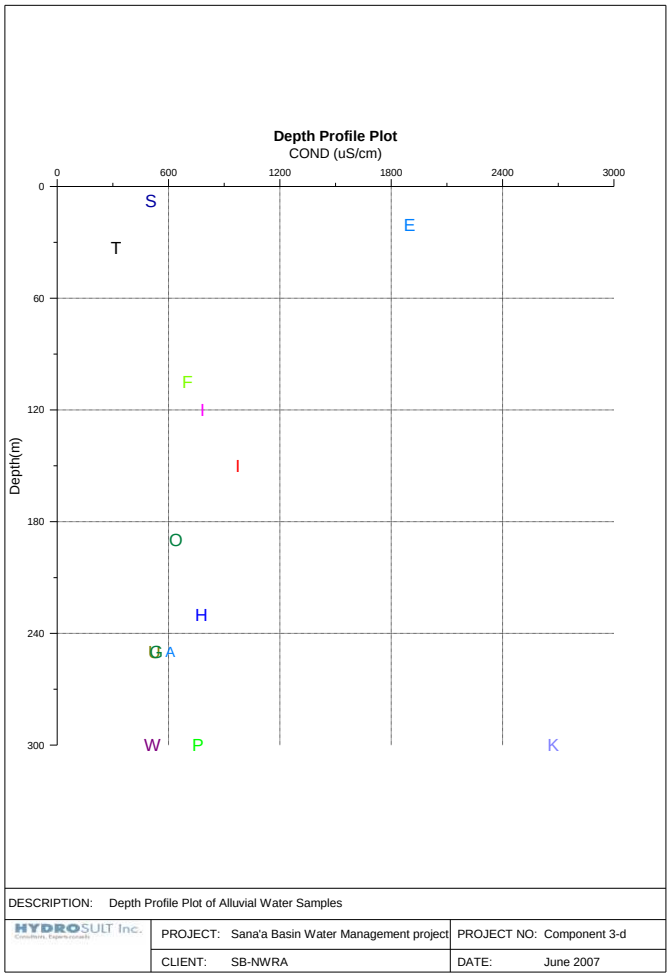

Figure 6-1 Depth profile plot for alluvial water quality samples based on Hydrosult data (2007)

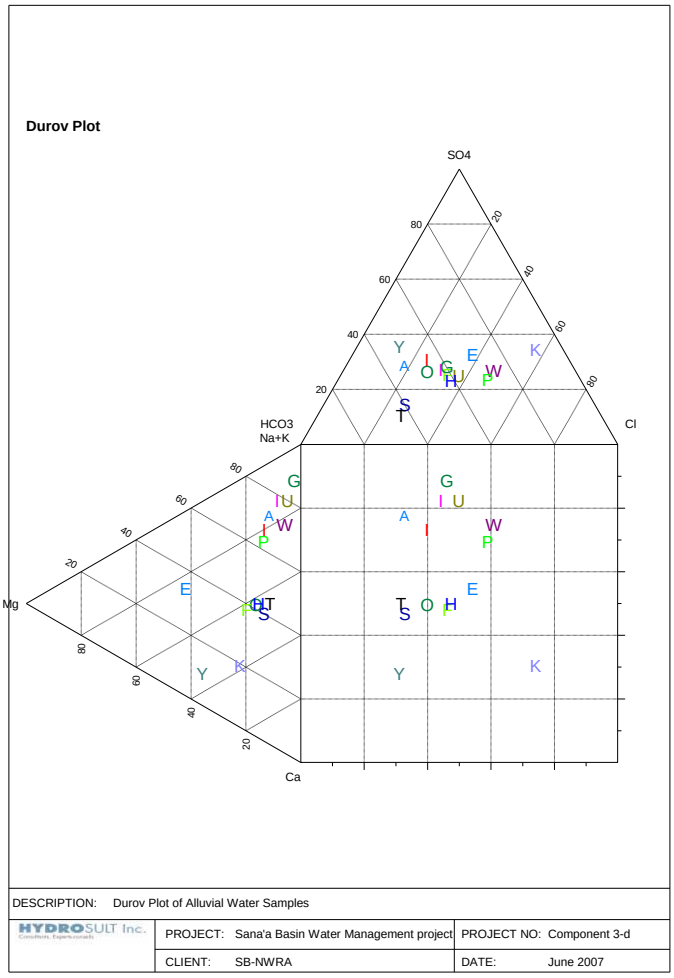

Figure 6-2 Durov plot for alluvial water quality samples based on Hydrosult data (2007)

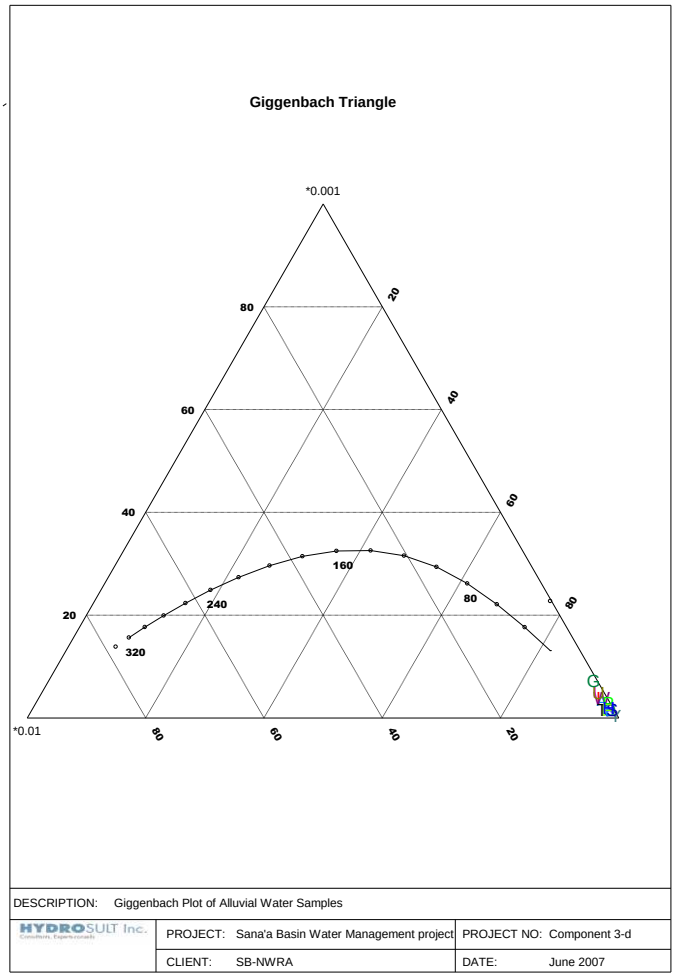

Figure 6-3 Giggenbach plot for alluvial water quality samples based on Hydrosult data (2007)

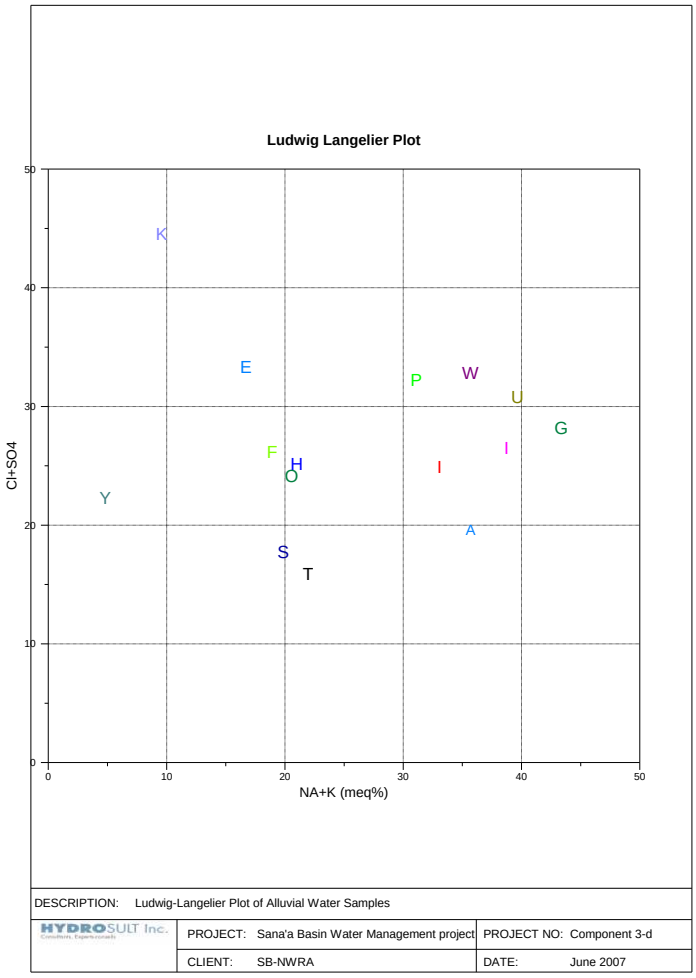

Figure 6-4 Ludwig-Langelier plot for alluvial water quality samples based on Hydrosult data (2007)

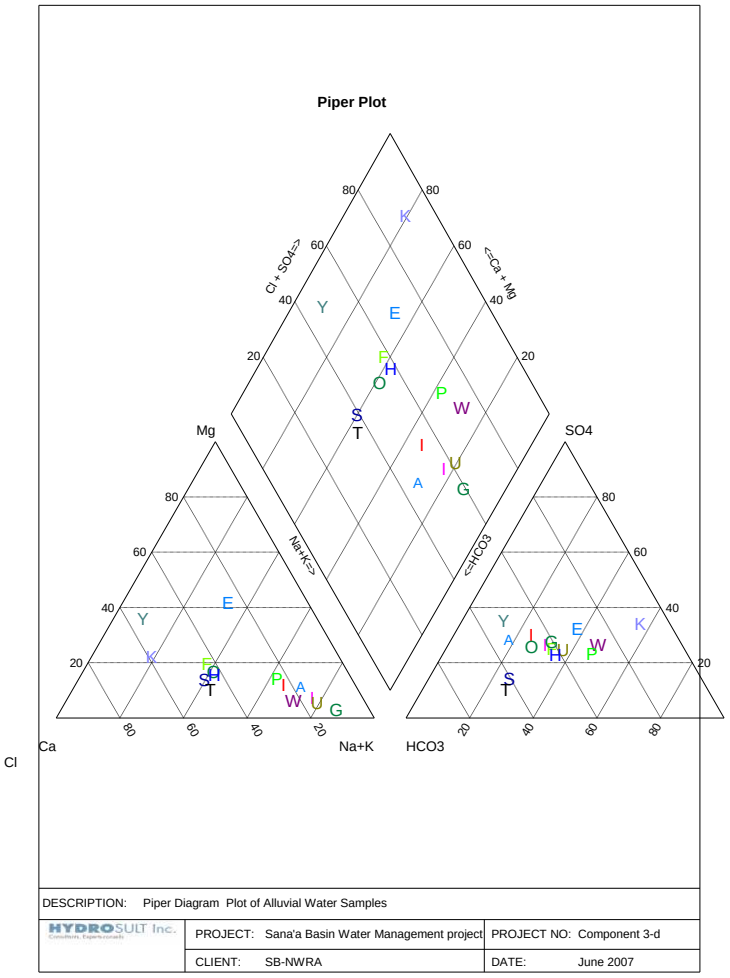

Figure 6-5 Piper diagram for alluvial water quality samples based on Hydrosult data (2007)

Figure 6-6 Ternary plot for alluvial water quality samples based on Hydrosult data (2007)

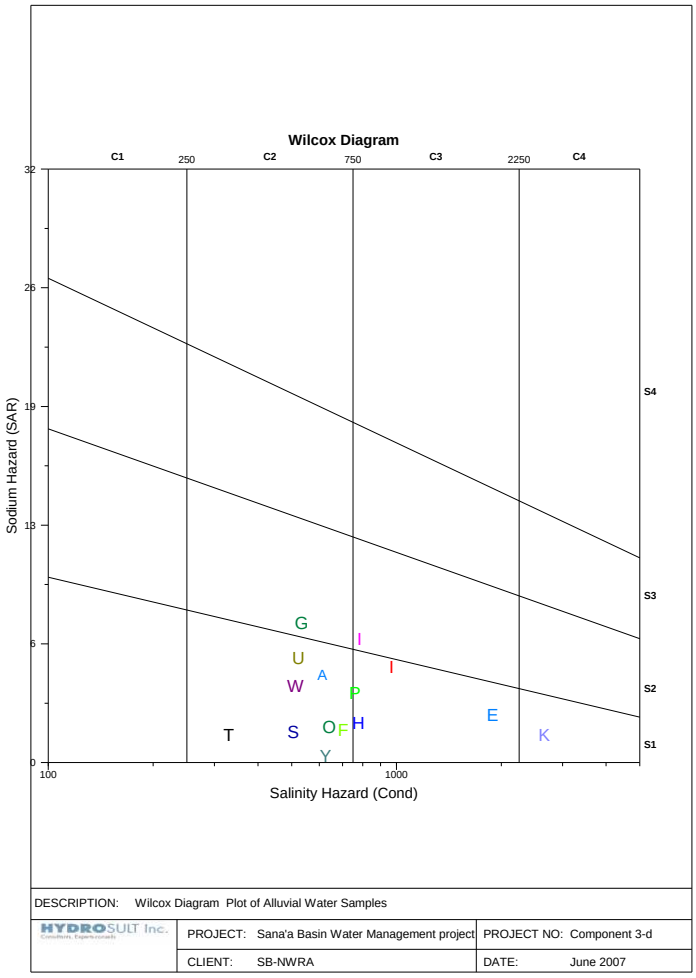

Figure 6-7 Wilcox diagram plot for alluvial water quality samples based on Hydrosult data (2007)

Limestone Aquifer

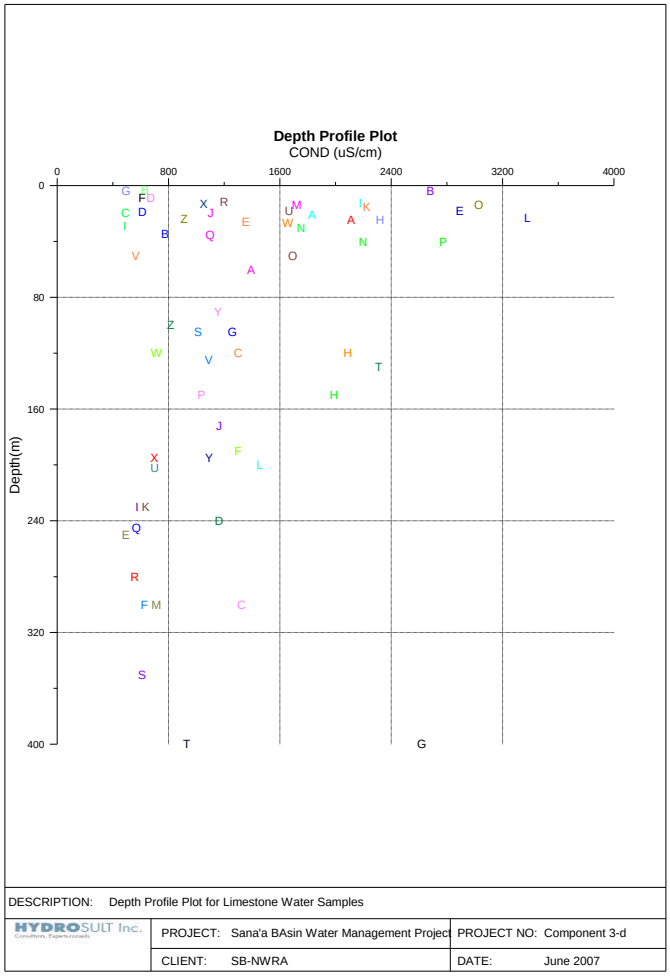

Figure 6-8 Depth profile plot for limestone water quality samples based on Hydrosult data (2007)

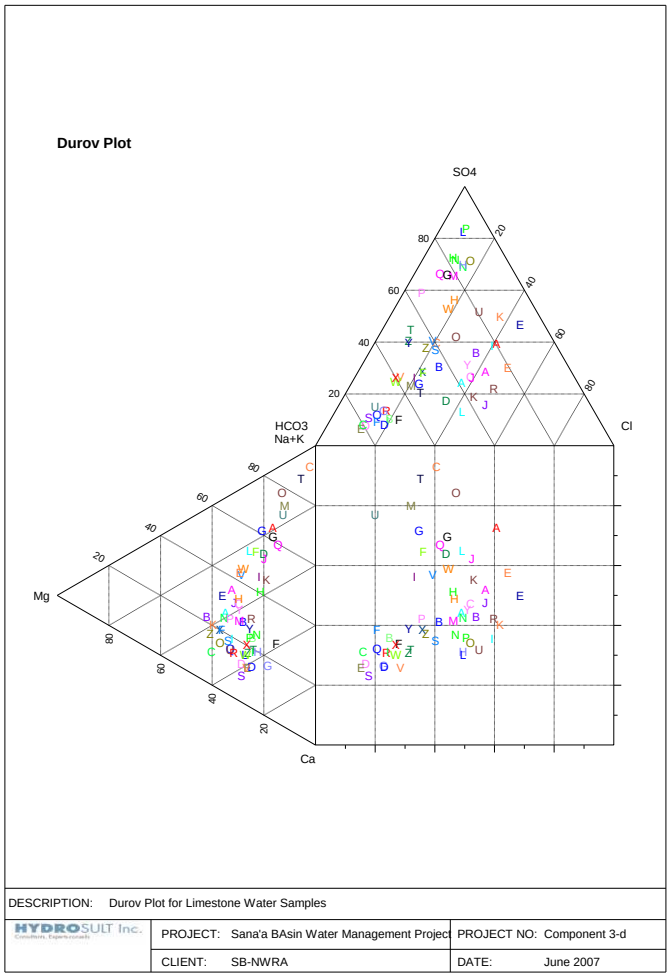

Figure 6-9 Durov plot for limestone water quality samples based on Hydrosult data (2007)

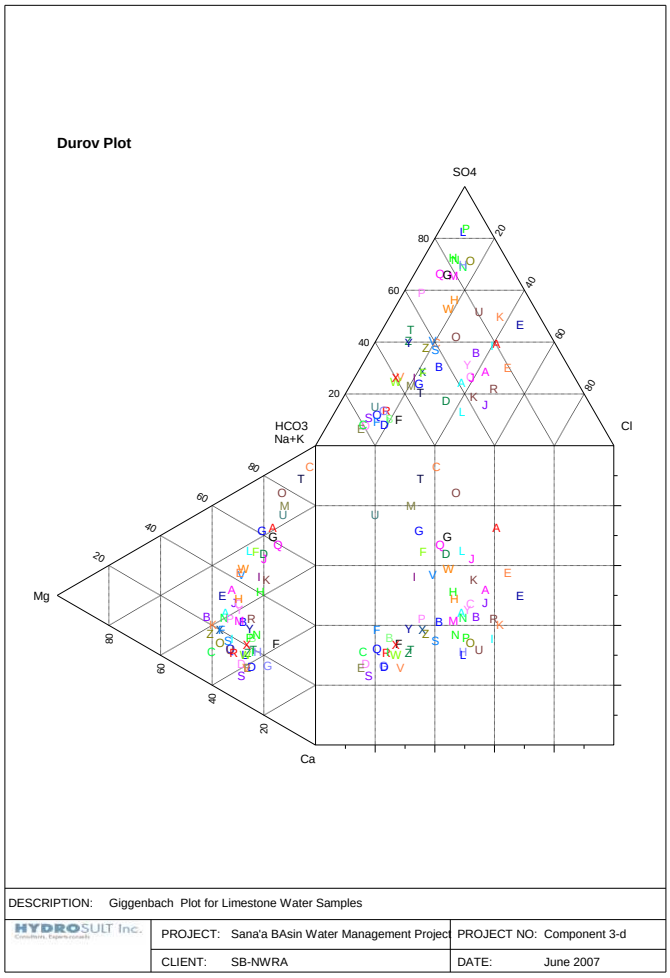

Figure 6-10 Giggenbach plot for limestone water quality samples based on Hydrosult data (2007)

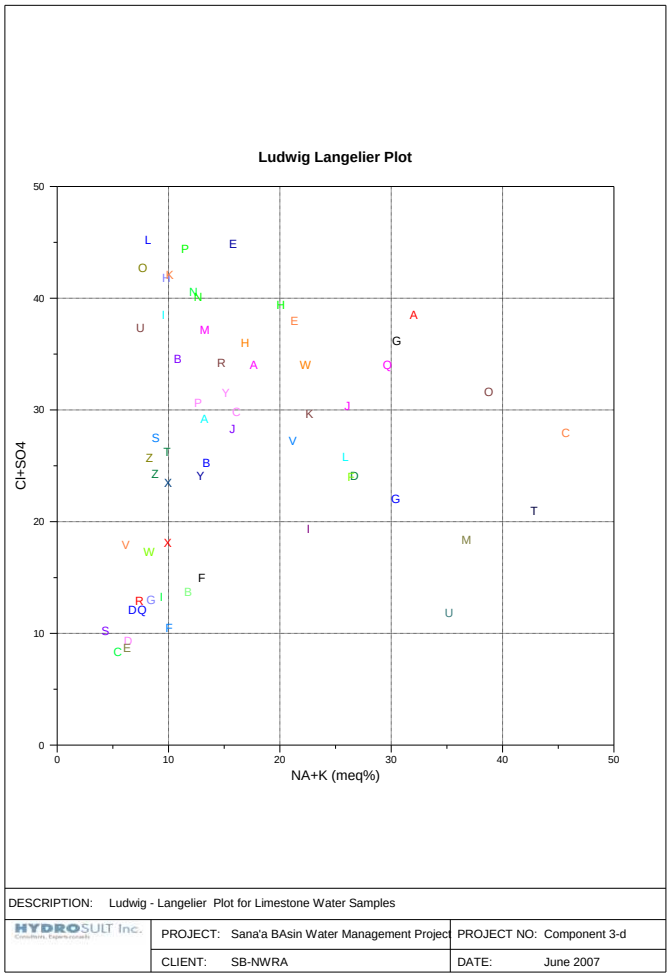

Figure 6-11 Ludwig-Langelier plot for limestone water quality samples based on Hydrosult data (2007)

Figure 6-12 Piper diagram plot for limestone water quality samples based on Hydrosult data (2007)

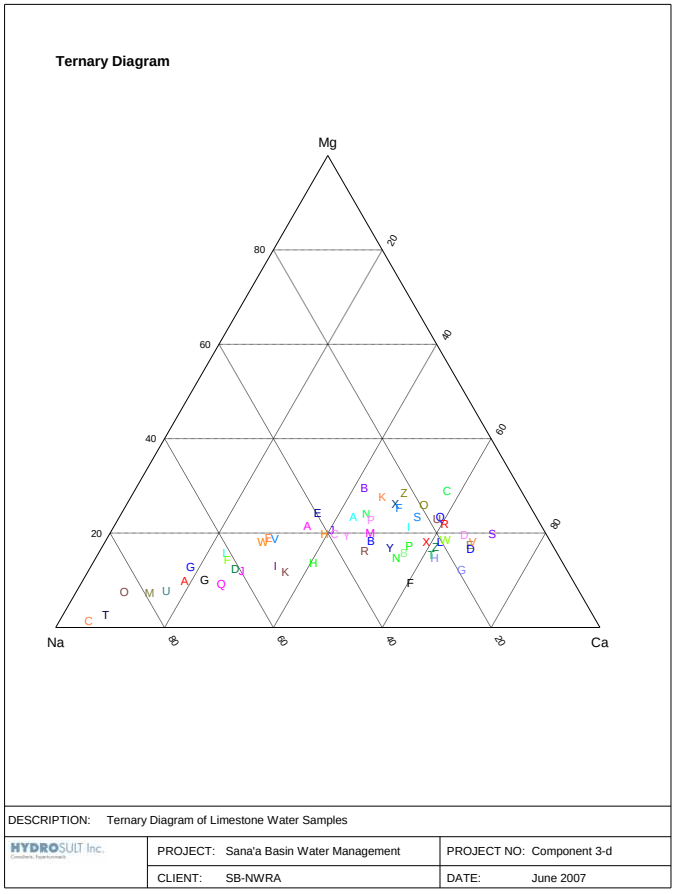

Figure 6-13 Ternary diagram plot for limestone water quality samples based on Hydrosult data (2007)

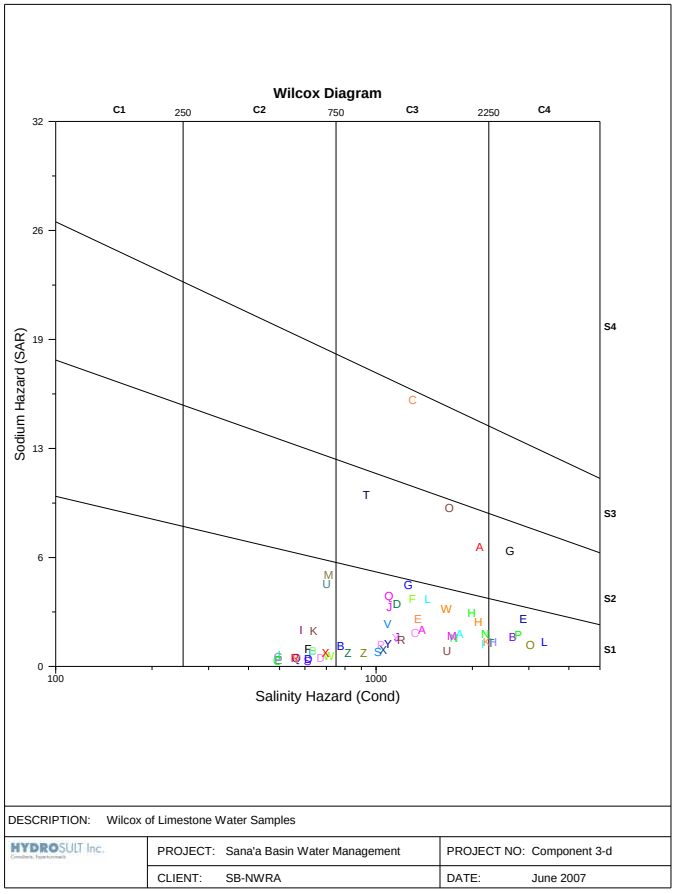

Figure 6-14 Wilcox diagram plot for limestone water quality samples based on Hydrosult data (2007)

Sandstone Aquifer

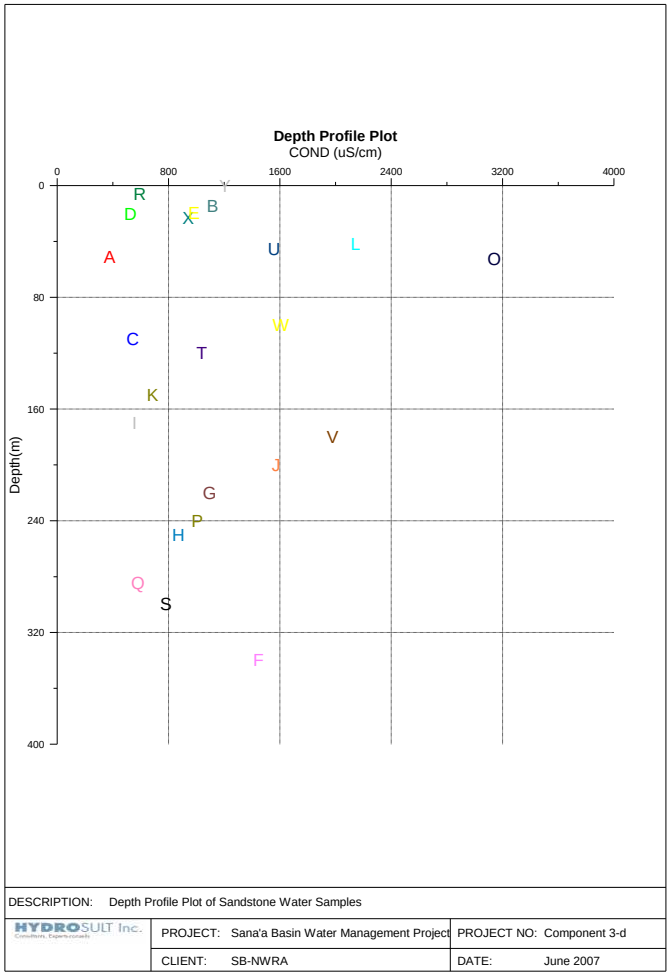

Figure 6-15 Depth profile plot for sandstone water quality samples based on Hydrosult data (2007)

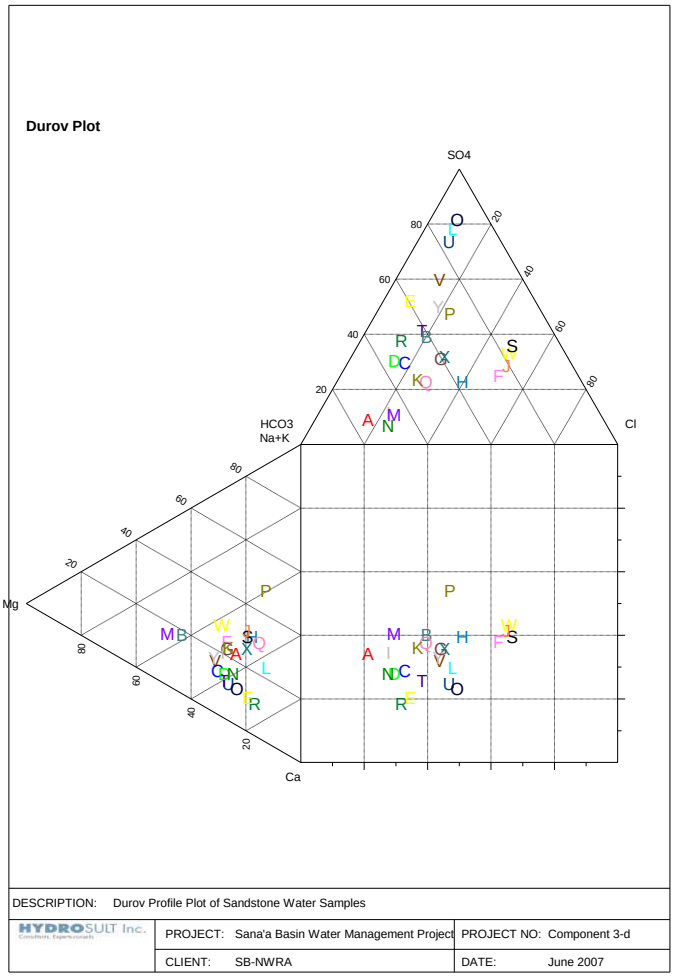

Figure 6-16 Durov profile plot for sandstone water quality samples based on Hydrosult data (2007)

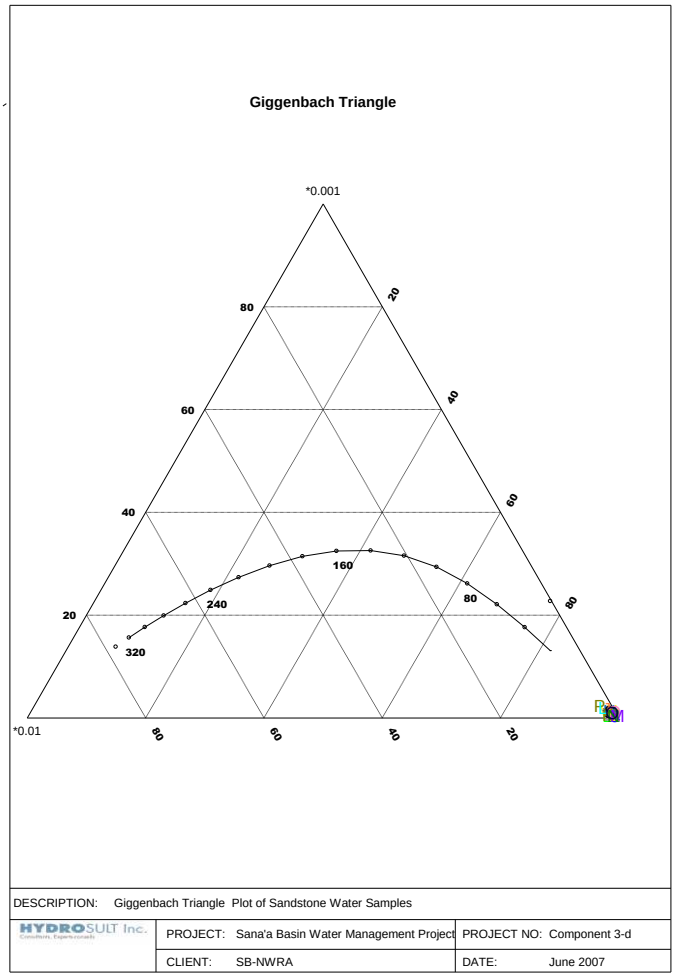

Figure 6-17 Giggenbach triangle plot for sandstone water quality samples based on Hydrosult data (2007)

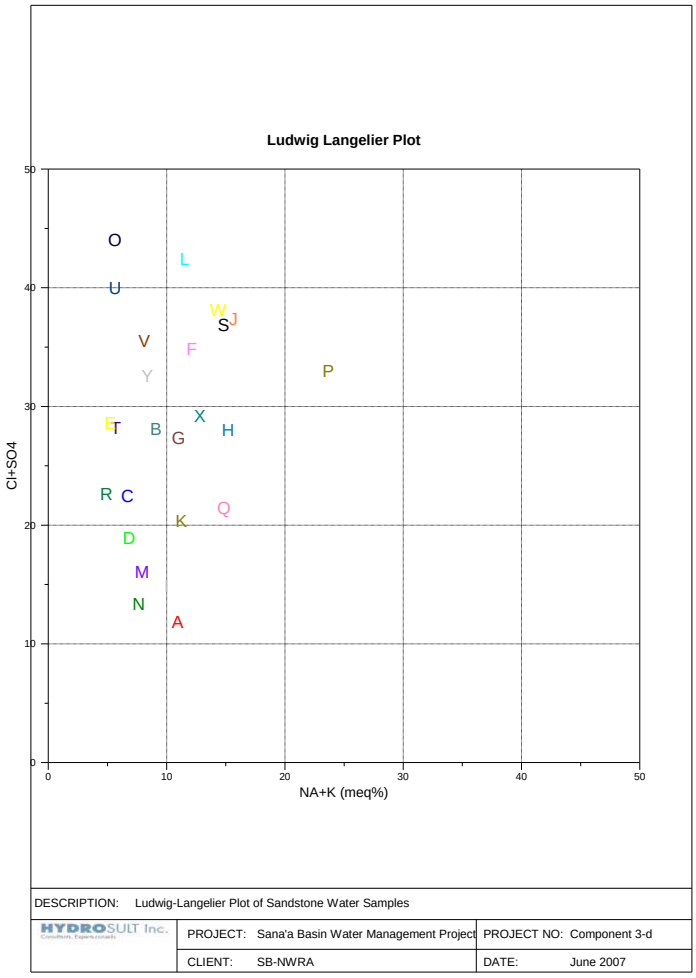

Figure 6-18 Ludwig-Langelier plot for sandstone water quality samples based on Hydrosult data (2007)

Figure 6-19 Piper plot for sandstone water quality samples based on Hydrosult data (2007)

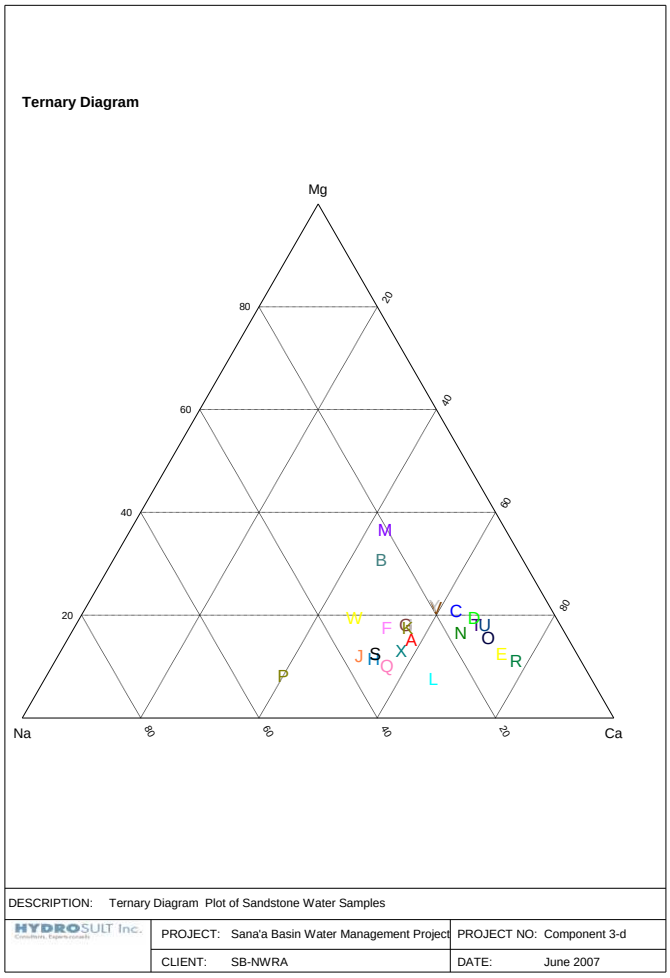

Figure 6-20 Ternary diagram plot for sandstone water quality samples based on Hydrosult data (2007)

Figure 6-21 Wilcox diagram plot for sandstone water quality samples based on Hydrosult data (2007)

Volcanic Aquifer

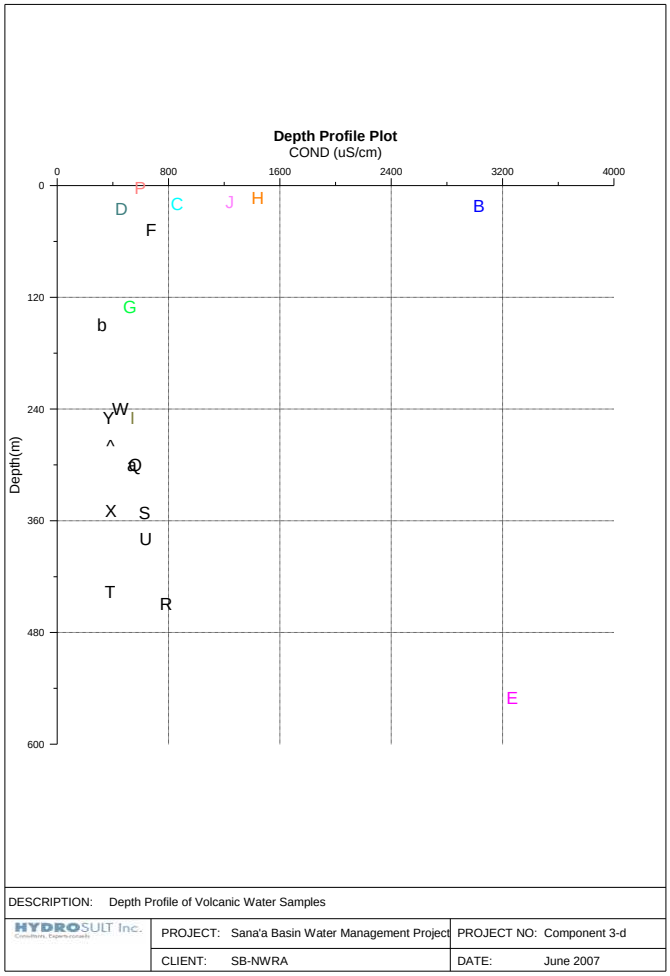

Figure 6-22 Depth profile plot for volcanic water quality samples based on Hydrosult data (2007)

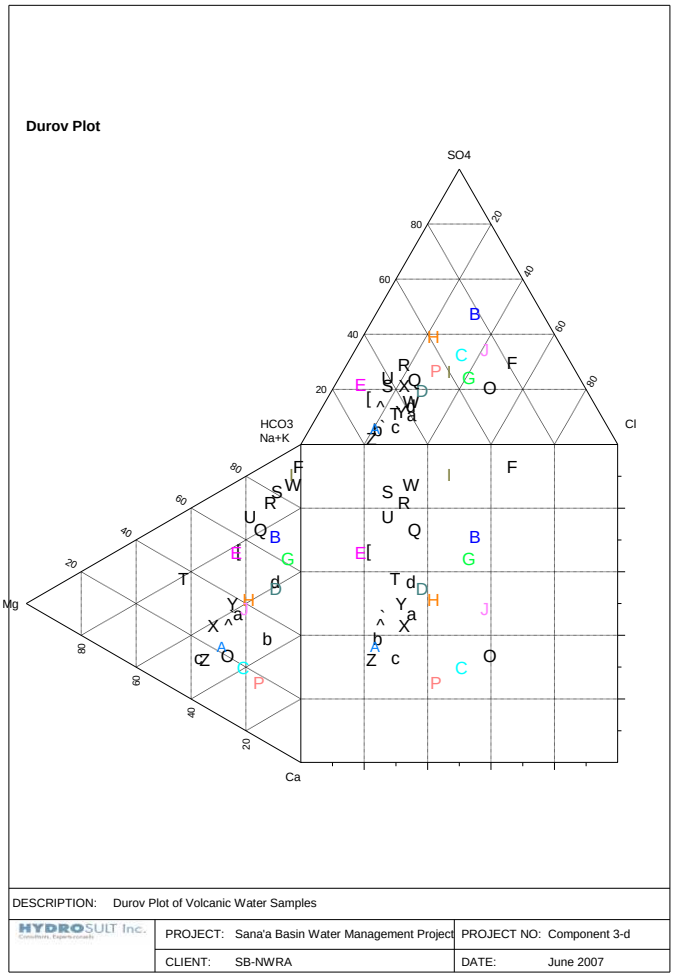

Figure 6-23 Durov plot for volcanic water quality samples based on Hydrosult data (2007)

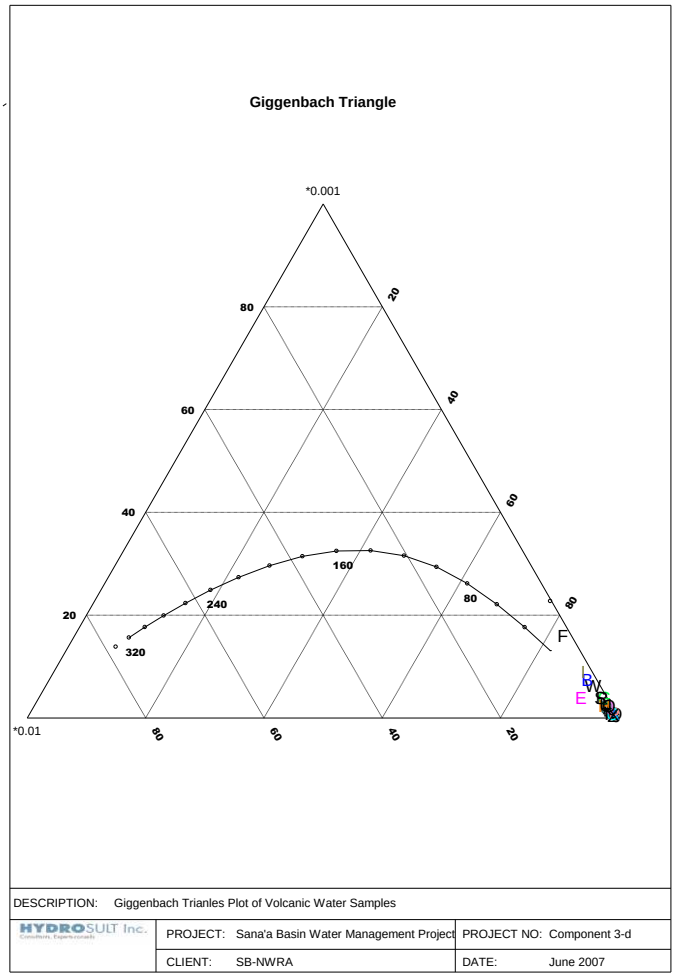

Figure 6-24 Giggenbach triangle plot for volcanic water quality samples based on Hydrosult data (2007)

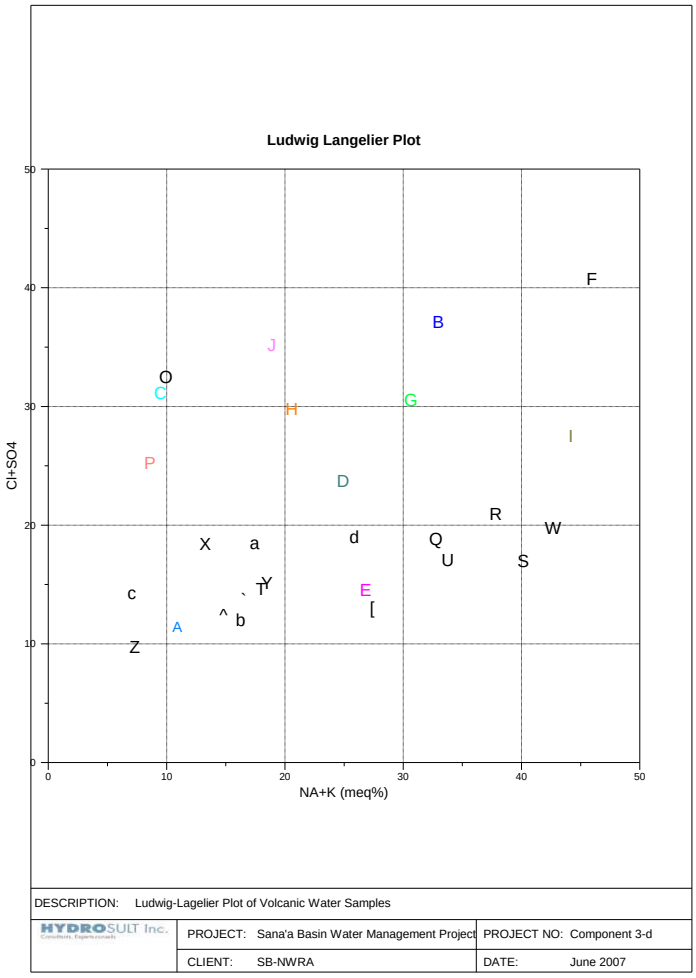

Figure 6-25 Ludwig-Lagelier plot for volcanic water quality samples based on Hydrosult data (2007)

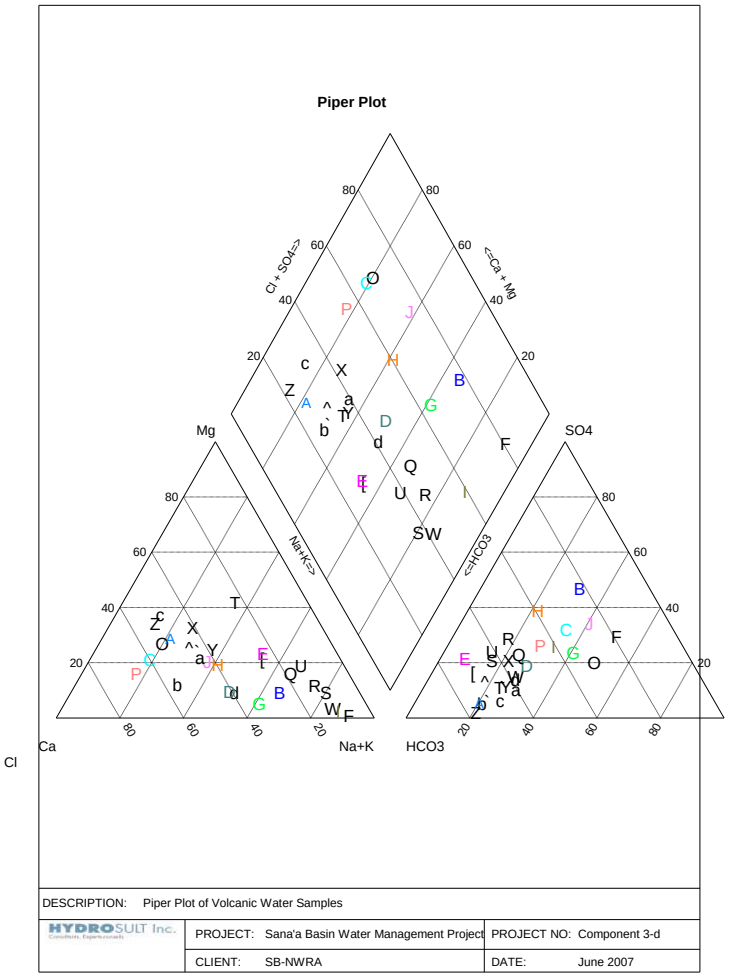

Figure 6-26 Piper diagram plot for volcanic water quality samples based on Hydrosult data (2007)

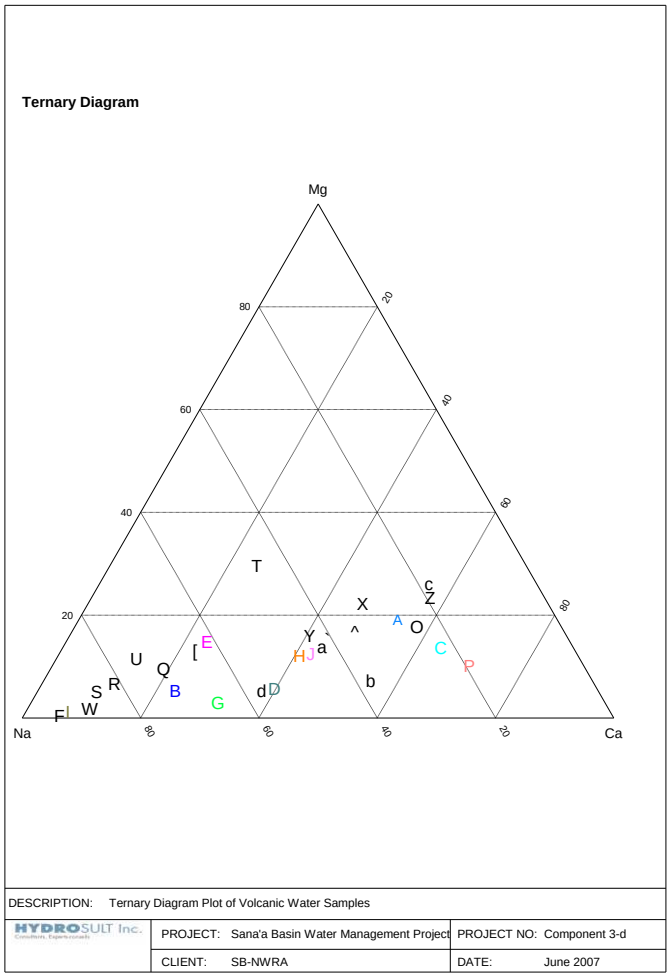

Figure 6-27 Ternary diagram plot for volcanic water quality samples based on Hydrosult data (2007)

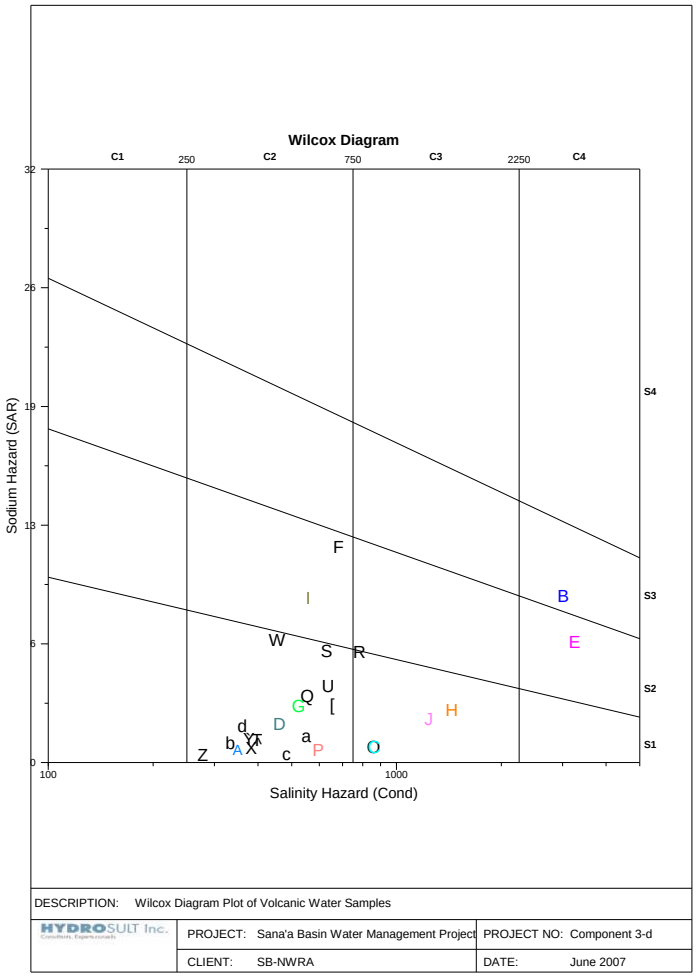

Figure 6-28 Wilcox diagram plot for volcanic water quality samples based on Hydrosult data (2007)

Chapter 7. FINAL WATER QUALITY MONITORING STATIONS FOR THE SANA'A BASIN

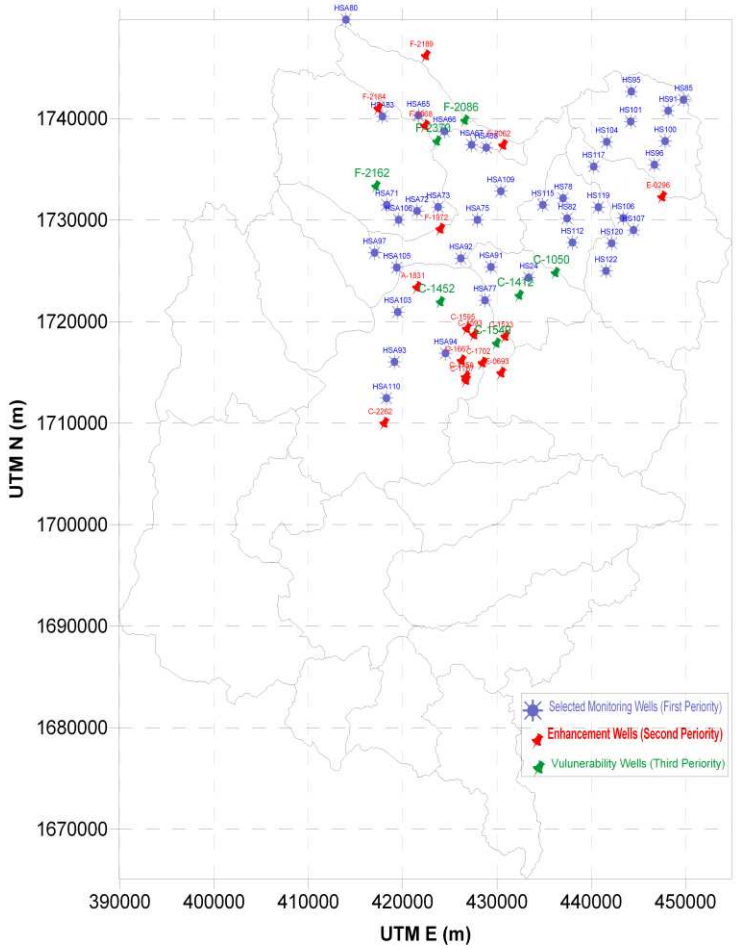

Figure 7-1 Map showing the locations for the water quality monitoring stations within the limestone aquifer.

The priority for installation is as follows: First priority for the selected monitoring stations (blue stars), second priority for enhancement locations (red pins), and the third priority for vulnerability wells (green pins).

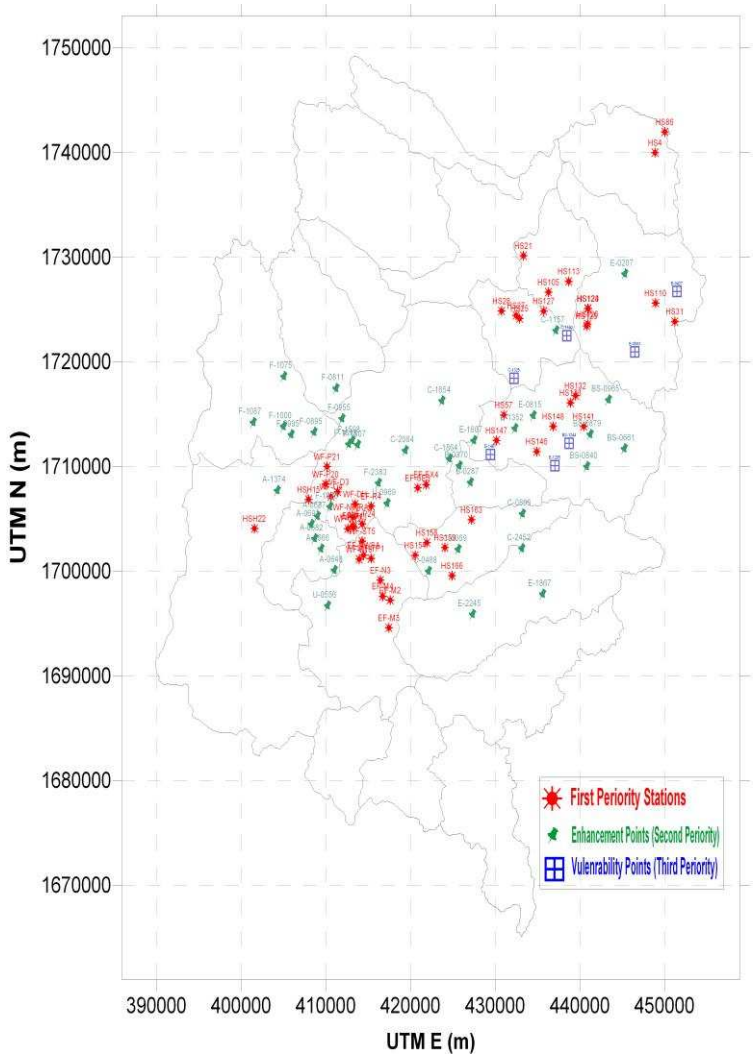

Figure 7-2 Map showing the locations for the water quality monitoring stations within the sandstone aquifer

The priority for installation is as follows: first priority for the selected monitoring stations (red stars), second priority for enhancement locations (green pins) and third priority for vulnerability wells (blue boxes).

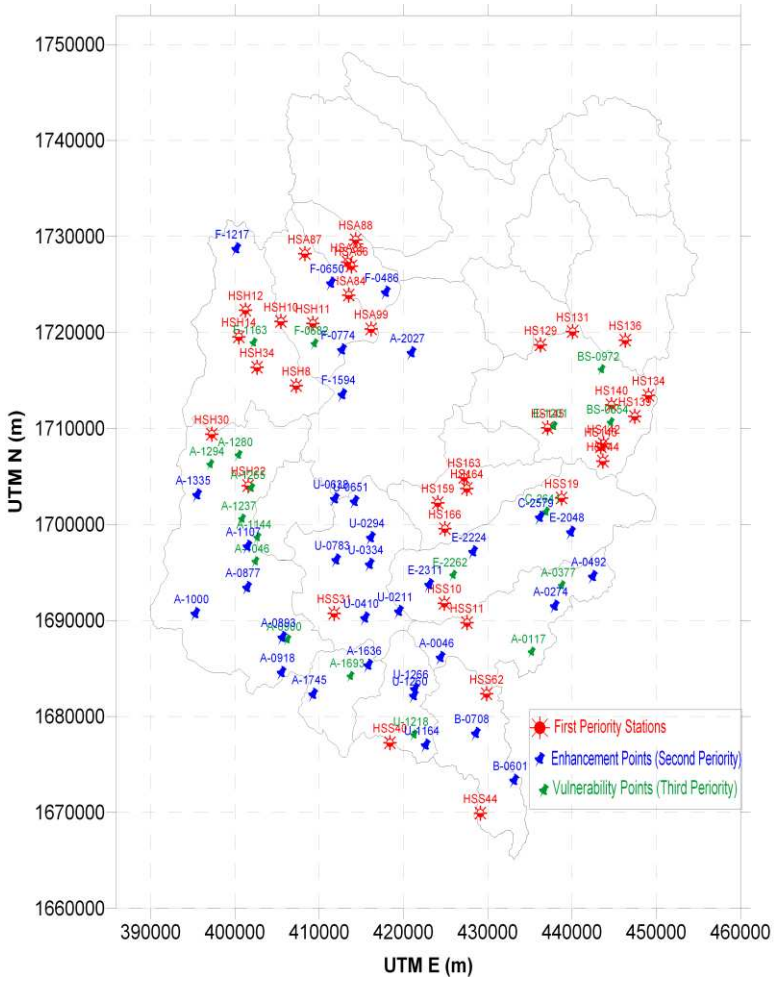

Figure 7-3 Map showing the locations for the water quality monitoring stations within the volcanic aquifer.

The priority for installation is as follows: first priority for the selected monitoring stations (red stars), second priority for enhancement locations (blue pins) and third priority for vulnerability wells (green pins).

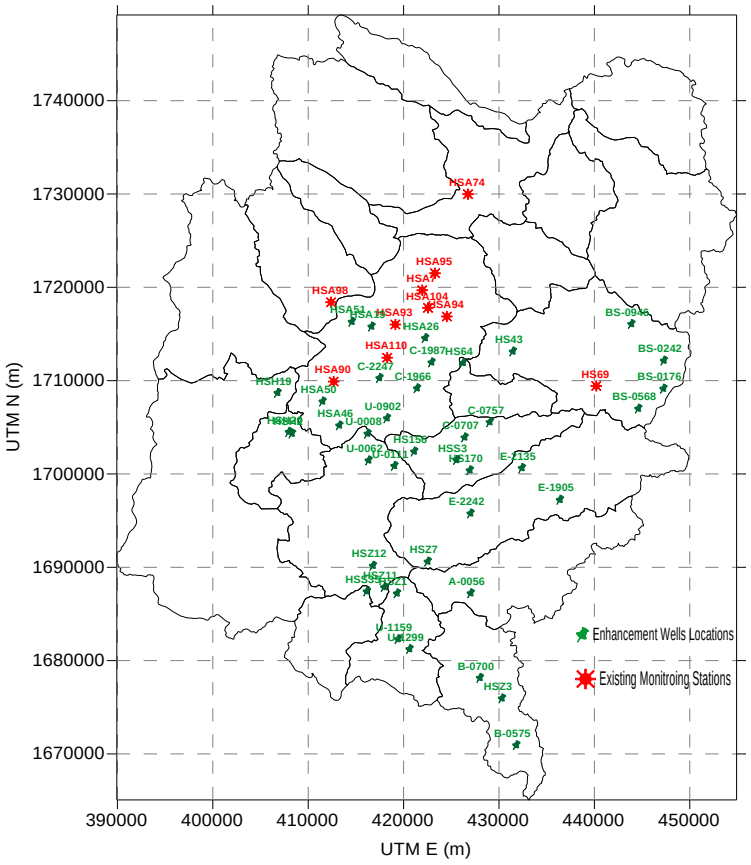

Figure 7-4 Map showing the locations for the water quality monitoring stations within the alluvial aquifer.

The priority for installing is as follows: first priority for the selected monitoring stations (red stars), second priority for enhancement locations (green pins)

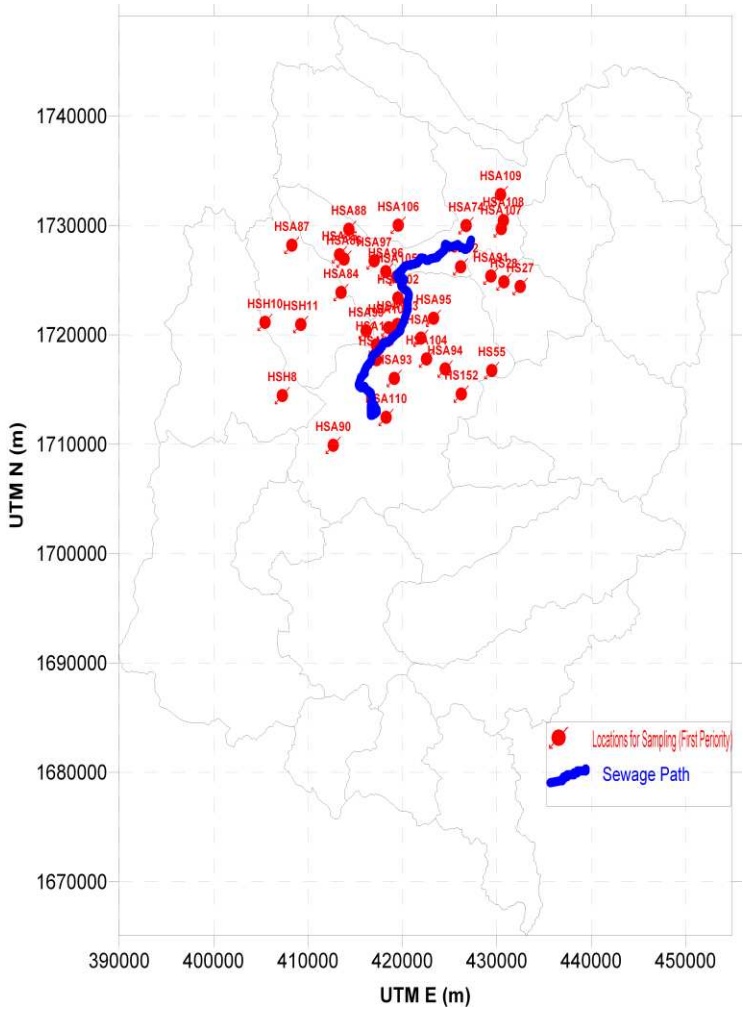

Figure 7-5 Map showing the locations for the water quality monitoring stations for the area in the vicinity of sewage path (red circles)

Ser No	Well ID	UTM (E)	UTM(N)	Ser No	Well ID	UTM (E)	UTM(N)
1	HSA83	417850	1740194	23	HS119	440747	1731266
2	HSA65	421656	1740289	24	HS24	433352	1724317
3	HSA66	424439	1738751	25	HSA77	428717	1722095

Ser No	Well ID	UTM (E)	UTM(N)	Ser No	Well ID	UTM (E)	UTM(N)
4	HSA67	427306	1737420	26	HSA94	424535	1716871
5	HSA68	428859	1737137	27	HSA93	419134	1716018
6	HSA71	418317	1731495	28	HSA110	418279	1712455
7	HSA72	421515	1730889	29	HSA72	421515	1730889
8	HSA73	423760	1731279	30	HSA73	423760	1731279
9	HSA75	427928	1730022	31	HSA105	419380	1725310
10	HSA109	430402	1732830	32	HSA92	426167	1726223
11	HS115	434859	1731484	33	HSA91	429370	1725365
12	HS82	437433	1730165	34	HSA77	428717	1722095
13	HS78	437008	1732149	35	HS122	441564	1724984
14	HS101	444166	1739703	36	HS104	441635	1737691
15	HS91	448148	1740768	37	HS101	444166	1739703
16	HS100	447830	1737774	38	HSA106	419567	1730016
17	HS95	444245	1742667	39	HS112	438002	1727781
18	HS96	446690	1735446	40	HSA103	419477	1720943
19	HS117	440254	1735268	41	HS107	444468	1729011
20	HS122	441564	1724984	42	HSA80	413979	1749744
21	HS120	442159	1727703	43	HS85	449783	1741843
22	HS106	443383	1730190	44	HSA97	417010	1726772

Table 7-1 First priority water quality monitoring stations in the limestone aquifer

Ser No	Well ID	UTM (E)	UTM(N)
1	F-2189	422017	1745489
2	F-2184	416979	1740288

Ser No	Well ID	UTM (E)	UTM(N)
3	F-2368	421924	1738577
4	F-1972	423569	1728398
5	F-2062	430214	1736665
6	C-1593	427144	1717991
7	C-1595	426382	1718589
8	C-2262	417627	1709275
9	C-1533	430448	1717839
10	C-1667	425820	1715432
11	C-1702	428033	1715227
12	C-1758	426240	1713841
13	C-1767	426298	1713511
14	E-0693	430015	1714227
15	E-0296	447083	1731578

Table 7-2 Second priority water quality monitoring stations in the limestone aquifer (well ID based on WEC 2001 Survey)

Ser No	Well ID	UTM (E)	UTM(N)	Ser No	Well ID	UTM (E)	UTM(N)
1	HS123	440981	1725057	16	HS146	434905	1711413
2	HS127	435733	1724826	17	HS147	430155	1712477
3	HS4	448870	1739967	18	HS57	431026	1714902
4	HS86	450033	1741936	19	HS148	436845	1713808
5	HS25	432883	1724121	20	HS21	433332	1730112
6	HS105	436297	1726629	21	HSA85	413350	1727319
7	HS110	448929	1725596	22	HS27	432478	1724413

Ser No	Well ID	UTM (E)	UTM(N)	Ser No	Well ID	UTM (E)	UTM(N)
8	HS31	451212	1723827	23	HS28	430758	1724836
9	HS113	438693	1727668	24	HS154	420565	1701499
10	HS124	440946	1725071	25	HS158	421924	1702707
11	HS125	440794	1723402	26	HS159	424075	1702243
12	HS126	440909	1723588	27	HS163	427202	1704895
13	HS132	439478	1716748	28	HS166	424917	1699550
14	HS133	438891	1716072	29	HSH15	407966	1706823
15	HS141	440459	1713806	30	HSH22	401575	1704051

Table 7-3 First priority water quality monitoring stations in sandstone aquifer (well ID based on Hydrosult 2007 survey)

Ser No	Well ID	UTM (E)	UTM(N)	Ser No	Well ID	UTM (E)	UTM(N)
1	P7	409000	1707850	24	EX3	421251	1706952
2	P10	413503	1703816	25	EX4	421852	1708250
3	P13	413296	1704211	26	TP2	415540	1702000
4	P14	410593	1706303	27	SE3	420860	1707950
5	P15	409405	1709557	28	B	418463	1701355
6	P16	413945	1701124	29	C	417228	1701068
7	P17	409559	1708837	30	D	417264	1702475
8	P19	414028	1700030	31	SF	419219	1703783
9	P20	409972	1708292	32	G	419194	1702725
10	P21	410159	1709961	33	K	419480	1704601
11	P22	414479	1700679	34	M	420642	1705129
12	P23	414401	1703554	35	M1	413204	1704330
13	P24	414301	1704500	36	M2	417609	1697217

Ser No	Well ID	UTM (E)	UTM(N)	Ser No	Well ID	UTM (E)	UTM(N)
14	DH	413470	1706400	37	M3	417458	1694581
15	ST5	414300	1702850	38	M4	416728	1697588
16	ST7	412400	1704800	39	M5	418091	1700298
17	ST13	412097	1707294	40	Q	419956	1703132
18	O3	411401	1707565	41	T	417885	1701005
19	O4	410628	1707093	42	W	416205	1700850
20	O11	413524	1703238	43	Y	417084	1700542
21	O12	412601	1704029	44	NWSA	414480	1701500
22	TP1	415350	1701200	45	R4	415355	1706200
23	NWRA3	413200	1705137	46	N3	416455	1699120

Table 7-4 Second priority water quality monitoring stations in sandstone aquifer (well ID based on NWSA survey)

Ser No	Well ID	UTM (E)	UTM(N)	Ser No	Well ID	UTM (E)	UTM(N)
1	C-1654	423361	1715694	21	F-0955	411567	1713996
2	C-2084	419031	1710949	22	F-1607	413404	1711492
3	F-1613	412347	1711572	23	F-0895	408257	1712694
4	F-1828	410120	1705575	24	F-0995	405549	1712468
5	F-2383	415862	1707830	25	F-1000	404645	1713233
6	A-0648	410645	1699504	26	F-1075	404692	1718019
7	A-0666	409076	1701553	27	F-1087	401070	1713638
8	C-1864	424219	1710168	28	A-1374	403912	1707134
9	BS-0661	444887	1711118	29	A-0682	408325	1702524
10	BS-0840	440454	1709420	30	A-0687	408653	1704681
11	BS-0879	440867	1712484	31	A-0691	407912	1703889

Ser No	Well ID	UTM (E)	UTM(N)	Ser No	Well ID	UTM (E)	UTM(N)
12	BS-0965	443018	1715791	32	E-0207	444965	1727815
13	E-0815	434127	1714281	33	C-1157	436825	1722405
14	E-1607	427134	1711891	34	U-0969	416887	1705905
15	B-0287	426735	1707900	35	U-0556	409866	1696112
16	B-0370	425417	1709489	36	C-2452	432807	1701582
17	C-0488	421760	1699425	37	E-1867	435252	1697227
18	C-0069	425269	1701517	38	E-2245	426970	1695301
19	C-0896	432857	1704901	39	E-1352	431985	1713054
20	F-0811	410857	1716883	40	F-1598	412739	1711882

Table 7-5 Third priority water quality monitoring stations in sandstone aquifer (well ID based on NWSA survey)

Ser No	Well ID	UTM (E)	UTM(N)
1	C-1325	432224	1718410
2	BS-1244	438735	1712206
3	E-1205	437039	1710062
4	E-1487	429429	1711137
5	C-1150	438450	1722482
6	E-0427	451455	1726695
7	E-0503	446484	1720921

Table 7-6 Fourth priority water quality monitoring stations in sandstone aquifer (well ID based on NWSA survey)

Ser No	Well ID	UTM (E)	UTM(N)	Ser No	Well ID	UTM (E)	UTM(N)
1	HS166	424917	1699550	19	HSS11	427537	1689763
2	HS159	424075	1702243	20	HSS19	438762	1702751

Ser No	Well ID	UTM (E)	UTM(N)	Ser No	Well ID	UTM (E)	UTM(N)
3	HS163	427202	1704895	21	HSH30	397248	1709399
4	HSH22	401575	1704051	22	HSS31	411771	1690739
5	HS129	436267	1718700	23	HSS40	418400	1677271
6	HS131	440083	1720084	24	HSS44	429126	1669927
7	HS134	449088	1713454	25	HSKK	402616	1716368
8	HS136	446320	1719200	26	HSKK	429864	1682361
9	HS139	447450	1711272	27	HSA84	413496	1723877
10	HS140	444695	1712454	28	HSA85	413350	1727319
11	HS142	443756	1708408	29	HSA86	413814	1726919
12	HS143	443420	1708089	30	HSA87	408295	1728198
13	HS144	443669	1706585	31	HSA88	414334	1729656
14	HS145	437115	1710061	32	HSH8	407277	1714451
15	HS164	427530	1703755	33	HSH10	405457	1721136
16	HSH12	401253	1722329	34	HSH11	409246	1720948
17	HSH14	400459	1719547	35	HSA99	416163	1720363
18	HSS10	424849	1691790	35	HSA99	416163	1720363

Table 7-7 First priority water quality monitoring stations in volcanic aquifer (well ID based on Hydrosult 2007 survey)

Ser No	Well ID	UTM (E)	UTM(N)	Ser No	Well ID	UTM (E)	UTM(N)
1	F-0486	417440	1723417	18	U-0334	415527	1695079
2	F-0650	410920	1724366	19	U-0410	414970	1689490
3	A-2027	420488	1717113	20	U-0651	413733	1701621
4	A-0877	400968	1692670	21	U-0783	411556	1695530
5	A-0893	405163	1687478	22	E-2048	439398	1698440

Ser No	Well ID	UTM (E)	UTM(N)	Ser No	Well ID	UTM (E)	UTM(N)
6	A-0918	405054	1683823	23	E-2224	427790	1696386
7	A-1000	394840	1689943	24	E-2311	422569	1692975
8	A-1745	408820	1681536	25	A-0046	423945	1685367
9	F-0774	412242	1717431	26	A-0274	437480	1690733
10	F-1594	412281	1712761	27	A-1636	415353	1684565
11	F-1217	399695	1727944	28	U-1164	422173	1676246
12	A-1107	401010	1696956	29	U-1260	420758	1681404
13	A-1335	395043	1702323	30	U-1266	420871	1682098
14	A-0492	441993	1693819	31	B-0601	432681	1672572
15	U-0638	411377	1701899	32	C-2579	435714	1699977
16	U-0211	418991	1690179	33	B-0708	428110	1677466
17	U-0294	415663	1697857	33	B-0708	428110	1677466

Table 7-8 Second priority water quality monitoring stations in volcanic aquifer (well ID based on WEC 2001 survey)

Ser No	Well ID	UTM (E)	UTM(N)
1	BS-0654	444207	1710013
2	BS-0972	443134	1715535
3	E-1201	437446	1709621
4	A-0900	405847	1687411
5	A-1693	413327	1683595
6	F-0682	409059	1718224
7	F-1163	401812	1718310
8	A-1046	402049	1695527
9	A-1144	402276	1698036

Ser No	Well ID	UTM (E)	UTM(N)
10	A-1237	400462	1699984
11	A-1265	401552	1703196
12	A-1280	400057	1706623
13	A-1294	396684	1705652
14	E-2262	425531	1694105
15	A-0117	434835	1686123
16	A-0377	438398	1693034
17	U-1218	420873	1677500
18	C-2641	436526	1700718

Table 7-9 Third priority water quality monitoring stations in volcanic aquifer (well ID based on WEC 2001 survey)

Ser No	Well ID	UTM (E)	UTM(N)
1	HS69	440194	1709431
2	HSA90	412671	1709899
3	HSA93	419134	1716018
4	HSA94	424535	1716871
5	HSA95	423296	1721513
6	HSA98	412395	1718404
7	HSA7	421957	1719694
8	HSA104	422559	1717798
9	HSA74	426751	1729981
10	HSA110	418279	1712455

Table 7-10 First priority water quality monitoring stations in the alluvial aquifer (well ID based on Hydrosult 2007 survey)

Ser. No.	Well ID	UTM E	UTM N	Ser. No.	Well ID	UTM E	UTM N
1	BS-0242	446971	1711659	21	U-0111	418715	1700374
2	BS-0946	443562	1715572	22	HSZ3	429988	1675461
3	C-0707	426077	1703424	23	HSZ1	418990	1686713
4	C-0757	428717	1705065	24	HSS35	415819	1686930
5	BS-0176	446918	1708650	25	HSZ11	417650	1687381
6	BS-0568	444286	1706509	26	HSZ12	416473	1689675
7	U-0902	417939	1705482	27	HSZ7	422211	1690122
8	U-0062	416013	1700961	28	HS170	426623	1699905
9	E-1905	436073	1696744	29	HSS3	425231	1701003
10	E-2135	432082	1700144	30	HS156	420794	1701918
11	E-2242	426695	1695279	31	HSH2	407985	1703832
12	A-0056	426716	1686726	32	HSH20	407651	1704018
13	U-1159	419094	1681809	33	HSA46	412944	1704711
14	U-1299	420302	1680741	34	HSA50	411185	1707277
15	B-0575	431497	1670446	35	HSH19	406473	1708203
16	B-0700	427684	1677661	36	HS64	425915	1711408
17	C-1966	421092	1708688	37	HS43	431132	1712635
18	C-1987	422614	1711466	38	HSA26	421938	1714069
19	C-2247	417151	1709783	39	HSA19	416322	1715307
20	U-0008	415907	1703830	40	HSA51	414258	1715814

Table 7-11 Second priority water quality monitoring stations in the alluvial aquifer (well ID based on Hydrosult 2007 survey and WEC 2001 Survey)

Ser No	Well ID	UTM (E)	UTM(N)	Aquifer
1	HSA84	413496	1723877	Volcanic

Ser No	Well ID	UTM (E)	UTM(N)	Aquifer
2	HSA85	413350	1727319	Volcanic
3	HSA86	413814	1726919	Volcanic
4	HSA87	408295	1728198	Volcanic
5	HSA88	414334	1729656	Volcanic
6	HSA90	412671	1709899	Alluvial
7	HSH8	407277	1714451	Volcanic
8	HSH10	405457	1721136	Volcanic
9	HS152	426243	1714598	Sandstone
10	HS55	429466	1716736	Sandstone
11	HS27	432478	1724413	Limestone
12	HS28	430758	1724836	Limestone
13	HSA91	429370	1725365	Limestone
14	HSA92	426167	1726223	Limestone
15	HSA93	419134	1716018	Alluvium
16	HSA94	424535	1716871	Alluvium
17	HSA95	423296	1721513	Alluvium
18	HSA96	418236	1725785	Volcanic -Limestone
19	HSA97	417010	1726772	Limestone
20	HSH11	409246	1720948	Volcanic
21	HSA99	416163	1720363	Volcanic
22	HSA16	417248	1717731	Alluvium -Limestone
23	HSA100	417243	1719087	alluvial-Volcanic
24	HSA101	418561	1720651	alluvial-Volcanic
25	HSA102	419534	1723364	Limestone

Ser No	Well ID	UTM (E)	UTM(N)	Aquifer
26	HSA103	419477	1720943	Limestone
27	HSA7	421957	1719694	Alluvium
28	HSA104	422559	1717798	Alluvium
29	HSA105	419380	1725310	Limestone
30	HSA106	419567	1730016	Limestone
31	HSA74	426751	1729981	Alluvium
32	HSA107	430467	1729702	Limestone
33	HSA108	430695	1730438	Limestone
34	HSA109	430402	1732830	Limestone
35	HSA110	418279	1712455	Alluvium

Table 7-12 First priority water quality monitoring stations in the vicinity of treated wastewater passage (well ID based on Hydrosult 2007 survey)